Winter 12-15-2015

The Mechanism and Regulation of Mammalian Photoreceptor Dark Adaptation

Yunlu Xue
Washington University in St. Louis

WASHINGTON UNIVERSITY IN ST. LOUIS

Division of Biology and Biomedical Sciences
Neurosciences

Dissertation Examination Committee:
Vladimir Kefalov, Chair
Joseph Corbo
Daniel Kerschensteiner
Peter Lukasiewicz
Paul Taghert

The Mechanism and Regulation of Mammalian Photoreceptor Dark Adaptation
by
Yunlu Xue

A dissertation presented to the
Graduate School of Arts & Sciences
of Washington University in
partial fulfillment of the
requirements for the degree
of Doctor of Philosophy

December 2015
St. Louis, Missouri

Table of Contents

List of Figures

Chapter 4

List of Tables

Chapter 3

List of Abbreviations

cGMP: cyclic guanosine monophosphate

CKO: conditional knock out

CNG channel: cyclic nucleotide-gated ion channel

CRALBP: cellular retinaldehyde binding protein

DES1: dihydroceramide desaturase-1

GAP: GTPase-activating-protein

GCL: ganglion cell layer

GDP: guanosine diphosphate

GPCR: G-protein coupled receptor

GRK: G-protein coupled receptor kinases

GTP: guanosine triphosphate

IPL: inner plexiform layer

IPM: interphotoreceptor matrix

INL: inner nuclear layer

IS: inner segment

KO: knock out

LRAT: lecithin retinol acyltransferase

MFAT: multifunctional O-acyltransferase

ONL: outer nuclear layer

OPL: outer plexiform layer

OS: outer segment

PDE: phosphodiesterase

PL: photoreceptor layer

RDH: retinol dehydrogenase

RDH10: retinol dehydrogenase 10

RGR: RPE-retinal G protein-coupled receptor

RPE: retinal pigment epithelium

<u>Acknowledgments</u>

First of all, my deepest acknowledgement goes to my thesis advisor, Dr. Vladimir Kefalov. I want to thank him for 5 years marvelous mentorship and unreserved support both in and out of my academic life. I also want to thank my thesis committee, Dr. Joseph Corbo, for the great collaboration on my major projects, as well as Drs. Daniel Kerschensteiner, Peter Lukasiewicz and Paul Taghert, who chaired this committee before the defense, for their enlightening and helpful advice over the years.

I am grateful to Dr. Andreas Burkhalter, who brought me to visual neuroscience and continuously encouraged me in graduate school, as well as Dr. Shiming Chen, who served on my qualification exam committee and has provided tremendous amount of moral support since then.

I thank my current and former colleagues at Kefalov lab, Frans Vinberg, Alexander Kolesnikov, Jinshan Wang, Keisuke Sakurai and Shiya Sato for the fun of working together and discussions on science and engineering.

Lastly, I want to thank my late grandparents, my parents, uncles and aunts for their love, support and understanding in my life.

Yunlu Xue

Washington University in St. Louis

September 2015

Dedicated to my grandfathers.

ABSTRACT OF THE DISSERTATION

The Mechanism and Regulation of Mammalian Photoreceptor Dark Adaptation

by

Yunlu Xue

Doctor of Philosophy in Biology and Biomedical Sciences

Neurosciences

Washington University in St. Louis, 2015

Professor Vladimir Kefalov, Chair

The visual perception of vertebrates begins in rod and cone photoreceptors. Both photoreceptors require visual pigments to detect light. At the first step of light detection, a chromophore molecule (i.e. 11-*cis* retinal), which is conjugated to the visual pigment in photoreceptor outer segment, absorbs a photon. Photoisomerization of the chromophore activates the visual pigment, triggers the phototransduction cascade, and produces electrical signals. After photoisomerization, the chromophore is ultimately converted to all-*trans* retinol, which must be recycled to regenerate the visual pigment. This visual pigment regeneration process is called the visual cycle. It is the rate-limiting step of the photoreceptor dark adaptation after extensive light activation.

The chromophore is recycled through retinal pigment epithelium (RPE) cells. In addition, cones can access a second visual cycle through the retinal Müller cells. This second visual cycle is cone-specific and fast-operating. However, it is unknown how important this retina visual cycle is to mammalian cone function and dark adaptation. To address this question, we studied whether this pathway could be impaired by deleting one of its components, the cellular retinaldehyde binding protein (CRALBP), and how this impairment would affect cone function

and survival. We found that the deletion of CRALBP in mice led to impaired retina visual cycle and cone overall dark adaption, causing chronic chromophore deprivation, which desensitized M-cones, mislocalized M-opsin, and decreased M-cone numbers. We discovered that only rescuing the retina, but not RPE visual cycle, could partially restore the cone function.

Considering the changes in ambient luminance, chromophore consumption is vastly different at day compared to at night. It is not clear whether the efficiency of the RPE visual cycle is modulated to reflect this chromophore consumption difference. To explore this question, we conducted rod dark adaptation experiments at subjective day, subjective night and objective day using electroretinography (ERG) on both melatonin-proficient and melatonin-deficient mouse strains. We observed that in melatonin-proficient mice the RPE visual cycle during the day is slightly down-regulated by the circadian clock and dramatically down-regulated by light exposure. We did not observe any such differences in melatonin-deficient strains, suggesting that this daytime down-regulation is melatonin-dependent.

Cones, but not rods can oxidize the 11-*cis* retinol produced by the retina visual cycle. However, the 11-*cis* retinol dehydrogenase (RDH) driving this reaction in cones has not been unidentified. To address this question, we examined how knocking out RDH10, an 11-*cis* RDH candidate, selectively in cones or in the retina affects the retina visual cycle. We did not observe any alteration in cone function and the retina visual cycle, suggesting that RDH10 is not necessary for the retina visual cycle. In addition, the transgenic RDH10 rods did not accelerate rod dark adaptation in vivo, suggesting that RDH10 is not sufficient for rods to access the retina visual cycle. The identity of the cone 11-*cis* RDH(s) is still unclear.

In summary, we first reported that the retina visual cycle supports cone function and dark adaptation. CRALBP plays a crucial role in retina visual cycle, whereas RDH10 appears not to

be involved in this pathway. The RPE visual cycle is down-regulated to decrease the chromophore turnover for saturated rods during the day. These findings strongly support the existence of a functional retina visual cycle and provide hints for future study on the evolution of this pathway.

"A basic characteristic of the scientific enterprise is its continuity. It is an organic growth, to which each worker in his time brings what he can; like Chartres or Hagia Sofia, to which over the centuries a buttress was added here, a tower there."

George Wald

Chapter 1: Introduction

1.1 Structure of mammalian retina

Vision begins at photoreceptor cells in the mammalian retina. The retina is a transparent thin layer of cells lining the back of the eye. It converts the light into electrical signals, and computationally processes these signals for higher visual perception in the brain. Because the brightest natural light is ~9 log-unit stronger than the dimmest condition, the retina has to adapt its functional operation accordingly to produce visual signals. The process of visual adaptation to darkness in transition from extensive bright light is termed as dark adaptation. This dissertation sought to address the mechanism and regulation of dark adaptation in photoreceptors.

Before getting to the retina, light from the environment is first refracted by the cornea, intensity-adjusted by the pupil, refracted again by the lens, passes through the vitreous body, and is finally focused onto the retina (Figure 1.1A). The image of the world is presented in an inverted fashion on the retina. However, the brain can "correct" this inverted image to the normal orientation (Stratton, 1897; Gibson, 1933), so that we do not take right as left or up as down. Nonetheless, the dark adaptation occurs at the retinal level, instead of the brain.

1.1.1 Neuronal retina composition and function

The retina is a complex structure of cells. The anatomy of the mammalian retina was well characterized by Santiago Ramón y Cajal over a hundred years ago (Ramón y Cajal, 1900). The retina is composed of 5 classes of neurons (see Masland, 2012 for review), which are organized into six layers: photoreceptor layer (PRL), outer nuclear layer (ONL), outer plexiform layer

1

(OPL), inner nuclear layer (INL), inner plexiform layer (IPL) and ganglion cell layer (GCL) (Figure 1.1B). Traditionally, PRL, ONL and OPL are defined as the outer retina, and INL, IPL and GCL belong to the inner retina.

Counterintuitively, vertebrate photoreceptors are on the back of the retina, which means that light needs to travel through the retina before getting to the photoreceptors. Then the photoreceptors convert the light into electrical signals, which are processed first by the bipolar cells and then ganglions cells (Figure 1.1B). Two other types of retinal neurons are also involved in the retinal visual signaling processing: horizontal cells, which modulate the photoreceptor-to-bipolar signal transmission, and amacrine cells, which modulate the bipolar-to-ganglion transmission (Figure 1.1B). Subsequently, the processed visual signals enter the higher processing center in the brain from ganglion cells via the optic nerve. In this dissertation, we will focus on the photoreceptors and their dark adaptation.

Figure 1.1 (A) The schematic of human eye. Adapted from (Faimilyeyes.com). (B) The anatomy of mammalian retina. (Adapted from Ramón y Cajal, 1900).
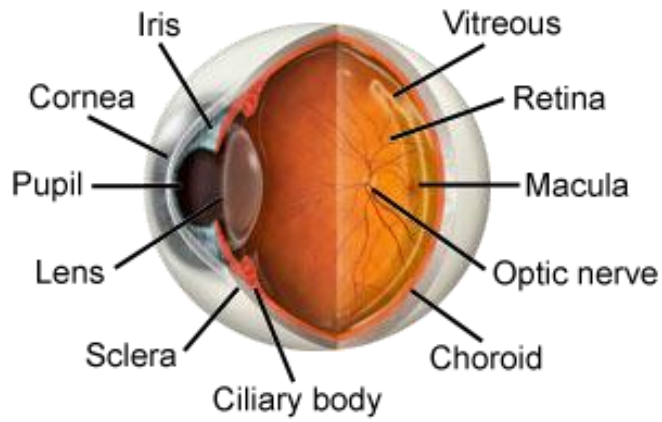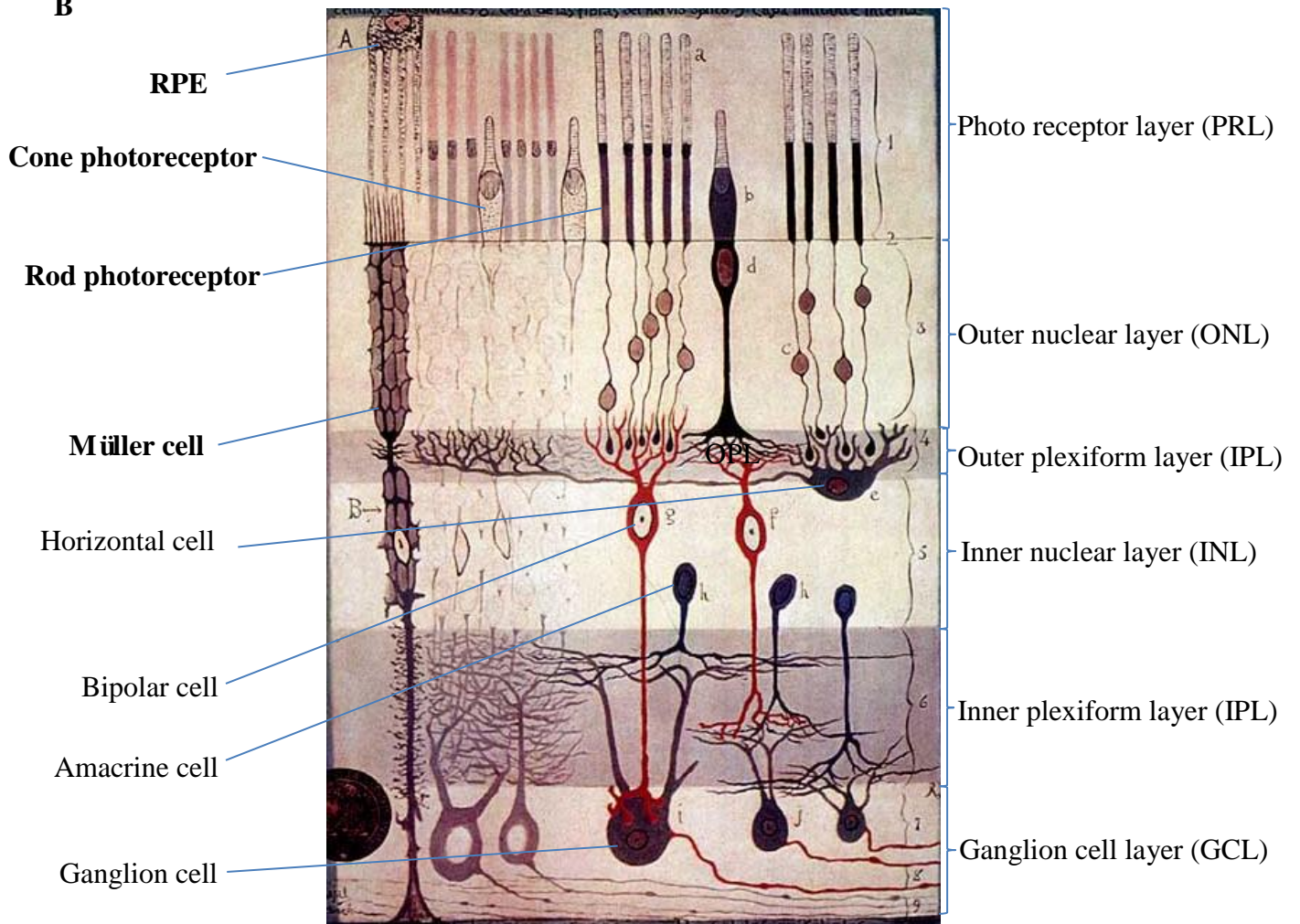
1.1.2 Photoreceptor morphology and function

In mammals, there are two types of photoreceptors, rods and cones (Figure 1.1B). Rods are responsible for vision in dim light conditions, and cones are for color vision in bright light conditions. The rods are very sensitive to light and can respond to a single photon, but get saturated during the day. Cones are less sensitive than rods, but can function in a wide range of light intensities. Cones can adapt rapidly from/to different light intensities and to darkness, while rods cannot. In addition, because rods dominate our vision at night, problems with rod dark adaptation are more noticeable. As a result, dark adaptation of rods is better studied than the dark adaptation of cones.

Rods emerged later than cones in evolution (Lamb et al., 2007). Mice and humans have only one type of rod, but in some amphibian species like frog, there are two types of rods (green and red), which have different spectral sensitivity (Papermaster et al., 1982; Matthews, 1983). In mouse and human retinas, rods are the dominant type, and cones only make up 3% and 5% of all the photoreceptors, respectively (Jeon et al., 1998; Purves et al., 2001). There are three type of human cones - blue, green and red, helping us to perceive colors (Curcio et al., 1991). In mice, most of the cones express a mixture of S-opsin and M-opsin in different ratios with a ventral-dorsal gradient pattern (Applebury et al., 2000).

Both rods and cones are composed of four parts: a modified cilium called the outer segment (Richardson, 1969), an organelle-rich inner segment, a nucleus and a synaptic terminal. The morphology of rods and cones is quite different (Figure 1.1B). The rods have long and slim outer segments, which enclose packed floating disc sacs, while cone outer segments are short and their discs are open to the interphotoreceptor matrix (IPM). Rod nuclei are scattered in the outer

4

nuclear layer, while cone nuclei are positioned close to the inner segments and well aligned on the apical side of the outer nuclear layer. Rod spherules, the rod synaptic terminals, are small in size, while cone pedicles, the cone synaptic terminals, are large and have a bigger active zone to fulfill the active synaptic transmission needed for day vision (Kolb, 1970; Lamb, 2013). These morphological differences could contribute to the rod/cone difference in dark adaptation, which will be discussed in Chapter 5.

1.1.3. Müller cells and retinal pigment epithelium (RPE)

The dark adaptation of photoreceptor needs the support from other cells. Like other neurons in the brain, photoreceptors get the nutritional and structural support from glia cells. In the retina, there are two types of endogenous glia cells, retinal microglia cells, which are mobile and believed to be responsible for immune reactions, and retinal macroglia, which are also called Müller cells and span the thickness of the retina (Wang and Wong, 2014). In addition, the retinal astrocytes enter the retina from the brain at early development stage (Stone and Dreher, 1987). In addition to the glia cells, retinal pigment epithelium (RPE) cells lie between the retina and choroid, which is rich in blood vessels. RPE cells are connected through tight junctions, forming the blood-brain-barrier between the blood vessels and the retina (Steinberg, 1985; Bok, 1993). RPE supports the photoreceptor function in many ways, such as chromophore recycling (see Section 1.4), nutrients supply, photoreceptor outer segment renewal by autophagy (Goldman et al., 1980; Kim et al., 2013). To support dark adaptation, RPE and Müller cells recycle the chromophore for photoreceptors. The mechanisms of this recycling process will be introduced in Section 1.4 in this chapter.

Anatomically, both the RPE and Müller cells are adjacent to the photoreceptors (Figure 1.1B). The apical side of RPE presents processes in close contact with the photoreceptors (Bok, 1993). The Müller cells stem processes have intimate contact with all the neurons in the retina (Reichenbach and Bringmann, 2010). Particularly, the processes of Müller cells form a sheath-like structure which wraps around the cone inner segments, and defines the outer limiting membrane with the photoreceptor inner segments (Reichenbach and Bringmann, 2010). Müller cells also have microvilli, which extend into IPM and are physically close to the photoreceptor inner segments. Anatomical adjacency of the RPE processes and Müller cell microvilli to photoreceptors facilitates the visual cycle, and further allows the phototransduction of rods and cones.

1.2 Phototransduction

1.2.1 Activation

Photoreceptors convert the light signal into electrical signals through a series of biochemical reactions termed the phototransduction cascade (see Pugh and Lamb, 1993; Yau and Hardie, 2009 for reviews). The light sensitivity molecule is rhodopsin in rods and cone opsin (also known as photopsin) in cones. These opsins are seven-transmembrane-helix proteins on the disc membrane in photoreceptor outer segments (Mustafi et al., 2009; Zhou et al., 2012). They are G-protein coupled receptors (GPCRs). The opsin molecules have a pocket-like structure to covalently bind with the chromophore, 11-*cis* retinal, by forming a Schiff base with a lysine. 11-*cis* retinal absorbs a photon and gets isomerized to all-*trans* retinal, activating the opsin molecule (Figure 1.2). The activated opsin molecule then activates the transducin, which is a G-protein, triggering the activation of phosphodiesterase (PDE) (see Arshavsky et al., 2002 for review). The activated PED hydrolyzes the cyclic GMP (cGMP) to GMP.

In darkness, photoreceptors are depolarized by an inward current called the "dark current", which drives the synaptic terminal to continuously release glutamate to bipolar cells. The dark current is induced by the influx of cations through the cyclic nucleotide-gated (CNG) channels on the outer segment membrane and a balancing efflux of cations at the inner segment (Hagins et al., 1970). The operation of CNG channels is determined by cGMP concentration in the outer segment.

Upon light activation, PDE-induced hydrolysis of cGMP leads to a reduction of cGMP concentration, which subsequently closes the CNG channels (Figure 1.2). The closure of CNG channels decreases the dark current, thus hyperpolarizing the photoreceptor and decreasing the

glutamate release at the synaptic terminal. This light-induced hyperpolarization is conceptually equivalent to "darkness-induced depolarization", which means the darkness "activates" the photoreceptor and releases synaptic transmitters. One possible evolutionary explanation is that it is more critical for the vertebrate ancestor to detect shadows made by prey or predators, than to detect bright objects (Reuter, 1969, 2011).

1.2.2 Deactivation

Because the temporal resolution of vision is on the millisecond scale, prolonged signaling will compromise the accuracy of vision. Therefore the timely shut down of the phototransduction cascade is very important. To completely deactivate the phototransduction, all phototransduction components need to be deactivated, and cGMP concentration returned to dark level. The deactivation process is complicated and many details are still under investigation (see Fu and Yau, 2007 for review), especially for cones (Sakurai et al., 2015).

In general, the activated opsin is first phosphorylated by G protein-coupled-receptor-kinase 1 (GRK1), followed by arrestin binding, which completely deactivates the opsin (Figure 1.2). The active transducin, which is the transducin α-subunit/GTP, is deactivated by GTPase, to transducin α/GDP, facilitated by GTPase-activating-protein (GAP). The deactivated transducin also subsequently deactivates PDE by freeing the PDE γ-subunit (PDE-αβ-subunit is the cGMP catalytic part, inhibited by free PDE γ-subunit). Then the cGMP level is restored by guanylate cyclase, thus reopening the CNG channels. In dark adaptation, phototransduction deactivation initiates rapidly after transition to darkness and is completed faster than chromophore recycling, thus it is not considered as part of the photoreceptor dark adaptation.

8

Figure 1.2 Schematic of phototransduction cascade in rod photoreceptor (adapted from Yau and Hardie, 2009).
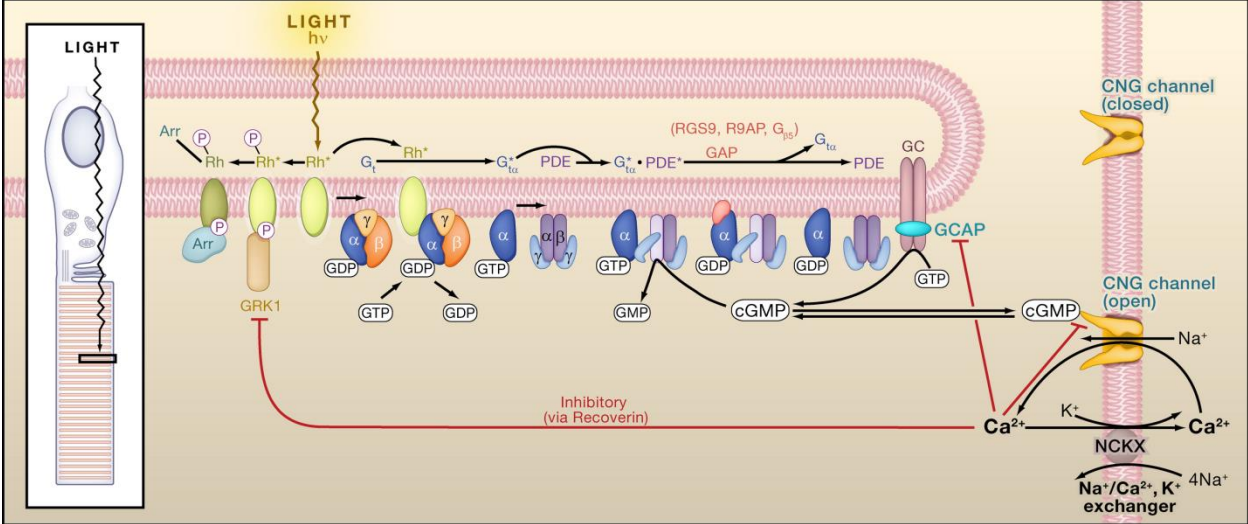
1.3 Dark adaptation

1.3.1 Dark adaptation is slow

On the surface of the earth, the ambient light intensity varies about 9 log units from overcast night to bright sunny day. Usually, we do not realize how incredible it is that our vision can function in such an expanded light range. From an engineer's perspective, the eye is facing two difficulties. First, how to adapt rapidly to light without "over exposure", which means saturation of system, and second, how to detect light at the extremely dim environment. To tackle the first challenge, cone photoreceptors have fast Ca^{2+} feedback signaling for quick light adaptation (Vinberg and Koskelainen, 2010; Sakurai et al., 2011, 2015). To solve the second challenge, rod photoreceptors evolved after cones to amplify the signal from a single photon, at the cost of getting saturated in bright conditions (see Lamb et al., 2007 for review). As a result, we can see faster and better without perceiving the transition from the dimmest to brightest condition, except feeling uncomfortable for just a few seconds if the transition happens too fast.

On the other hand, there is one property that would be relatively easy to achieve in engineering, but seems to be challenging for the eye. This is the ability to regain sensitivity in dark conditions immediately after intense illumination. To deal with this bright to dark scenario, the pupil first expands to allow more light into the eye, driven by a neural muscular reflex together with the intrinsic light response of the iris (Xue et al., 2011). However, the time-course of complete dark adaptation is much longer than that of the pupillary reflex. Because visual pigments have been partially bleached by the bright light, they need to be regenerated before photoreceptors regain their high sensitivity. It takes minutes for the visual pigments to regenerate. This overall process of visual sensitivity recovery is called dark adaption.

1.3.2 Psychophysical studies

The history of dark adaptation research has been thoroughly reviewed previously (Lamb and Pugh, 2004; Reuter, 2011). The earliest investigation of dark adaptation started with psychophysics experiments on humans. In these studies, subjects reported the dimmest light they could see following bright light exposure. These classic psychophysical tests revealed a fast recovery phase, which was completed in 3 to 4 minutes and a slow recovery phase, which was completed in 30 minutes after the illumination (Hecht et al., 1937) (Figure 1.3). In Hecht et al.'s result, the initial fast recovery phase is believed to be driven by the dark adaptation of cones, and the slow recovery phase is believed to be driven by rods.

In modern psychophysical dark adaptation research, a more careful examination at different photobleach levels revealed three phases: a fast S1 component, a constant-speed linear S2 component, and a slow S3 component (Lamb and Pugh, 2004). The S1 component is believed to be the cone-driven dark adaptation together with unclear contribution from the deactivation of rod phototranduction cascade. The S2 component is due to the regeneration of rhodopsin (see details in Section 1.3.3). The mechanism of S3 component is still unknown, possibly due to the dephosphorylation of opsin by phosphatase (Lamb and Pugh, 2004 and unpublished PP2A rod CKO data form Kefalov lab).

The above psychophysical phenomenon of dark adaptation is believed to originate from the eye but not from higher processing centers in brain, because if the two eyes were kept in different illumination, they demonstrate different sensitivity. This eye origination of dark adaptation was later confirmed by recordings on frog ganglion cells (Donner and Reuter, 1967). Similar recovery curve shape was observed in the ganglion cells threshold dark adaptation.

11

Figure 1.3 Classic human psychophysical dark adaptation curves following various bleaching level (i.e. adapting intensities). (Adapted from Hecht et al., 1937).
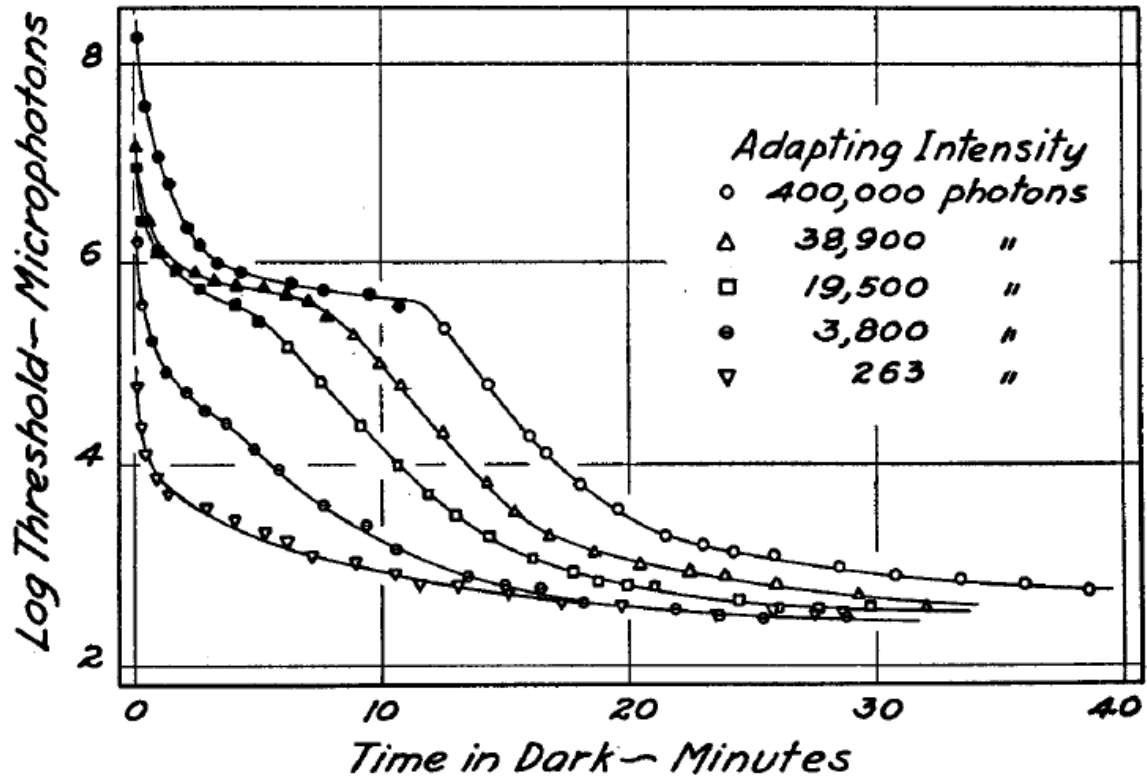
1.3.3 Dowling—Rushton relation for rod dark adaptation

Psychophysical test is a subjective method. How can we objectively study dark adaptation with a functional approach? Is there a correlation to the psychophysics using this approach? Electroretinography (ERG) is a powerful tool to measure the function of the retina, thus opening a window for the retinal dark adaptation in vivo (details in section 1.5 Common Experimental Procedures). The ERG b-wave (originated by on-bipolar cells) sensitivity threshold recovery was carefully measured in albino rats after full photobleach (Dowling, 1960). The b-wave sensitivity recovery was complete within two hours, and the logarithmic b-wave sensitivity was found proportional to the rhodopsin level, measured from the extract of the eyes (Dowling, 1960). For the dark adaptation time constant, 50% of Rat rhodopsin was regenerated in 30 minutes after darkness (Dowling, 1960).

After Dowling, Rushton reported the relationship between psychophysics and in vivo rhodopsin level in humans using reflection densitometry (Rushton, 1961). In this study, the regeneration of rhodopsin was reported to be faster in humans (50% regenerated in 7 minutes) than in rats (Rushton, 1961). The slower regeneration in rats was likely due to the effect of anesthesia in ERG, as well as the differences between species. Nevertheless, in agreement with Dowling's results, the log psychophysical sensitivity was proportional to the rhodopsin level in humans. In the end, the proportional relationship between log sensitivity and rhodopsin content was named the Dowling-Rushton relation.

The Dowling-Rushton relation correlated the ERG sensitivity with rhodopsin level, and the rhodopsin level with psychophysical sensitivity. Therefore, it was inferred that the ERG sensitivity is correlated with the psychophysical sensitivity. To establish the direct correlation

between the ERG sensitivity and the psychophysical sensitivity relation in humans, first, the recovery of ERG a-wave maximal amplitude was measured at various levels of photobleach (Thomas and Lamb, 1999). Then, the psychophysical sensitivity was measured as the time of 50% recovery of S2 component at various level of photobleach (Lamb and Pugh, 2004). With the two data sets, it was confirmed that the ERG maximal responses well correlated with psychophysical sensitivity as a function of photobleach intensity (Lamb and Pugh, 2004). In addition, the linear and constant-speed shape of the S2 component at all bleaching level suggests that the rate of rhodopsin regeneration is linear (Lamb and Pugh, 2004).

Taken together, Dowling, Rushton, Lamb and Pugh established a clear relation among psychophysics (S2 component), scotopic ERG response, and rhodopsin level in rod-mediated dark adaptation, suggesting the rhodopsin regeneration to be the rate-limiting step of rod dark adaptation.

1.3.4 Cone-mediated dark adaptation

It should be noticed that unlike rod-mediated dark adaptation, cone-mediated dark adaptation so far does not have a well-established Dowling-Rushton relation, due to technical challenges. These include the fast kinetics of cone-dark adaptation (3-4 minutes in human psychophysical tests), the scarce number of cones, diverse types of cones, and the fovea-peripheral differences in human. Nonetheless, photopic ERG results (Mahroo and Lamb, 2012) correlate well with the fovea cones opsin content measured by reflection densitometry (Rushton and Henry, 1968), and dark adaptation recovery fits better with a rate-limited fashion, implying that cone opsin regeneration is likely to be the rate-limiting step for cone-mediated dark adaptation (Mahroo and Lamb, 2012).

These studies also provided the foundation for the research presented in this dissertation that ERG can be used to test the cone-mediated dark adaptation.

1.4 Visual cycle

In the previous section, we introduced the notion that visual pigment regeneration is the rate-limiting step in photoreceptor dark adaptation. What drives the visual pigment regeneration? Indeed, it is a biochemical process termed the visual cycle, in which chromophore is recycled through RPE and Müller cells (see Lamb and Pugh, 2004; Wang and Kefalov, 2011; Kefalov, 2012 for reviews).

1.4.1 Metarhodopsin conversion

Visual pigment regeneration is composed of two parts, a fast opsin cycle, and a slow chromophore cycle. The fast opsin cycle starts with the phototransduction deactivation, which was briefly introduced in Section 1.2.2. For rods, after phototransduction activation, rhodopsin gets into the metarhodopsin I (M1) configuration in microseconds. In 1 millisecond, M1 converts to metarhodopsin II (M2), which is also the activated rhodopsin (R*), triggering the phototransduction cascade (Figure 1.2). After conversion, M2 is rapidly phosphorylated by GRK1 and capped by arrestin, thus losing its activity. The deactivated M2 then decays to metarhodopsin III (M3) to an equilibrium-state relation (Kolesnikov et al., 2003). M3 is also inactive, and it decays into free opsin in several minutes, releasing all-*trans* retinal and awaiting 11-*cis* retinal binding to regenerate rhodopsin.

Cone opsins undergo a similar cycle to rhodopsin. Because cones are scarce in the rod-dominant retina, the studies on cone visual pigments were done on cone-dominant species such as chicken. Although the existence of a cone meta III is controversial, the decay of chicken green "meta III" is much faster (in seconds) than rhodopsin M3 (Shichida et al., 1994).

The final step of the visual pigment cycle involves the binding of 11-*cis* retinal (i.e. chromophore) to free opsin to regenerate visual pigment. Therefore, the slower chromophore supply becomes the rate-limiting step for visual pigment regeneration, and ERG-psychophysical dark adaptation. Thus, visual cycle will only refer to the biochemical process of chromophore recycling, which rate-limits photoreceptor dark adaptation, in this dissertation.

1.4.2 Canonical RPE visual cycle

The slow chromophore cycle was first described by George Wald in frog (*Rana pipiens* and *Rana esculenta*) eyes using absorption spectrum measurements (Wald, 1935). In this pioneer study, he reported that "visual purple", was bleached by light to "visual yellow", releasing the previously undefined carotenoid retinene. Wald also described retinene decomposition to a clear product of Vitamin A. Wald found that Vitamin A was abundant in the combination of RPE and choroid, sparse in retina from light adapted eyes, and only present in trace amounts in retina from dark adapted eyes, but abundant in isolated retina after light bleach. Taking these observations together with the knowledge that Vitamin A deprivation led to compromised synthesis of visual purple and night blindness, Wald believed that Vitamin A was both the precursor and decomposition product of the visual purple. Thus he concluded that this "Vitamin A cycle" was vital for the visual function.

80 years after Wald's study, now we have a better understanding of this Vitamin A cycle and its significance to photoreceptor dark adaptation (See Lamb and Pugh, 2004; Wang and Kefalov, 2011; Saari, 2012; Kiser et al., 2014 for reviews). Now we know that the visual purple is rhodopsin, the visual yellow is the metarhodopsin, and the retinene is 11-*cis* retinaldehyde (retinal) and all-*trans* retinal.

11-*cis* retinal is the light-sensing molecule, which covalently binds to the free opsin. Its photoisomerization to all-*trans* retinal triggers the phototransduction cascade (see Section 1.2). Then the all-*trans* retinal is reduced by retinol dehydrogenases (RDHs) to all-*trans* retinol (i.e. Vitamin A). All-*trans* retinol was previously thought to be carried by interphotoreceptor retinoid-binding protein (IRBP) through interphotoreceptor matrix (IPM) to the RPE (Okajima et al., 1989). In the RPE, it is recycled back to 11-*cis* retinal (Figure 1.4). However, the deletion on IRBP mice did not show significantly delayed rod dark adaptation (Kolesnikov et al., 2011), suggesting IRBP transportation is unlikely to be the rate-limiting step in the RPE visual cycle.

In the RPE, all-*trans* retinol first binds to Cellular retinol-binding protein (CRBP) (Napoli, 2000), before it is esterified by Lecithin retinol acyltransferase (LRAT) to all-*trans* retinyl ester (Ruiz et al., 1999; Mondal et al., 2000). The all-*trans* retinyl ester is then isomerized and hydrolyzed by RPE65 to 11-*cis* retinol (Redmond et al., 1998; Jin et al., 2005), which is carried by cellular retinaldehyde binding protein (CRALBP) (Saari et al., 2001). Then 11-*cis* retinol is oxidized to 11-*cis* retinal by RDHs, released from the RPE, and returned to the rod outer segment across the IPM to bind to free opsin, thus regenerating rhodopsin and completing the visual cycle (see Fain et al., 2001; Saari, 2012 for reviews).

For the supply to the eye, as envisioned by Wald (Wald, 1935), it is important to replenish the attrition in the visual cycle with dietary Vitamin A. Now we know that all-*trans* retinol is carried by retinol binding protein (RBP) in blood vessels, and delivered to the eyes through STRA6, a membrane receptor on the basolateral side of the RPE (Bok and Heller, 1976; Kawaguchi et al., 2007).

Because this visual cycle goes through the RPE, it is called the canonical RPE visual cycle (Figure 1.4). RPE visual cycle primarily serves the rods in rod-dominant species, such as mice and humans. However, during the day, when the chromophore recycling is higher with sustained light, rods are saturated by daylight. Therefore, RPE visual cycle is facing a dilemma, to function faster to meet the higher chromophore consumption? Or to function slower to preserve the energy wasted on the saturated rods? We will answer this question in Chapter 3.

Cones also use this RPE visual cycle, (Kolesnikov et al., 2011), however, the exact contribution of RPE visual cycle to cone dark adaptation is not clear. We will explore this question using CRALBP-deficient mouse model in Chapter 2.

Figure 1.4 Schematic of the canonical RPE visual cycle on a rod photoreceptor. Abbreviations:11cRAL, 11-*cis* retinal; 11cROL, 11-*cis* retinol; atRAL, all-*trans* retinal; atROL, all-*trans* retinol; 11cRE, 11-*cis* retinyl ester; atRE, all-*trans* retinyl ester; REH, retinyl ester hydrolase; CRALBP, cellular retinaldehyde binding protein; IRBP, Interphotoreceptor retinoid-binding protein; CRBP, Cellular retinol-binding protein. (Adapted from Wang and Kefalov, 2011).
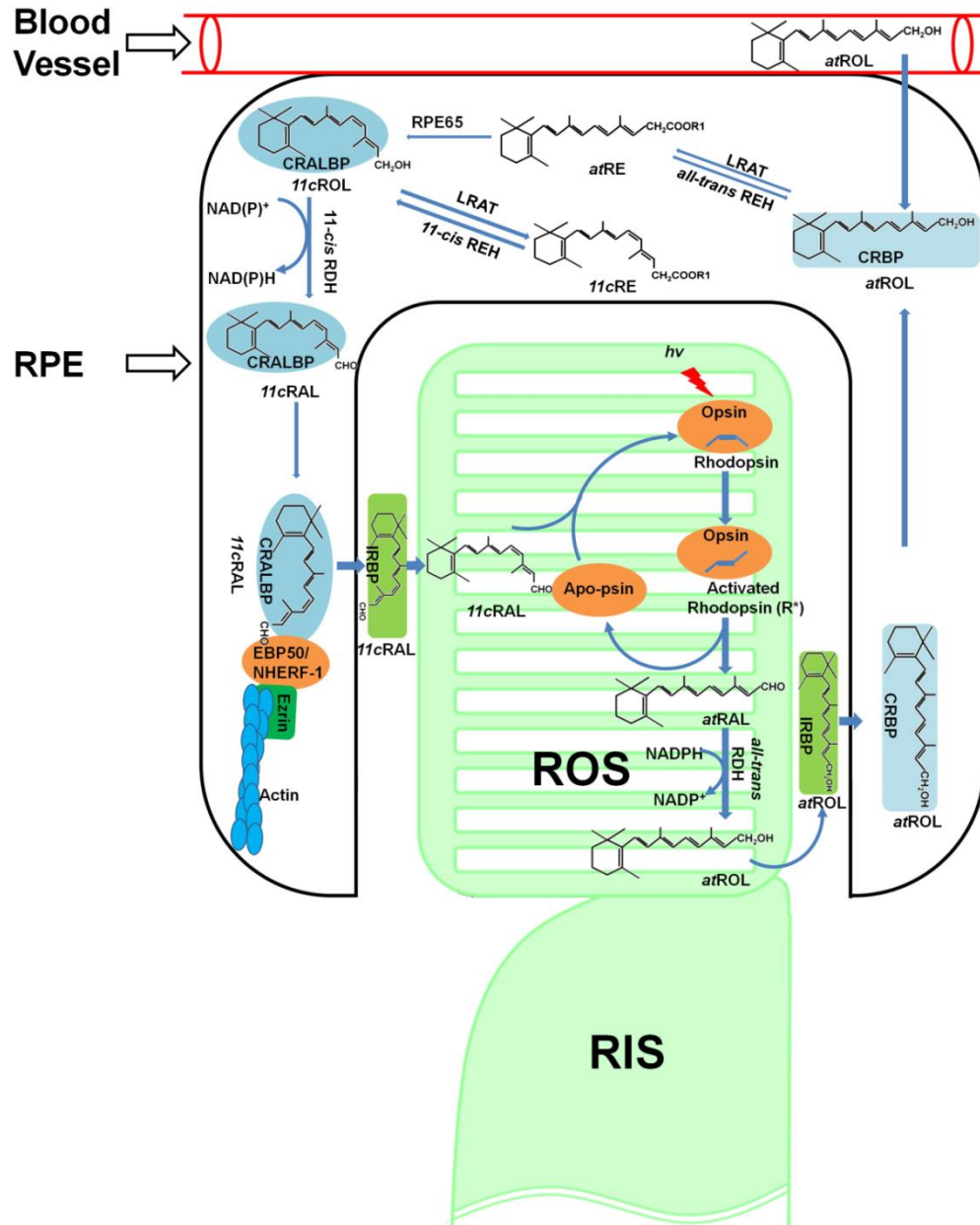
1.4.3 Novel retinal visual cycle

The RPE visual cycle slowly turns over chromophore and fully dark adapt rods in 30 minutes, which is unlikely to drive the rapid cone-mediated phase (3-4 minutes) observed in classic dark adaptation experiments (Hecht et al., 1937). Now we know that this fast cone dark adaptation is driven by a novel visual cycle within the retina (Wang and Kefalov, 2009; Wang et al., 2009), which supplies chromophore specifically to cones. In this retina visual cycle (Figure 1.5), all-*trans* retinol travels to the Müller cells in the retina, where it is isomerized to 11-*cis* retinol (Mata et al., 2002). The 11-*cis* retinol can travel back to the outer segment and be oxidized by unidentified 11-*cis* RDH(s) in cones, but not in rods, to 11-*cis* retinal for visual pigment regeneration (Jones et al., 1989; Mata et al., 2002; Miyazono et al., 2008). This retina visual cycle operates very rapidly and can regenerate the cone opsin to its maximal capacity within two minutes (Kolesnikov et al., 2011).

Unlike in canonical RPE visual cycle, the molecules involved in the retina visual cycle are largely unknown. Nonetheless, several RPE visual cycle proteins, such as CRALBP, are also found in Müller cells. In zebrafish, two orthologues of CRALBP are differentially expressed in the RPE and Müller cells, and knocking down the Müller cell CRALBP leads to impaired cone ERG (Fleisch et al., 2008). Could CRALBP also be involved in the mammalian retina visual cycle? What will happen to cone function and dark adaptation if we delete CRALBP in mice? In addition, why can cones, but not rods, access this retina visual cycle? Is it due to a cone-specific 11-*cis* RDH? What is the identity of this 11-*cis* RDH? Is it RDH10 (Farjo et al., 2009)? Is RDH10 the unidentified 11-*cis* RDH? These questions motivated us to conduct research in Chapter 2 and 4 to investigate the molecular mechanism of the retina visual cycle.

Figure 1.5 Schematic of the novel retina visual cycle and RPE visual cycle for cone photoreceptor. (Adapted from Wang and Kefalov, 2011).
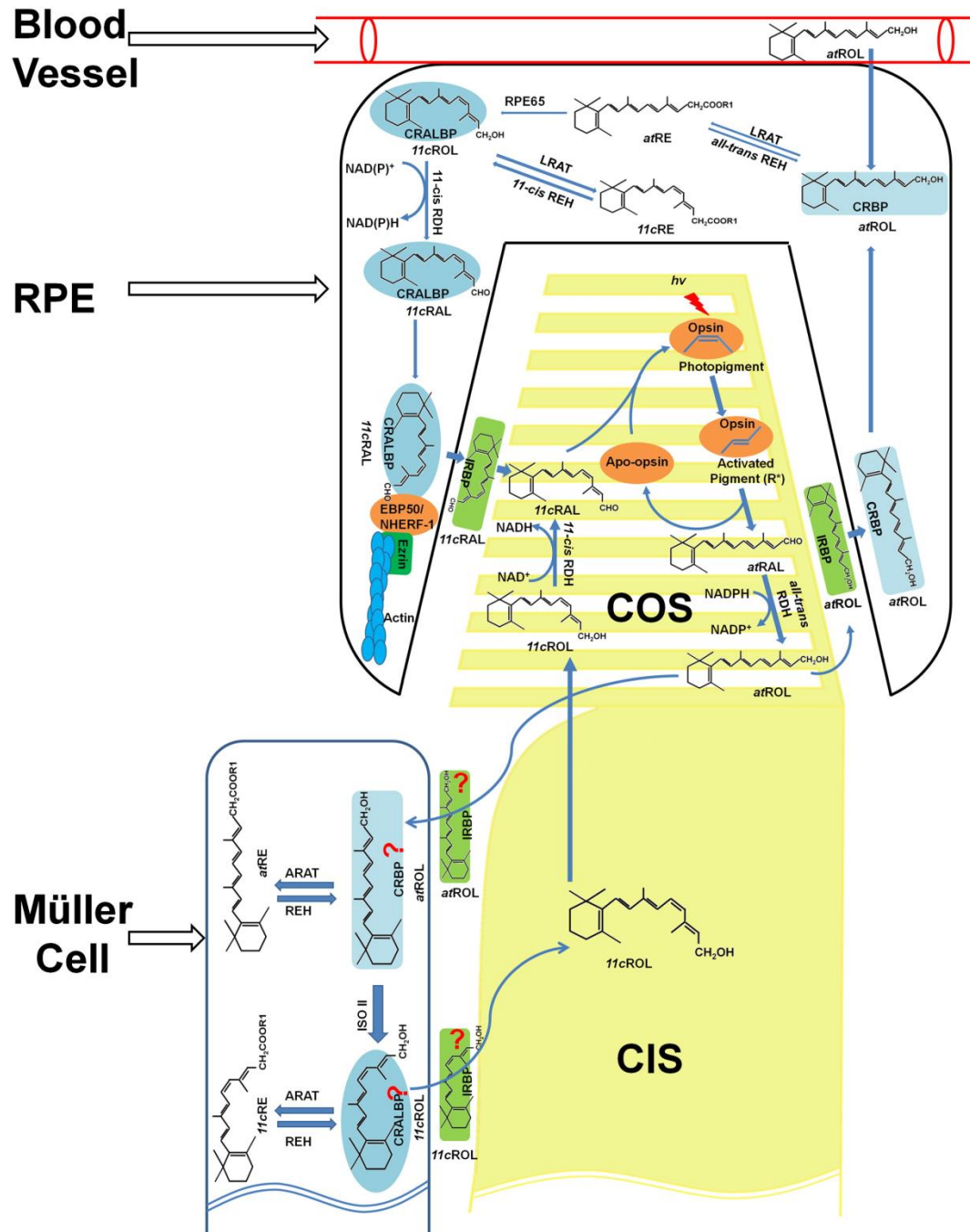
1.5 Research overview

As discussed in the previous section, there are many unknowns about the novel retina visual cycle, especially its molecular components (see Wang and Kefalov, 2011 for review). Therefore the existence of mammalian retina visual cycle is still challenged by a few experts in the field (Lamb and Pugh, 2004; Jacobson et al., 2015), even though several candidate molecules have been proposed recently, such as DES1 as the 11-*cis* isomerase (Kaylor et al., 2013) and MFAT as the 11-*cis* retinyl-ester synthase in Müller cells (Kaylor et al., 2014).

First, this dissertation will seek to resolve this debate, or at least add fresh perspectives, by demonstrating Müller cell CRALBP as the first functionally identified player in the retina visual cycle (Chapter 2).

Second, this dissertation will also make the first attempt to identify the 11-*cis* RDH in cones that enables the cones, but not rods, to access the retina visual cycle. We proposed RDH10 as the candidate molecule and tested this hypothesis by electrophysiological experiments combined with bio-molecular tools (Chapter 4).

Third, this dissertation will explore the differences in the RPE visual cycle at day versus night. During the day, rods do not function due to saturation by light, yet they keep consuming chromophore through the RPE visual cycle. This high chromophore turnover seems like it would be a waste of energy. Thus, we hypothesized that the RPE visual cycle efficiency is different between day and night. We tested this hypothesis by monitoring mouse rod dark adaptation using in vivo ERG, and found that in melatonin-proficient mice the RPE visual cycle is down-regulated during the day (Chapter 3).

Overall, this dissertation aims to demonstrate and explore the molecular mechanism of the retina visual cycle and the regulation of the RPE visual cycle to reveal the mechanisms of mammalian photoreceptor dark adaptation. These results also provide insights on how the two very different types of cells, rods and cones, collaborate to support vision, and provide insights into the evolution of the visual cycle.

1.6 Common experimental procedures

In this section, the common experimental procedures used in Chapters 2, 3 and 4 of this dissertation will be introduced. Each chapter has its specific section of Experimental Procedures with details on additional procedures.

1.6.1 Animals

The maintenance and treatment of all the animals followed the protocols approved by Washington University Animal Studies Committee. To facilitate the recording of cone responses, several mice strains used in this dissertation were bred to rod transducin α-subunit knockout (*Gnat1*$^{-/-}$) background, which was obtained from Janis Lem (Tufts University, Boston), to eliminate the rod photoresponse. In *Gnat1*$^{-/-}$ mice, the morphology of retina is normal (Calvert et al., 2000).

1.6.2 In vivo electroretinogram (ERG)

Because the neurons of the retina are well organized in layers, the electrical currents create a measurable cross-retina voltage potential difference. In vivo ERG recordings measures the composition of these cross-retina voltage changes originated from multiple cell types (Figure 1.6).

The in vivo ERGs were performed with a commercial LKC® system as previously described (Kolesnikov et al., 2011). The dark-adapted animals were anesthetized with ketamine/xylazine (100/20 mg/kg) and their pupils were dilated with atropine sulfate eye-drops. A mouse was placed onto a 37 ℃ heating pad and electrodes were connected to its cornea with 2.5% Gonak hypromellose ophthalmic demulcent solution to pick up electrical signals generated

by the retina. A reference electrode was inserted beneath the skin at the scalp between the two eyes. The animal was allowed to stabilize in darkness for 15 minutes before beginning the recordings. Test flashes of increasing intensity (530 nm LED until 25 cds m^{-2} limit and white Xenon flash for higher) were delivered by the Ganzfeld sphere, and the ERG signals were recorded to obtain the intensity-response curves.

To test the dark adaptation kinetics, bright green LED light (520 nm) was used to bleach an estimated 90% of the photopigments in 30 seconds. For rod dark adaptation test, the recovery of the ERG responses was monitored at fixed post-bleach time points within 2 hours after the bleach. The maximal response amplitude, r_{max}, was recorded at the brightest light intensity, and S_f was estimated as the ratio of dim flash response amplitude and the corresponding flash intensity in the linear range of the intensity-response curve, about 20% to 30% of the maximum. The post-bleach maximal amplitude (r_{max}) and sensitivity (S_f) were normalized to their dark adapted pre-bleach level, r^{DA}_{max} and S_f^{DA}, respectively. For cone dark adaptation test, the cone sensitivity S_f was recorded at pre-set time intervals until 52 minutes after the photobleach. The cone b-wave flash sensitivity was normalized to the pre-bleach value to get the sensitivity recovery curve.

Figure 1.6 The waveform of scotopic ERG and cellular origination of the wave components. (Adapted from Cameron et al., 2008).
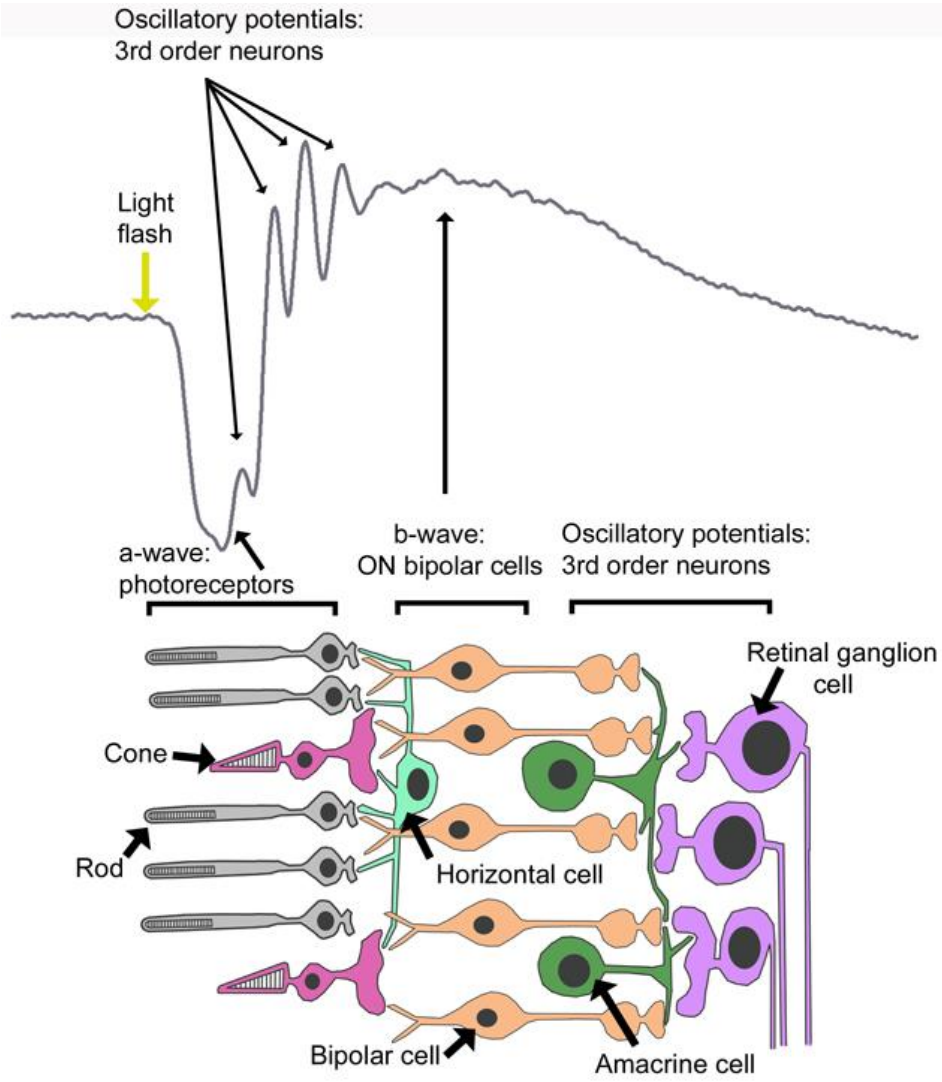
1.6.3. Transretinal recordings

Similar to in vivo ERG, Transretinal recordings measure the ERG signals ex vivo with isolated mouse retina as previously described (Sundermeier et al., 2014a, 2014b). The isolated retina was carefully mounted on a custom-made chamber for transretinal voltage recording (Vinberg et al., 2014). The retina was perfused with Locke's solution bubbled with O_2/CO_2 and supplemented with 30 μM DL-AP4 to block the ON-pathway synaptic transmission. This allowed isolation of the ERG a-wave, which is originated from the photoreceptors. As described in Section 1.6.2, the ERG a-wave signal is a reflection of the photoreceptor dark current changes, making transretinal recording a faithful tool to test the overall photoreceptor physiology.

After setting up the recording chamber, the retina was allowed to stabilize for 15 minutes before any recording. The responses of cones to 1 ms 505 nm LED-generated test flashes of various intensities were amplified and recorded on a desktop computer with pClamp10 software (Molecular Dynamics). Dim flash analysis was performed with responses of amplitude <30% of the maximal for each retina (Pugh and Lamb, 1993). For dark adaptation tests, pre-programed protocols were used to precisely monitor the fast recovery of cone sensitivity during the first 12 minutes following an estimated 90% photobleach of the visual pigments. The cone sensitivity was normalized to the pre-bleach level to generate the sensitivity recovery curve.

27

Chapter 2: CRALBP is required for the mammalian retina visual cycle and M-cone vision

2.1 Abstract

Mutations in human Cellular Retinaldehyde Binding Protein (CRALBP) can lead to severe cone photoreceptor-mediated vision loss. The mechanism of this disease and the role of CRALBP in supporting cone function are unknown. Here, we report that the deletion of CRALBP in mice impairs the retina visual cycle. The resulting M-opsin mislocalization and M-cone loss incapacitate cone-driven visual behavior and light responses. M-cone dark adaptation is also largely suppressed in the absence of CRALBP. Dark rearing CRALBP knockout mice prevented the deterioration of cone function but did not rescue cone dark adaptation. Restoring CRALBP expression specifically in the M üller cells, but not the retinal pigment epithelium (RPE) cells, of knockout mice rescued the retina visual cycle and M-cone sensitivity. Our results identify M üller cell CRALBP as key component of the retina visual cycle and demonstrate the significance of this pathway for maintaining normal cone-driven vision and accelerating cone dark adaptation.

2.2 Introduction

Photoactivation of a visual pigment molecule in vertebrate rod and cone photoreceptors rapidly triggers a light response and concomitantly renders the activated pigment unable to detect a subsequent photon of light. Regeneration of the visual pigment back to the ground state requires recycling its chromophore from the "bleached" all-*trans* retinal to the light-sensitive 11-*cis* retinal. This process, known as the visual cycle, requires export of the all-*trans* chromophore out of the photoreceptors and its conversion to the 11-*cis* form in retinal pigment epithelium (RPE) cells (for both rods and cones) or in retinal Müller glia (for cones only). The 11-*cis* chromophore is then imported back into photoreceptors, where it combines with a molecule of free opsin to regenerate the visual pigment (Wang and Kefalov, 2011; Saari, 2012). The cone-specific visual cycle (Mata et al., 2002) has been suggested to enable cones, but not rods, to quickly recover from bright light exposure and to function over a wide range of light intensities (Wang and Kefalov, 2009; Wang et al., 2009; Kolesnikov et al., 2011). While an active area of research (Kaylor et al., 2013, 2014), to date none of the putative molecular components in this pathway have been shown to actually affect mammalian cone function, casting doubt on the significance of this pathway.

Cellular Retinaldehyde-Binding Protein (CRALBP) is a retinoid binding protein expressed in the RPE and Müller glia and believed to be involved in the retina visual cycle (Saari, 2012). CRALBP is a 36 kDa water-soluble protein with two conformational states facilitating the intracellular transportation of hydrophobic 11-*cis* retinoids (Liu et al., 2005). In zebrafish, two distinct orthologues, *cralbp a* and *cralbp b*, are expressed in RPE and Müller cells, respectively (Collery et al., 2008; Fleisch et al., 2008). Notably, knockdown of either of the

two isoforms leads to decreased cone-driven ERG responses (Fleisch et al., 2008), suggesting a role of the Müller cell-expressed CRALBP in zebrafish cone function (see also ref. (Babino et al., 2014)). In mammals, CRALBP is encoded by a single gene, *Rlbp1,* expressed in both RPE and Müller cells. Mutations in human *RLBP1* cause several autosomal recessive retinal diseases, such as autosomal recessive retinitis pigmentosa (Maw et al., 1997), Bothnia dystrophy (Burstedt et al., 1999, 2001, 2003), retinitis punctata albescens (Morimura et al., 1999), fundus albipunctatus (Katsanis et al., 2001; Naz et al., 2011), and Newfoundland rod-cone dystrophy (Eichers et al., 2002). These visual disorders are characterized by early-onset night blindness and may be followed by functional defects in the macular region (Thompson and Gal, 2003). CRALBP is required for the proper function of the RPE visual cycle and for the timely recovery of mammalian rod and cone ERG responses (Saari et al., 2001). However, the role of Müller cell-expressed CRALBP in the mammalian retina visual cycle is unknown. It is also not clear whether CRALBP in RPE, Müller cells, or both is required for the normal function of mammalian cones. Here, we used behavioral and electrophysiological assays in $Rlbp1^{-/-}$ mice to examine the overall effect of CRALBP deletion on M-cone function. We also used molecular tools to explore the mechanism by which the lack of CRALBP causes cone function deterioration. We then used adeno-associated virus (AAV)-mediated gene transfer to selectively restore CRALBP in RPE or Müller cells and examine the distinct roles of the two visual cycles in supporting mammalian M-cone function.

2.3 Experimental procedures

Animals. CRALBP-deficient mice (Saari et al., 2001) were kindly provided by John Saari (University of Washington, Seattle). To facilitate cone recordings, the CRALBP knockout mice were crossed with the rod transducin α knockout mice ($Gnat1^{-/-}$) (Calvert et al., 2000) obtained from Janis Lem (Tufts University, Boston) to eliminate rod responses. The role of CRALBP in cone function and morphology was then determined by comparing adult (6 weeks to 6 months old) control ($Gnat1^{-/-}$) and $Rlbp1^{-/-}$ (CRALBP-deficient $Gnat1^{-/-}$) mice. All mice used in this study were confirmed to be free of the *rd8* mutation (Mattapallil et al., 2012). For dark-rearing experiments, newborn mice were transferred to a lightproof cabinet and briefly exposed to ambient light only once a week during cage changing. All other mice were raised in 60 Lux 12:12 hour light-dark cycle. Animals were dark-adapted for 18 hours before electrophysiological recordings and at least 30 minutes prior to pupillary light reflex tests. The animals used for the optomotry tests were light-adapted before the experiment. In addition, $Rpe65^{-/-}$ ($Gnat1^{+/+}$) mice were used as control animals for pupillary light reflex and exogenous chromophore treatment experiments.

Photopic vision measured from optomotor responses. The threshold of contrast sensitivity was measured with a commercially available Optomotry® system (Cerebral Mechanics) as previously described (Kolesnikov et al., 2011). The intensity of the background light of the system was controlled with a custom-made cylinder of neutral density filter film, wrapped around the mouse stand. The contrast sensitivity threshold at a 0.128 cycles/degree grating spatial frequency was measured by an automated computer program when mice failed to provide optomotor responses. The tests started from brightest (1.84 Log cds m^2) to dimmest (-

3.56 Log cds m^2) background light intensity. Intriguingly, we observed that two of the tested CRALBP-deficient *Gnat1*$^{-/-}$ mice (*Rlbp1*$^{-/-}$) did not respond normally to the moving bar in the test and instead rotated their head to the direction opposite to the moving bar. Therefore, we excluded the results from these two mice from our analysis.

Electrophysiology. See Chapter 1.3. Common Experimental Procedures.

For exogenous chromophore application experiments, 300 μg 9-*cis* retinal was dissolved in 200 μL NaCl/BSA (bovine serum albumin) solution (with 10% ethanol) and administered by intraperitoneal injection. The treated animals were dark-adapted overnight prior to in vivo ERG recordings. In addition, 300 μg 11-*cis* retinal was dissolved in 4 mL 0.01% ethanol Locke's solution, and an isolated retina was incubated with 0.5-1 ml of that solution for 1 hour in darkness. Cone responses from the treated retinas were then obtained using transretinal recordings.

Frozen sections. Eyes were fixed in 4% paraformaldehyde in phosphate buffered saline (PBS) for 2 hours at room temperature, rinsed with PBS, and then cryoprotected in 30% sucrose. The lens was removed prior to embedding in Tissue-Tek OCT compound (Sakura). Frozen blocks were cryosectioned at a thickness of 12-14 μm. For immunohistochemical staining, sections were blocked for ~1 hour at room temperature, followed by overnight incubation at 4 ℃ with primary antibody, except for anti-CRALBP, which was incubated for 2 hours at room temperature. The following primary antibodies were used: rabbit anti-red/green cone opsin (Millipore AB5405) at 1:600, rabbit anti-blue cone opsin (Millipore AB5407) at 1:200, and rabbit anti-CRALBP (UW55 polyclonal antibody isolated from rabbits immunized with human recombinant CRALBP, gift from John Saari, University of Washington, Seattle (Saari et al.,

2001, 2009)) at 1:200. The following fluorescently labeled secondary antibodies were used, respectively: AlexaFluor 555 donkey anti-rabbit (Molecular Probes A-31572) at 1:800, AlexaFluor 488 donkey anti-rabbit (Molecular Probes A-21206) at 1:500, and AlexaFluor 555 donkey anti-rabbit (Molecular Probes A-31572) at 1:800. Secondary antibodies were applied for 30 minutes at room temperature, followed by DAPI staining, application of Vectashield (Vector Labs), and coverslipping. The following blocking solutions were used: 0.1% Triton X-100 and 5% normal donkey serum in PBS for staining of opsins, and 0.5% Triton X-100 and 2% normal donkey serum in PBS for staining of CRALBP. Primary and secondary antibodies were diluted in block. Slides were stored at -20 ℃ until imaging. Images were taken as multi-plane captures using an Olympus BX61WI microscope and Hamamatsu ORCA-AG CCD camera and processed with MetaMorph software and Adobe Photoshop, except for Figure 2.6E and 2.6F, which were taken as single-plane captures using an Olympus BX51 microscope and Olympus DP70 camera and processed with SlideBook software and Adobe Photoshop.

Whole mount immunostaining. Retinas were dissected in PBS with the lens intact, fixed for 30 minutes at room temperature with 4% paraformaldehyde in PBS, and rinsed with PBS prior to removal of the lens. Retinas were blocked for ~1 hr at room temperature, followed by overnight incubation at 4 ℃ with primary antibody. The following primary antibodies were used: rabbit anti-red/green cone opsin (Millipore AB5405) at 1:500 and goat anti-blue opsin (Santa Cruz sc-14363) at 1:500. The following fluorescently labeled secondary antibodies were used, respectively: AlexaFluor 555 donkey anti-rabbit (Molecular Probes A-21206) at 1:800 and AlexaFluor 488 donkey anti-goat (Molecular Probes A-11055) at 1:800. Secondary antibodies were applied for 30 min at room temperature. The following blocking solution was used: 0.5% Triton X-100 and 2% normal donkey serum in PBS. Primary and secondary antibodies were

diluted in block. Retinas were stored light-protected in PBS at 4 ℃ until imaging, whereupon

they were whole-mounted with glass shards at the corners of the slide and coverslipped.

Cone quantification. Whole mounted retinas were imaged using 10X objective lens with

an Olympus BX51 microscope and Olympus DP70 camera as single-plane captures. Image files

were annotated in Adobe Photoshop with dots to mark opsin staining. The dots were quantified

using the "Analyze Particles" feature in ImageJ. Quantification was conducted in 170 μm x 170

μm fields located in the dorsal, nasal, temporal, and ventral quadrants.

AAV vector preparation and injection. Four types of AAV vectors were used for the

injection: shH10-scCAG-Rlbp1 (expressing CRALBP in Müller cells, Müller-CRALBP), 7m8-

scVMD2-Rlbp1 (expressing CRALBP in RPE cells, RPE-CRALBP), shH10-scCAG-GFP

(expressing GFP in Müller cells, GFP control) and 7m8-scVMD2-GFP (expressing GFP in RPE

cells, GFP control). The Müller glia-specific viruses (shH10-scCAG-Rlbp1/GFP) were

constructed using a Müller glia-specific AAV serotype shH10 and the ubiquitous synthetic CAG

promoter (Klimczak et al., 2009). The RPE-specific viruses (7m8-scVMD2-Rlbp1/GFP) were

built using a pan-retinally expressing AAV serotype 7m8 and a RPE specific promoter VMD2

(Esumi et al., 2004; Dalkara et al., 2013). To generate the scCAG-Rlbp1 viral transfer plasmid,

Rlbp1 was reverse-transcribed from purified wild type mouse retina total mRNA. Then the GFP

open reading frame of a self-complementary AAV vector expressing GFP under CAG promoter

control was replaced with the Rlbp1 cDNA using restriction enzymes. This plasmid was then

further processed to generate the scVMD2-Rlbp1 transfer plasmid through the replacement of the

CAG promoter with the PCR purified VMD2 promoter. The control scCAG-GFP and scVMD2-

GFP viral plasmids were created using the same process without the replacement of the GFP

open reading frame. For the generation of each virus, 293T cells at 80% confluence were

cotransfected with the appropriate transfer plasmid, pHelper plasmid, and the AAV rep/cap plasmid (shH10 or 7m8) in a molar ratio of 1:1:1. At 72 hours after transfection, cells were collected, pelleted, resuspended in lysis buffer, freeze–thawed, and then treated with Benzonase. Cell debris was removed by centrifugation, and the supernatant was loaded onto an iodixanol gradient and subjected to ultracentrifugation. The 40% virus-containing iodixanol fraction was removed from the gradient, and the iodixanol was replaced via buffer exchange using Amicon Ultra-15 Centrifugal units in PBS. Titers were determined by quantitative PCR relative to a standard curve (Aurnhammer et al., 2012). An aliquot of 1 - 1.5 µL of the virus was injected into the vitreous of anesthetized 4 week old mice using a Hamilton syringe. Animals were harvested 4-5 weeks after the injection for cone electrophysiology experiments, and 8 weeks after the injection for immunohistochemistry.

Pupillary light reflex. All mice were awake and manually restrained while a 480 nm LED light was directed to one eye (the left eye). The light stimulus lasted for 30 seconds, after which the mouse was returned to its cage to dark-adapt until to the next light stimulus. Individual frames of the movie were taken from VLC Media Player. The images were analyzed in ImageJ. Pupil area in darkness and following 30 seconds of light exposure were compared to generate a ratio. For dose-response curves, the data were fitted with a variable slope sigmoidal dose response curve with the top constrained to 1.0 and the bottom constrained between 0 and 0.1.

Statistical analysis. See Chapter 1.3 Common Experimental Procedures.

Study approval. The maintenance and treatment of the animals followed the protocols approved by Washington University Animal Studies Committee.

2.4 Results

The deletion of CRALBP suppresses mammalian cone visual function

In addition to causing well-documented rod-driven scotopic visual disorders (Morimura et al., 1999; Burstedt et al., 2001), mutations in CRALBP also disrupt cone-driven photopic vision in humans (Maw et al., 1997; Eichers et al., 2002; Burstedt et al., 2003). It is believed that the pathophysiology for both rods and cones is based on inefficient chromophore recycling (Maw et al., 1997; Burstedt et al., 1999). However, the exact mechanisms of cone dysfunction in CRALBP-related diseases, and the relative contributions of the RPE visual cycle and the retina visual cycle to cone dark adaptation, are unknown. To address these questions, we first examined how the deletion of CRALBP affects the cone-driven photopic visual performance of CRALBP knockout mice by optomotor response behavioral tests. All functional experiments were performed with knockout mice lacking the rod transducin alpha subunit ($Gnat1^{-/-}$). This facilitated the isolation of cone function by ablating rod photoresponses while preserving normal retina morphology and cone function (Calvert et al., 2000; Kolesnikov et al., 2011). The experiments were performed with LCD monitor white light which would be expected to selectively activate mouse M-cones (peak absorption at 508 nm) but not S-cones (peak absorption at 360 nm) (Nikonov et al., 2006). We found that the background light intensity required to achieve half-maximal cone-driven contrast sensitivity of 6-week old $Rlbp1^{-/-}$ mice was ~10-fold higher than in controls (-0.4 and -1.3 Log cds m^{-2}, respectively). Thus, the absence of CRALBP caused a substantial desensitization of cone-driven vision.

We then asked whether the vision loss observed at a behavioral level was caused by the deterioration of cone function in the absence of CRALBP. We conducted in vivo ERG recordings to examine the dark-adapted cone b-wave responses of 6- to 13-week old $Rlbp1^{-/-}$

36

mice. We used 530 nm LED flashes to selectively excite M-cones (Nikonov et al., 2006) up to the system's 25 cds m^{-2} intensity limit, and Xenon flash for higher intensities. We observed a significant 40% ($p < 10^{-4}$) decrease of maximal M-cone b-wave amplitude in $Rlbp1^{-/-}$ mice compared to both $Rlbp1^{+/+}$ (control) and $Rlbp1^{+/-}$ mice (Figure 2.1A & B). In addition, we found a dramatic 20-fold decrease in photopic sensitivity, as measured by the corresponding increase in $I_{1/2}$ (the flash intensity required to achieve half-maximal response) of the $Rlbp1^{-/-}$ cone b-wave responses (Figure 2.1B). Surprisingly, light sensitivity in the absence of CRALBP was diminished to such an extent that even the brightest light stimulus of the ERG system (697 cds m^{-2}, Xenon flash) could not generate a saturated photopic b-wave response (Figure 2.1B, red circles). In contrast, light sensitivity in $Rlbp1^{+/-}$ mice was comparable to that of control mice (Figure 2.1B, blue triangles, inset).

In the course of these recordings, we noticed that the older $Rlbp1^{-/-}$ mice had smaller cone b-wave amplitudes than young adult mice. We compared the ERG b-wave responses from 6-7 week and 13-16 week old mice to examine the long-term effect of CRALBP knockout on mouse photopic vision. In control animals, cone b-wave amplitude showed ~10% (not significant, N.S.) reduction with age (Figure 2.1C). In contrast, the cone b-wave amplitude of $Rlbp1^{-/-}$ mice decreased by nearly 50% ($p < 0.001$) over the same two-month period (Figure 2.1D). The light sensitivity, as estimated from the $I_{1/2}$ of the respective normalized intensity-response curves, remained unchanged for both groups within the 2 months of aging (Figure 2.1C & D, insets). Thus, the deletion of CRALBP caused a dramatic and progressive reduction in cone-driven visual performance.

Figure 2.1. The deletion of CRALBP reduces photopic in vivo ERG response amplitude and sensitivity. (A) Representative in vivo cone ERG responses from control (black traces), $Rlbp1^{-/-}$ (red traces), and $Rlbp1^{+/-}$ (blue traces) mice. Test flash intensities increased from 2.27 x 10^{-2} cds m^{-2} (bottom traces) to 697 cds m^{-2} (top traces) in steps of ~0.5 log-unit. (B) Ensemble-averaged cone b-wave intensity-response curves for control (n=10), $Rlbp1^{-/-}$ (n=12), and $Rlbp1^{+/-}$ mice (n=10). (C) Cone b-wave intensity-response curves for control mice of 6-7 weeks (filled squares, n=8) and 13-16 weeks (open squares, n=10) of age. (D) Cone b-wave intensity-response curves for $Rlbp1^{-/-}$ mice of 6-7 weeks (filled circles, n=6) and 13-16 weeks (open circles, n=6) of age. Insets in B-D show the corresponding normalized intensity-response curves. Results are shown as mean ±SEM.
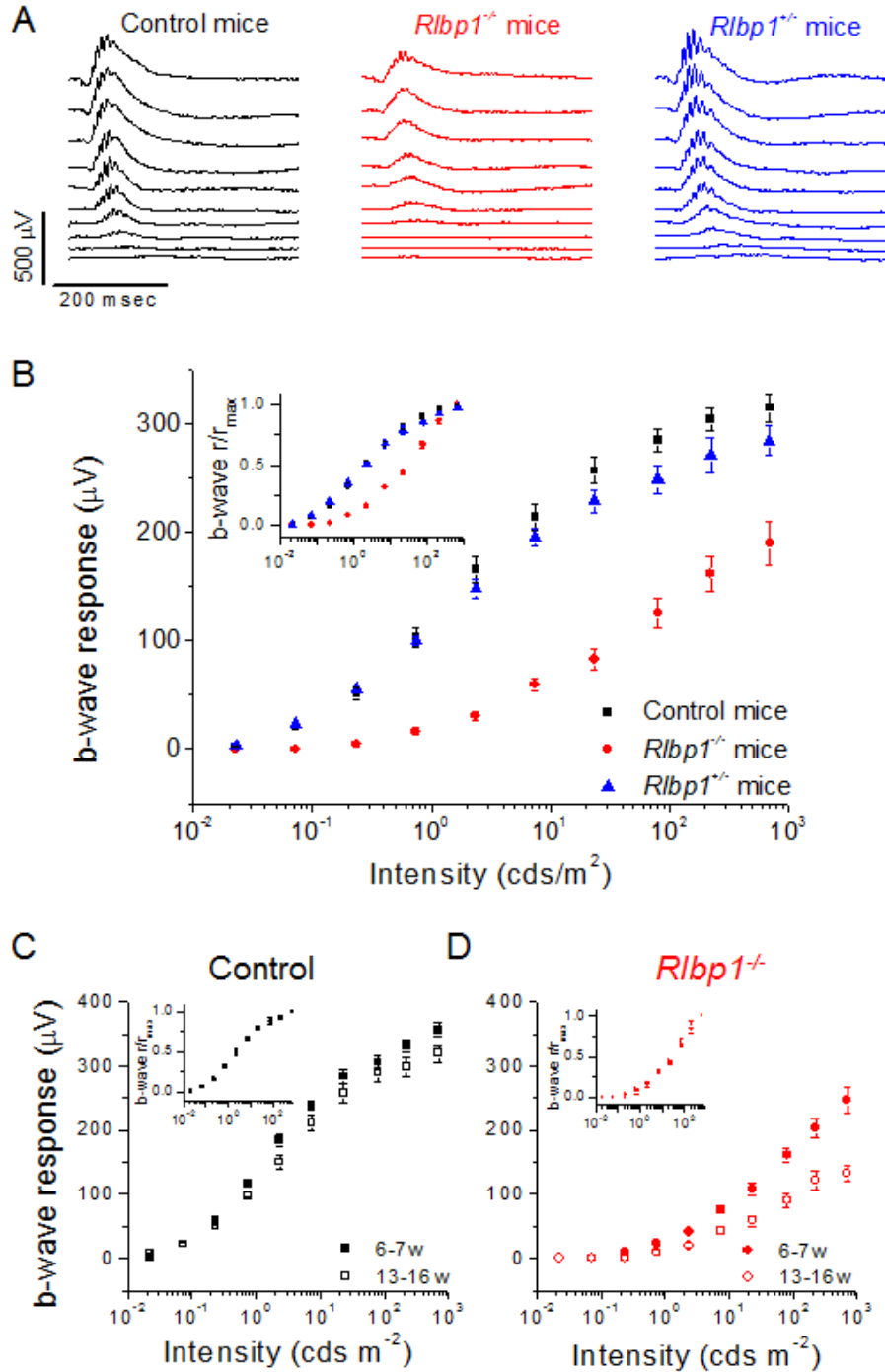
The deletion of CRALBP desensitizes mammalian cones and lowers their phototransduction amplification

The reduced photopic b-wave amplitude and sensitivity of CRALBP-deficient mice could be caused by a deficit either in cone phototransduction or in cone-to-bipolar cell synaptic transmission. To distinguish between the two possibilities, we determined whether cone phototransduction was affected directly by the deletion of CRALBP by performing ex vivo recordings from isolated retina. This technique allowed us to pharmacologically block synaptic transmission (see Methods) and isolate the cone (a-wave) response. We used 505 nm LED flash light to stimulate the M-cones in these recordings. Similar to the in vivo ERG b-wave results above, the ex vivo transretinal responses from $Rlbp1^{-/-}$ cones were smaller than those from control cones, with more than 50% ($p < 0.05$) decrease in maximal amplitude (Figure 2.2A & B). Indicative of their reduced sensitivity, the responses of $Rlbp1^{-/-}$ M-cones could not be saturated even at the maximal possible light intensity of our system (Figure 2.2B). The analysis of their corresponding intensity-response functions showed a 20-fold lower sensitivity (higher $I_{1/2}$) compared to control cones (Figure 2.2B, inset). The absence of CRALBP also resulted in somewhat accelerated cone response inactivation (Figure 2.2C). In addition, consistent with their reduced light sensitivity, CRALBP-deficient cones had a 9-fold smaller phototransduction amplification compared to control cones (Figure 2.2D), revealed by the corresponding scaling factor required to match the rising slopes of the fractional dim flash responses to 103 photons μm^{-2} for control cones and 1,387 photons μm^{-2} for $Rlbp1^{-/-}$ cones. Taken together, these results demonstrate that the deletion of CRALBP in mice leads to severe desensitization and altered cone phototransduction in dark-adapted M-cones, which in turn produces a desensitized cone b-wave and suppressed cone-mediated vision.

Figure 2.2. The deletion of CRALBP reduces transretinal cone response amplitude and sensitivity. (A) Representative transretinal cone responses from control (left panel) and *Rlbp1*^{-/-} (right panel) retinas. Test flash intensities increased from 23 photons μm^{-2} to 1.40×10^6 photons μm^{-2} in steps of 0.5 log-units. For both panels, the flash intensity producing the response shown in red was 1.39×10^4 photons μm^{-2}. (B) Ensemble-averaged absolute and normalized (inset) cone intensity-response curves for control (n=13) and *Rlbp1*^{-/-} (n=13) retinas. (C) Ensemble-averaged normalized cone dim flash responses from control (n=12) and *Rlbp1*^{-/-} (n=13) retinas. (D) Ensemble-averaged dim flash responses from control (n=13) and *Rlbp1*^{-/-} (n=11) cones normalized to r_{max} and flash intensity and with matched rising slopes to determine the change in phototransduction amplification. Results are shown as mean $\pm$ SEM.

40
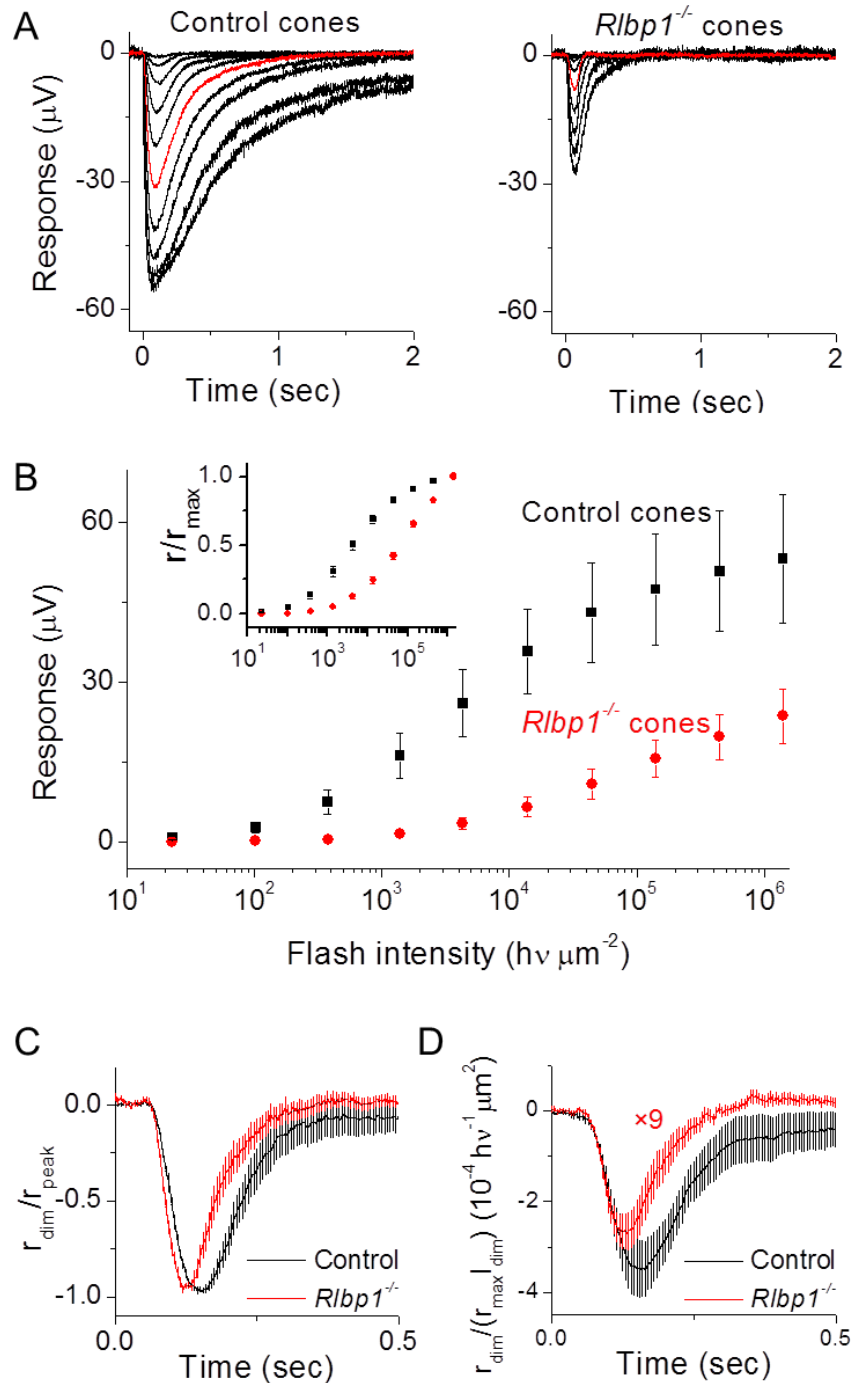
The deletion of CRALBP severely impairs mammalian cone dark adaptation

We next sought to determine the effect of CRALBP deletion on the RPE and retina visual

cycles in the context of cone dark adaptation. First, we determined the overall effect of CRALBP

deletion on cone dark adaptation. Using in vivo ERG recordings, we examined the cone b-wave

sensitivity recovery of control and *Rlbp1*^{-/-} mice following exposure to a brief bright green light

estimated to photoactivate (bleach) 90% of the M-cone visual pigment (see Methods for details).

As expected, cone b-wave sensitivity in the control mice underwent robust recovery following

the bleach, and returned within 50 minutes to an estimated 50% of the prebleach level (Figure

2.3A, black squares). An incomplete photoreceptor dark adaptation following a bleach in ERG

recordings from wild type mice is not unusual (Kolesnikov et al., 2011), and is most likely

caused by the general anesthetics (Keller et al., 2001). In striking contrast to the ERG response

recovery in controls, M-cones in *Rlbp1*^{-/-} mice recovered only a slight fraction of their sensitivity

following an identical bleach (Figure 2.3A, red circles). Thus, cone dark adaptation in vivo,

driven through the combined action of the RPE and Müller cell visual cycles, was severely

compromised by the deletion of CRALBP. Notably, the effect of CRALBP deletion on the

recovery of cone sensitivity was more pronounced than the previously reported delay in recovery

of cone b-wave response amplitude (Saari et al., 2001).

Next, to determine the specific effect of CRALBP deletion on the Müller cell visual

cycle, we performed cone dark adaptation experiments in retina dissected free of RPE, in which

cone pigment regeneration can be driven only by the retina visual cycle. Following an initial

>100-fold desensitization caused by the bleach, within seconds, cones in both control and *Rlbp1*^{-}

[/-] retinas showed a rapid initial increase of sensitivity (Figure 2.3B). This partial recovery, which

was most likely due to the inactivation of the phototransduction cascade following the bleach,

was comparable in the two mouse strains. However, the *Rlbp1*$^{-/-}$ cone sensitivity failed to recover further during the 12 minutes of postbleach recordings, while control cones recovered to within 5-fold of their pre-bleach level (Figure 2.3B). We conclude that the deletion of CRALBP has a dramatic effect on the ability of the retina visual cycle to promote mouse cone dark adaptation. Taken together, these results demonstrate that CRALBP plays a role in both the RPE and the retina visual cycles and that its deletion severely impairs the ability of both pathways to promote mammalian cone dark adaptation.

Figure 2.3. The deletion of CRALBP suppresses cone dark adaptation. (A) Normalized cone b-wave sensitivity (b-wave S_f / b-wave S_f^{DA}) from in vivo ERG recordings during dark adaptation following 90% pigment bleach at t=0 for control (n=10) and *Rlbp1$^{-/-}$* (n=10) mice. (B) Normalized cone sensitivity (S_f / S_f^{DA}) from transretinal recordings during dark adaptation following 90% pigment bleach at t=0 for control (n=9) and *Rlbp1$^{-/-}$* (n=10) isolated retinas. Results are shown as mean $\pm$ SEM.
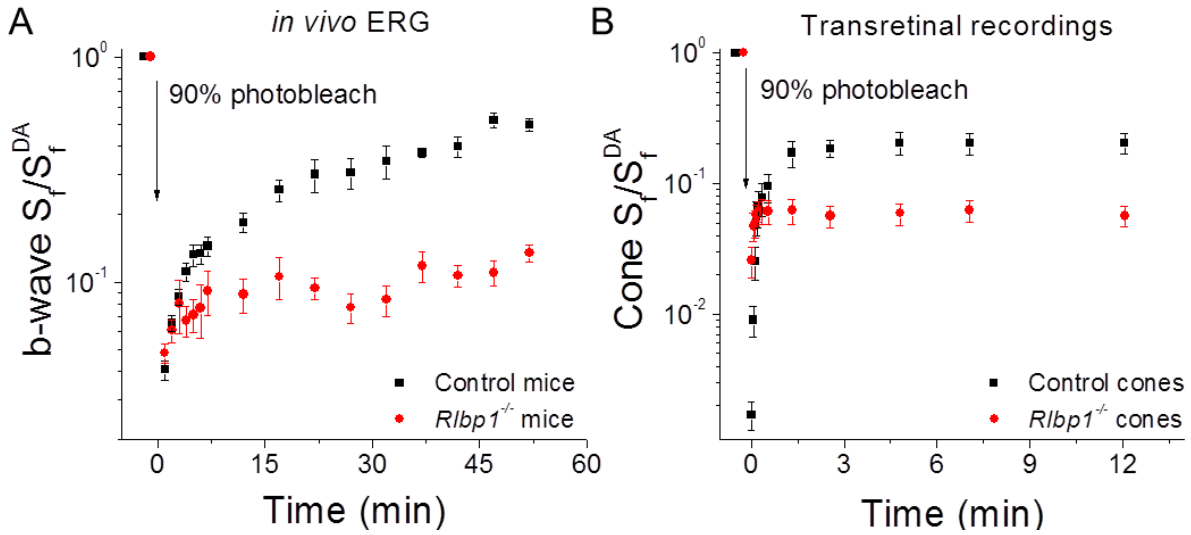
Dark rearing of CRALBP-deficient mice restores cone function but not cone dark adaptation

It is believed that the role of CRALBP in both the RPE and retina visual cycles is to accelerate the production of 11-*cis* retinoid (Saari, 2012). We hypothesized that in the absence of CRALBP, both visual cycles would still remain functional but would fail to provide sufficient chromophore for sustaining normal cone function in 12:12 hour cyclic-light conditions. To test this idea, we first attempted to restore cone function in *Rlbp1$^{-/-}$* mice by supplying them with exogenous chromophore in order to regenerate any free cone opsin into visual pigment. However, the application of either 9-*cis* retinal in vivo (Figure 2.4A) or 11-*cis* retinal ex vivo (Figure 2.4B) failed to rescue M-cone sensitivity. In contrast, treatment of chromophore-deficient *Rpe65$^{-/-}$* retinas with exogenous 11-*cis* retinal ex vivo and application of 9-*cis* retinal to *Rpe65$^{-/-}$* mice in vivo resulted in a robust increase in rod sensitivity and maximal response (data not shown), as previously reported (Ablonczy et al., 2002; Rohrer et al., 2003). These results demonstrate that free opsin is not present in *Rlbp1$^{-/-}$* cones at detectable amounts, and therefore is not the cause for the reduced sensitivity and response amplitude of cones in CRALBP-deficient mice.

We next examined whether the suppressed M-cone function in CRALBP knockout mice is caused by a long-term chromophore deficiency. We raised *Rlbp1$^{-/-}$* newborn mice in near-complete darkness to substantially slow down the consumption of chromophore in their eyes and lower the demand for recycled chromophore by the cones. It was recently shown that raising mice in complete darkness leads to an eventual decline in cone-to-bipolar cell synaptic transmission (Dunn et al., 2013). However, the occasional brief exposure to room light during routine animal care was sufficient to maintain normal cone function in our control mice and

resulted only in a slight increase in the maximal amplitude of their in vivo ERG b-wave response (Figure 2.4C). Importantly, the photopic b-wave sensitivity of control mice, as measured from their normalized intensity-response curve, was unchanged by the dark rearing (Figure 2.4C, inset). In contrast, raising $Rlbp1^{-/-}$ mice in darkness not only restored cone b-wave maximal response (Figure 2.4D), but also boosted cone sensitivity to the level of control cones (Figure 4D, inset). However, a subsequent exposure to bleaching light unmasked the deficiency in cone pigment regeneration, as the dark adaptation in CRALBP-deficient mice was identical for animals raised in darkness and in cyclic light (Figure 2.4E). Together, these results demonstrate that the dark rearing of $Rlbp1^{-/-}$ mice slows down the consumption of chromophore enough to preserve cone function. However, dark rearing alone does not address the underlying deficit in the RPE and/or retina visual cycles.

Figure 2.4. Dark rearing but not acute treatment with exogenous chromophore rescues CRALBP-deficient cone sensitivity. (A) Normalized in vivo ERG cone b-wave intensity-response curves for untreated control (replotted from Figure 2.2B inset) and 9-*cis* retinal treated (n=6) *Rlbp1*$^{-/-}$ mice. (B) Normalized transretinal cone intensity-response curves for control (black, n=6) and *Rlbp1*$^{-/-}$ (red, n=6) retinas in control solution (filled symbols; replotted from Figure 2.3B inset) and after treatment with exogenous 11-*cis* retinal (open symbols, n=6). 9cRal, 9-*cis* retinal; 11cRal, 11-*cis* retinal. (C) Cone b-wave intensity-response curves from in vivo ERG recordings for control mice raised in cyclic light (filled squares, n=14) and in darkness (open squares, n=10). (D) Cone b-wave intensity-response curves from in vivo ERG recordings for control (black squares; replotted from Figure 2.1B) and *Rlbp1*$^{-/-}$ mice raised in cyclic light (red filled circles; replotted from Figure 2.1B), and *Rlbp1*$^{-/-}$ mice raised in darkness (open red circles, n=10). Insets in A and B show the corresponding normalized intensity-response curves. (E) Normalized cone b-wave sensitivity (b-wave S_f / b-wave S_f^{DA}) from in vivo ERG recordings during dark adaptation following 90% pigment bleach at t=0 for control (black squares) and *Rlbp1*$^{-/-}$ mice raised in cyclic light (filled red circles; replotted from Figure 2.3A), and for *Rlbp1*$^{-/-}$ mice raised in darkness (open red circles, n=10). Results are shown as mean ± SEM.
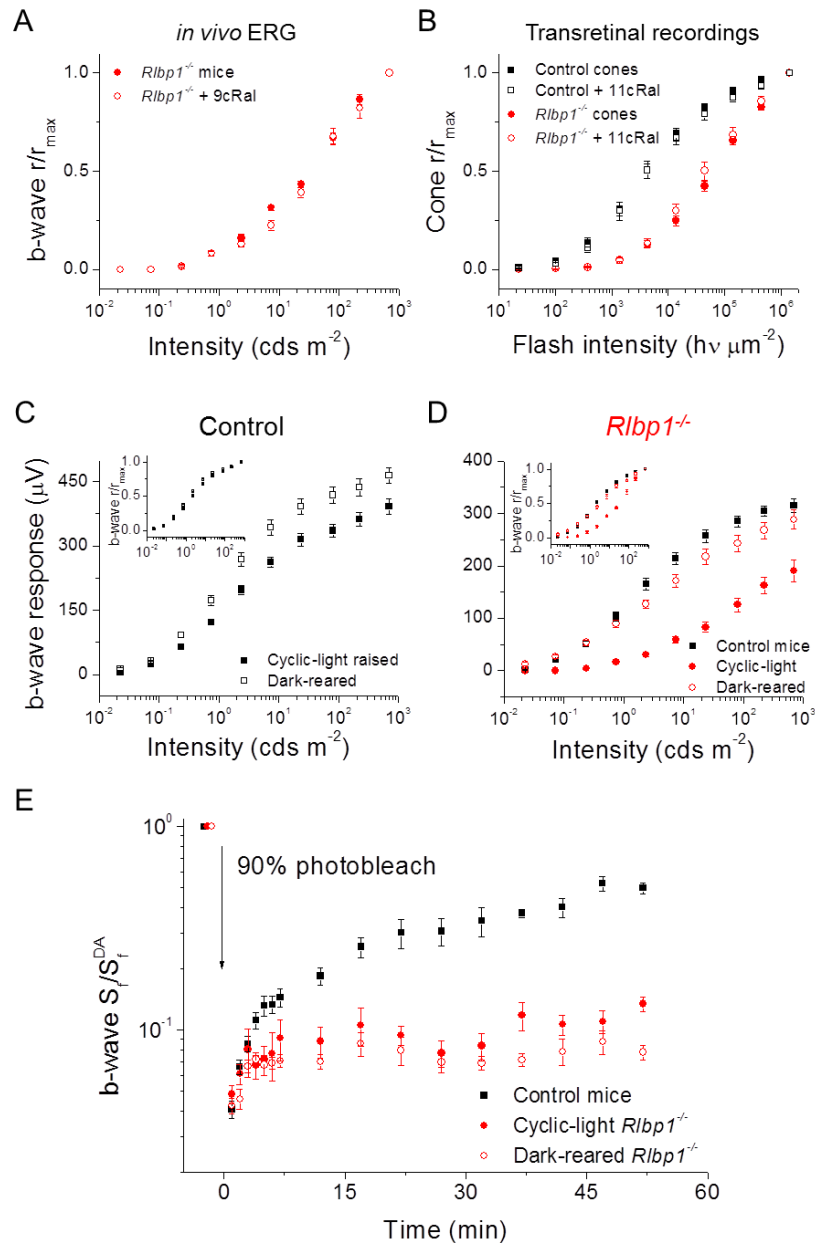
The deletion of CRALBP induces M-opsin mislocalization and loss of M-cones

What is the molecular mechanism underlying the functional deterioration in CRALBP-deficient cone? Based on the physiological results above, we hypothesized that CRALBP was required for proper localization of opsin protein. To test this hypothesis, we stained frozen sections from $Rlbp1^{-/-}$ and control retinas with cone opsin antibodies. Whereas M-opsin was localized to the cone outer segment of control retinas as expected, we observed striking mislocalization of M-opsin to the cone cell bodies, axons, and pedicles of young (6 week old) and old (4 to 6 months) $Rlbp1^{-/-}$ mice raised conventionally in cyclic light-dark conditions. Intriguingly, dark-rearing of $Rlbp1^{-/-}$ appeared to ameliorate M-opsin mislocalization to some extent (Figure 2.5A), consistent with the physiology results above. In contrast to M-opsin, S-opsin was appropriately localized to the cone outer segment in the retinas of both $Rlbp1^{-/-}$ mice and controls (Figure 2.5B). We also wondered whether the M-opsin mislocalization in $Rlbp1^{-/-}$ retinas was correlated with M-cone number. Quantification of whole mount antibody staining revealed a lower density of M-opsin-expressing cones in the dorsal retina of $Rlbp1^{-/-}$ mice compared to age-matched controls (Figure 2.5C), whereas the density of S-opsin expressing cones was not affected (Figure 2.5D). Thus, the deletion of CRALBP resulted in both mislocalization of M-opsin and M-cone loss. However, overall the cone density in $Rlbp1^{-/-}$ retinas did not change markedly with age, suggesting that the observed age-dependent decline in cone function was caused by progressive deterioration in the light responses of individual M-cones.

Figure 2.5. The deletion of CRALBP affects the localization of M-opsin and number of cones expressing M-opsin. Antibody staining of retinal frozen sections from *Rlbp1*^{-/-} and control mice for (A) M-opsin and (B) S-opsin. Representative images are shown. At least 3 retinas per condition were examined. Scale bar, 25 μm. COS, cone outer segment; ONL, outer nuclear layer; OPL, outer plexiform layer. For clarity, DAPI channel is not shown. (C) Quantification of whole mount M-opsin antibody staining (n = 4 retinas per condition). (D) Quantification of whole mount S-opsin antibody staining (n = 3 retinas per condition). D, dorsal; T, temporal; N, nasal; V, ventral. Young, 6-7 weeks old; Old, 3 to 6 months old. Results are shown as mean ± SEM. N.S., not significant. * p<0.05, ** p<0.01, two-tailed unpaired student's t test.
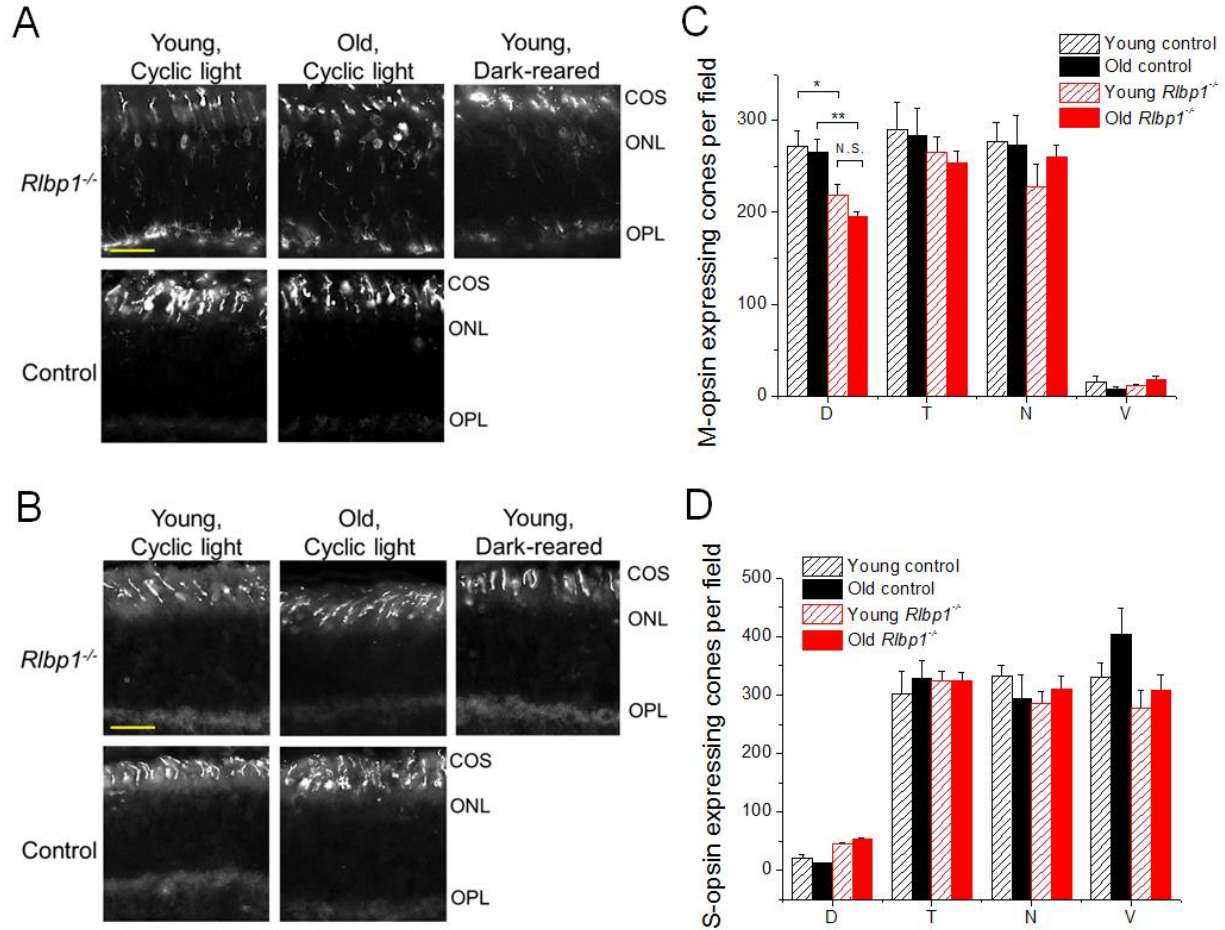
The retinal visual cycle is essential for cone function

In the above results, we demonstrated that CRALBP was crucial for maintaining normal M-cone function in cyclic-light environment and for proper cone dark adaptation. However, because in these experiments CRALBP was absent from both RPE and Müller cells, we were not able to determine the relative contribution of each visual cycle in maintaining normal cone function. To address this question, we used two separate AAV vectors to express CRALBP specifically in either RPE or Müller cells of adult $Rlbp1^{-/-}$ mice (see Section 2.3 for details). First, we verified that CRALBP was delivered via intravitreal AAV injection to the RPE (via the RPE-specific AAV construct, 7m8-scVMD2-Rlbp1) or to the Müller cells (via the Müller cell-specific AAV construct, shH10-scCAG-Rlbp1) in $Rlbp1^{-/-}$ retinas. As previously shown (Saari et al., 2001), antibody staining revealed robust CRALBP expression in the RPE and Müller cells of wild type mice (Figure 2.6A) and its complete absence in $Rlbp1^{-/-}$ eyes (Figure 2.6B). Notably, immunohistochemistry revealed expression of CRALBP specifically in the targeted cell type for both AAV constructs (Figure 2.6C & D). Moreover, the extent of intravitreal AAV infection appeared to be widespread, as demonstrated by the CRALBP expression in the targeted cell type along the length of the retina (Figure 2.6E & F).

Figure 2.6. The AAV-mediated delivery of CRALBP to Müller cells or RPE cells. Antibody staining shows expression pattern of CRALBP in (A) control retina, (B) *Rlbp1⁻ᐟ⁻* retina, (C) Müller cells of *Rlbp1⁻ᐟ⁻* retina after intravitreal injection with an AAV construct targeted for Müller cells, shH10-scCAG-Rlbp1, and (D) RPE of *Rlbp1⁻ᐟ⁻* retina after intravitreal injection with an AAV construct targeted for RPE, 7m8-scVMD2-Rlbp1. Scale bar, 50 μm. RPE, retinal pigmented epithelium; ONL, outer nuclear layer; INL, inner nuclear layer; GCL, ganglion cell layer. Widespread infection across the retina was achieved for both constructs, as seen in tiled images (scale bar, 200 μm) for (E) shH10-scCAG-Rlbp1 and (F) 7m8-scVMD2-Rlbp1. Red channel, anti-CRALBP. Blue channel, DAPI.
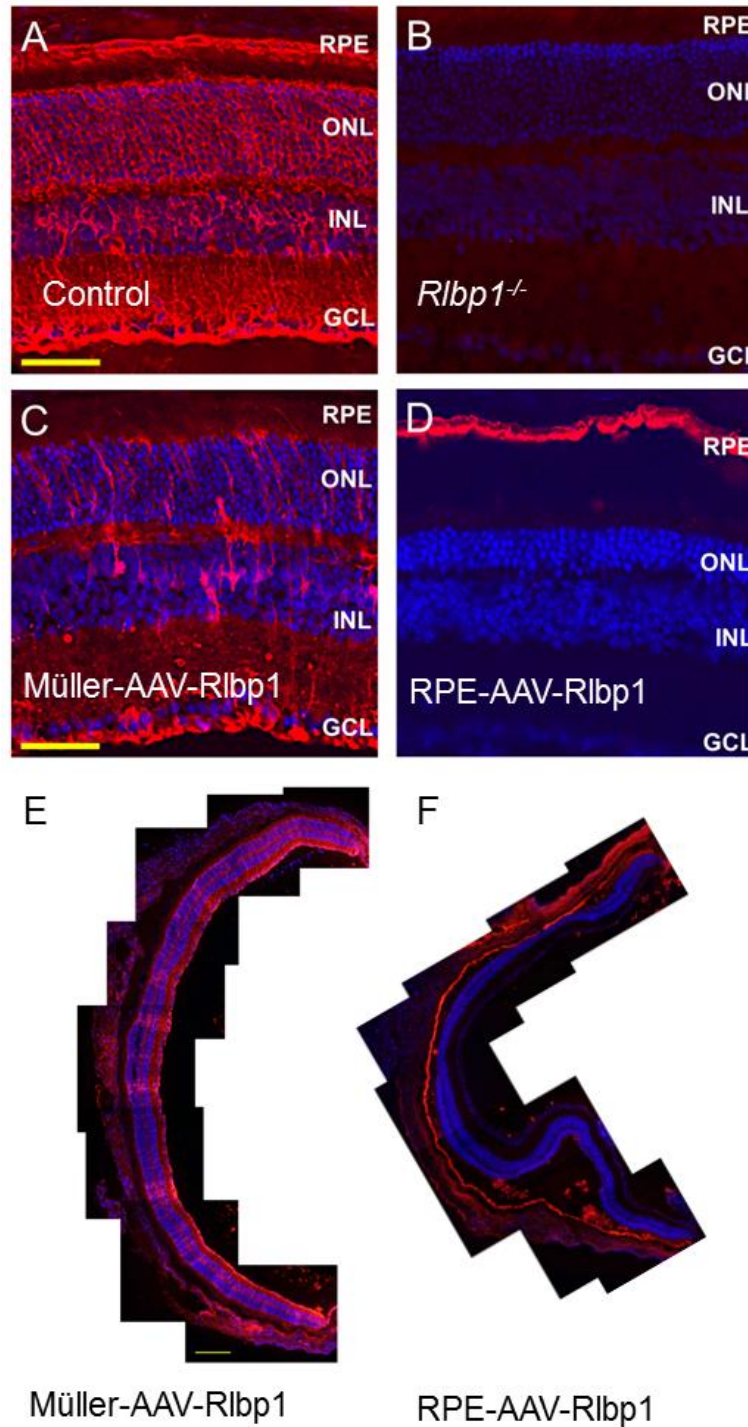
We then examined how the rescue of each visual cycle affected the dark-adapted function of M-cones, as well as their ability to recover light sensitivity rapidly following a bleach. The transretinal recordings revealed that dark-adapted cone sensitivity in Müller cell-CRALBP expressing $Rlbp1^{-/-}$ mice was improved by ~10-fold (Figure 2.7A), and the amplification of cone phototransduction was enhanced by 5.8-fold compared to controls (Figure 2.7B). In contrast, dark-adapted cone responses from RPE cell-CRALBP expressing $Rlbp1^{-/-}$ mice were indistinguishable from those of their AAV-GFP injected littermates (Figure 2.7A & B). This result demonstrates that the expression of CRALBP in Müller cells is required for the normal function of dark-adapted M-cones. The dim flash response kinetics, cone maximal response and cone b-wave maximal response were not affected by either RPE or Müller cell expression of CRALBP (data not shown), indicating an incomplete rescue of cone function. We also note that AAV-mediated CRALBP delivery to either the RPE or Müller cells failed to correct the M-opsin mislocalization defect (data not shown). Notably, in vivo cone dark adaptation was markedly improved by the AAV-mediated CRALBP rescue of either visual cycle with indistinguishable time courses (Figure 2.7C). In contrast, only the expression of CRALBP in the Müller cells resulted in the rescue of cone dark adaptation in the isolated RPE-free retina, whereas expression of CRALBP in the RPE had no effect on cone dark adaptation under these conditions (Figure 2.7D). Together, these results demonstrate the role of the retina visual cycle in supporting mammalian M-cone function and indicate that CRALBP in Müller cells plays a key role in this pathway.

51

Figure 2.7. AAV-driven expression of CRALBP in Müller cells rescues the sensitivity and dark adaptation of CRALBP-deficient cones. (A) Ensemble-averaged transretinal cone intensity-response curves for $Rlbp1^{-/-}$ mice injected with AAV driving expression of GFP in RPE or Müller cells (black squares, n=4), CRALBP in Müller cells (red circles, n=5), and CRALBP in RPE cells (green diamonds, n=3). (B) Transretinal dim flash responses of $Rlbp1^{-/-}$ mice showing the relative amplification for AAV-driven control GFP (black, n=4), Müller cell-specific CRALBP (red, n=5), and RPE-specific CRALBP (green, n=3) expression. (C) in vivo ERG recordings of cone b-wave dark adaptation (b-wave S_f / b-wave S_f^{DA}) following a 90% bleach of $Rlbp1^{-/-}$ mice with AAV-driven expression of control GFP (black, n=11), Müller cell-specific CRALBP (red, n=12), and RPE-specific CRALBP (green, n=8). (D) Transretinal recordings of cone dark adaptation (S_f / S_f^{DA}) following a 90% bleach of $Rlbp1^{-/-}$ retinas with AAV-driven expression of control GFP (black, n=4), Müller cell-specific CRALBP (red, n=5), and RPE-specific CRALBP (green, n=3). Results are shown as mean ± SEM.
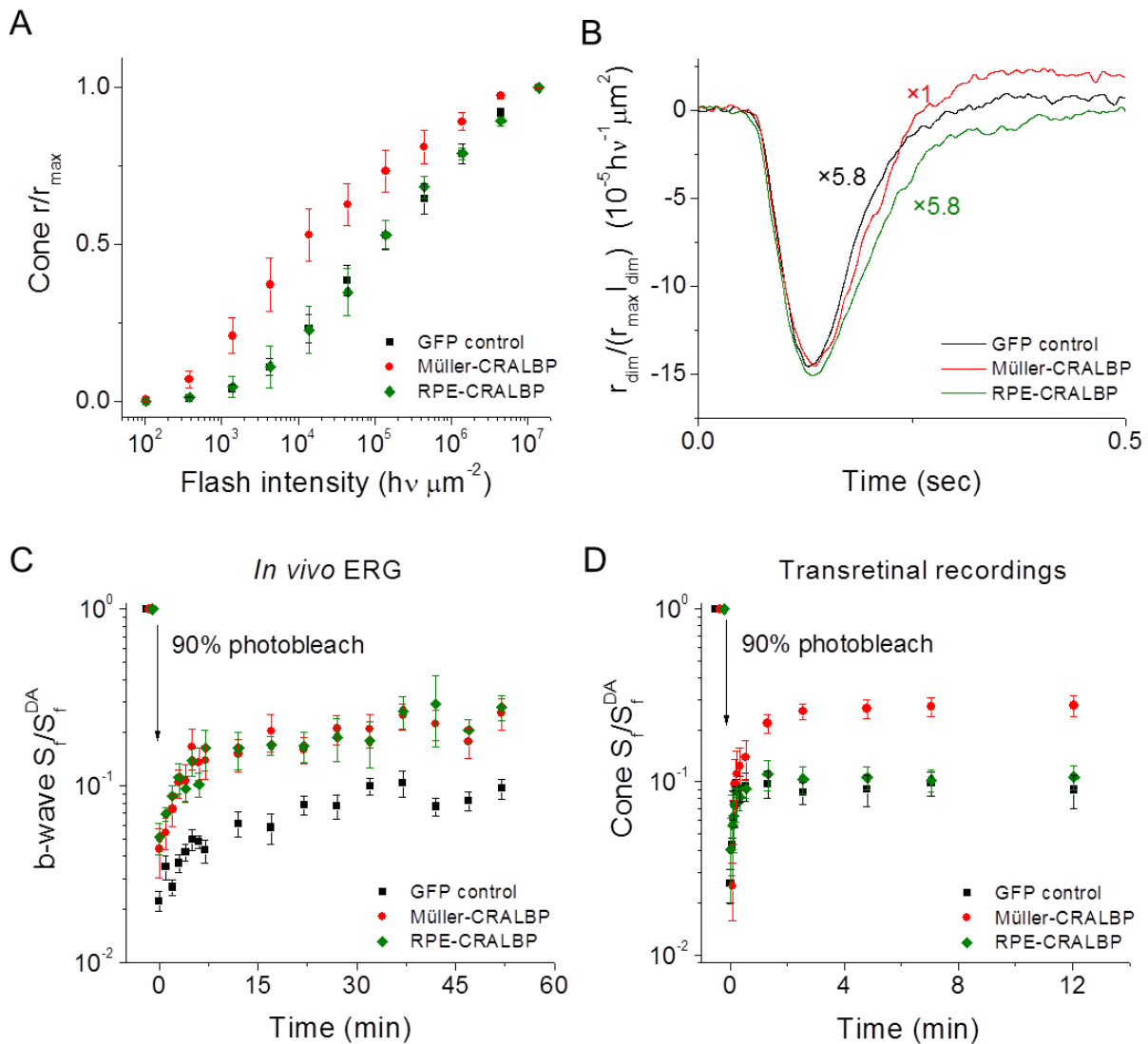
The deletion of CRALBP affects the pupillary light reflex

Besides rods and cones, another cell type in the retina that requires chromophore for its function is the intrinsically photosensitive retinal ganglion cells (ipRGCs) (Hattar et al., 2003). CRALBP in Müller cells was recently proposed to facilitate the supply of 11-*cis* retinal to the ipRGCs (Wong, 2013). We investigated this possibility by evaluating the effect of CRALBP deletion on the light-driven pupil constriction. Rods in both control and $Rlbp1^{-/-}$ mice do not respond to light due to the absence of GNAT1, and their pupillary light reflex is therefore mediated by the two remaining light-sensitive cell types in the retina, cones and ipRGCs (Xue et al., 2011). In melanopsin knockout animals that lack the melanopsin phototransduction but maintain normal cone function, there is a clear reduction in the magnitude of the pupillary light reflex, but only at high light intensities (Lucas et al., 2003). To determine whether melanopsin phototransduction is affected in the $Rlbp1^{-/-}$ mice, we exposed one eye to light and measured pupil constriction in the contralateral eye (Figure 2.8A). This enabled us to evaluate the overall sensitivity of the pupillary light reflex. Two-way ANOVA analysis showed an overall significant difference ($p < 0.001$) between the pupil constriction intensity-response curves of control and $Rlbp1^{-/-}$ mice. Further one-way ANOVA statistical analysis followed by Bonferroni correction on the p values at each intensity revealed significantly higher ($p < 0.05$) threshold for pupil constriction in $Rlbp1^{-/-}$ mice compared to controls (Figure 2.8B). The light intensity required to reach 50% constriction (EC_{50}) was also slightly higher in CRALBP-deficient mice compared to controls, but the difference was not statistically significant (Figure 2.8C). The maximal pupil constriction in bright light of $Rlbp1^{-/-}$ mice was comparable to that of controls suggesting that the function of ipRGCs is largely unaffected by the deletion of CRALBP (Lucas et al., 2003). In contrast, the maximal pupillary light reflex of $Rpe65^{-/-}$ mice, in which all photoreceptor function

is severely suppressed due to the lack of chromophore (Tu et al., 2006), was dramatically

reduced (Figure 2.8A & B). This analysis suggests that the pupillary light reflex is overall

different in $Rlbp1^{-/-}$ mice, with the difference restricted to relatively dim light levels, where the

pupil response is primarily driven by cone signals. The response at higher light intensities, which

is dominated by the ipRGC signals, was not affected by the deletion of CRALBP. Together,

these results indicate that CRALBP is not required for the delivery of chromophore to ipRGC

cells and the regeneration of melanopsin, and the decreased sensitivity of the pupillary light

reflex in $Rlbp1^{-/-}$ mice is most likely caused by the suppressed cone function. However, a

conclusive determination of this issue would require the generation of triple knockout animals

that lack both rod and melanopsin phototransduction pathways in addition to the $Rlbp1$ gene.

Figure 2.8. The deletion of CRALBP reduces the threshold of pupillary light reflex. (A) Comparison of pupil size in darkness and in the light (~14 log photons cm^{-2}s^{-1}) in control, *Rlbp1*$^{-/-}$ and *Rpe65*$^{-/-}$ (*Gnat1*$^{+/+}$) negative control mice. (B) Averaged intensity-response curves for control (n = 5), *Rlbp1*$^{-/-}$ (n = 5) and *Rpe65*$^{-/-}$ (n=4) mice. A significant difference was observed at threshold (* $p < 0.05$) between *Rlbp1*$^{-/-}$ and control mice by two-way ANOVA followed by Bonferroni's post-test. Results shown as mean ±SEM. (C) Intensity required to reach 50% constriction (EC$_{50}$) in control and *Rlbp1*$^{-/-}$ mice ($p = 0.10$, N.S., two-tailed unpaired student's t test).
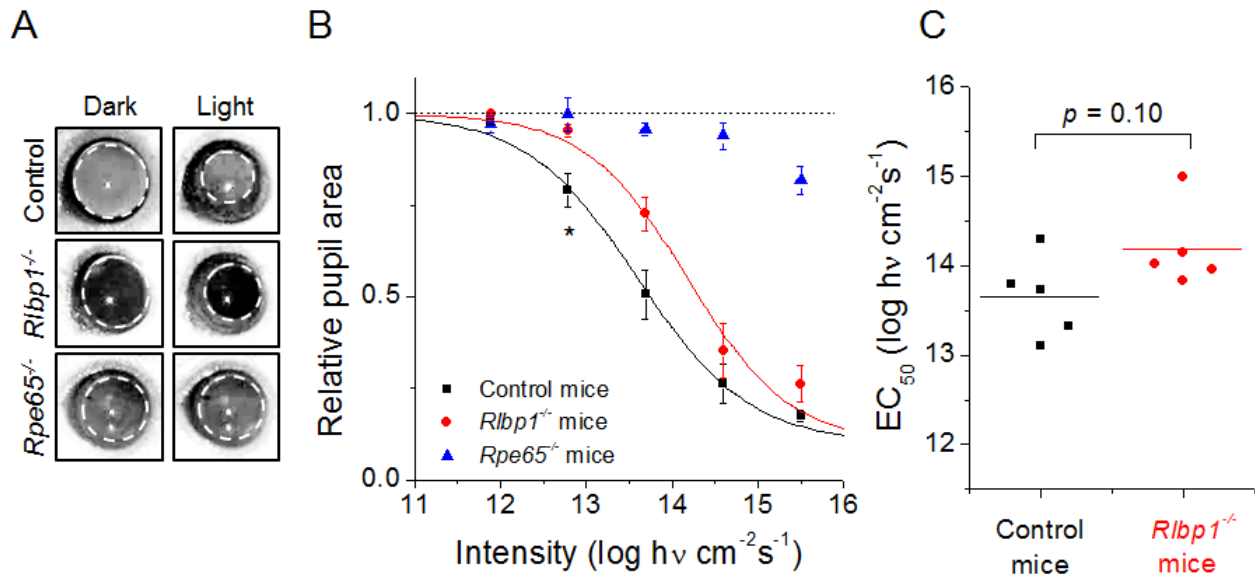
2.5 Discussion

Molecular evidence for the function of a mammalian retina visual cycle

The idea of a second, cone-specific visual cycle was first put forth in the 1970s (Goldstein, 1970) and has been gaining acceptance and experimental support in recent years (Mata et al., 2002; Muniz et al., 2009; Wang et al., 2009). This pathway was proposed to involve the conversion of spent all-*trans* retinol, released from cones, back into 11-*cis* retinol in the retinal Müller cells (Mata et al., 2002). Indeed, it was shown recently that the retina promotes pigment regeneration and dark adaptation in cones independently of the RPE, and that pharmacological ablation of Müller cells blocks this process (Wang and Kefalov, 2009). Recent biochemical studies have identified putative retinoid isomerase (Kaylor et al., 2013) and ester synthase activities (Kaylor et al., 2014) in Müller cells consistent with a retina visual cycle. However, the molecular mechanism involved in the trafficking and recycling of chromophore still remains largely unknown and skepticism still remains, partly due to the lack of experimental evidence for the involvement of any of the putative molecular players in this pathway in actually controlling the function of cones. Here, we settle this issue by demonstrating that the deletion of CRALBP in Müller cells prevents this pathway from promoting dark adaptation in mouse cones. Our results also reveal a previously unappreciated role of the retina visual cycle in the long-term maintenance of normal mammalian cone function.

The role of CRALBP in the retina visual cycle

We found that the deletion of CRALBP in mice resulted in a dramatic suppression of cone dark adaptation both in vivo, when driven by the combined action of the RPE and retina visual cycles (Figure 2.3A), and ex vivo, when driven only by the retina visual cycle (Figure

2.3B). Therefore, suppression of the RPE visual cycle by the deletion of CRALBP not only affects the rods as previously shown by Saari et al., 2001 (Saari et al., 2001), but also compromises the ability of the RPE to drive the dark adaptation of cones. More importantly, our results also clearly demonstrate that CRALBP in the Müller cells plays a similar role in the retina visual cycle to promote cone dark adaptation.

What is the mechanism of CRALBP function in the retina visual cycle? The rescue of cone function in dark-reared *Rlbp1*^{-/-} mice indicates that the deletion of CRALBP does not block the function of the retina visual cycle; rather, CRALBP likely regulates its efficiency or kinetics. In the RPE, CRALBP interacts with the isomerohydrolase to carry 11-*cis* retinol and facilitate its oxidation to 11-*cis* retinal (Saari and Crabb, 2005). A recent study suggests that in vitro CRALBP closely interacts with DES1, the proposed retinoid isomerase in Müller cells (Kaylor et al., 2013). Therefore, it is possible that CRALBP takes up 11-*cis* retinol from DES1 and facilitates the reisomerization of chromophore by the retina visual cycle. CRALBP also facilitates the release of chromophore from RPE cells and its subsequent uptake by photoreceptors (Bonilha et al., 2004; Nawrot et al., 2004). Thus, a second possibility is that CRALBP plays a similar role in Müller cells and accelerates the flow of chromophore to cones.

The influence of chromophore deficiency on cone function

Rods in CRALBP-deficient mice have normal sensitivity and maximal response after overnight dark adaptation (Saari et al., 2001). In striking contrast, dark-adapted cones in CRALBP-deficient mice have significantly reduced response amplitude and 20-fold lower sensitivity (Figure 2.1 & 2.2). Notably, this suppressed cone function can be rescued by raising the animals in darkness (Figure 2.4). This result indicates that unlike the other widely studied

57

chromophore-binding protein, IRBP (Jin et al., 2009; Parker et al., 2009), CRALBP is not required for the normal development and survival of cones. Instead, the preservation of normal cone function in dark-reared $Rlbp1^{-/-}$ mice suggests that the cone phenotype is caused by inadequate chromophore supply. One possibility is that the delayed recycling of chromophore in the absence of CRALBP leads to chronic chromophore deficiency, so that even after overnight dark adaptation of these mice, the pigment content of their cones is still not fully restored. However, considering that CRALBP-deficient rod responses are normal after 18 hours dark adaptation (Saari et al., 2001), it is unlikely that only cones would be affected by such incomplete dark adaptation. Indeed, our observation that application of exogenous chromophore failed to rescue cone function (Figure 2.4) rules out this possibility.

An alternative hypothesis is that the chronic deficiency of chromophore affects the cone opsin level. Evidence for this notion comes from studies of a key enzyme in the RPE visual cycle, RPE65. In contrast to the slowed down RPE visual cycle in $Rlbp1^{-/-}$ mice, $Rpe65^{-/-}$ mice lack this pathway completely and are unable to supply chromophore to their photoreceptors (Redmond et al., 1998). This results in mislocalization of cone opsin and very rapid degeneration of the cones (Znoiko et al., 2005; Jacobson et al., 2007), attributed to chromophore deficiency (Znoiko et al., 2005; Cottet et al., 2006). Consistent with the role of chromophore in supporting cone opsin folding and expression, a recent study demonstrated that proper cone opsin expression requires sufficient chromophore supply to the endoplasmic reticulum (Insinna et al., 2012). In addition, 11-*cis* retinal in the inner segment of cones also appears to facilitate the transport of several phototransduction proteins to the cone outer segments (Zhang et al., 2008). Thus, the deterioration of M-cone function that we observed in $Rlbp1^{-/-}$ mice is likely a direct result of the chromophore deficiency caused by the impairment of the retina visual cycle.

58

Notably, we found that S-cone opsin localization and expression were not affected in $Rlbp1^{-/-}$ mice (Figure 2.5B & D) indicating that apo S-opsin might be more stable than its M-opsin counterpart. It is intriguing in this context that mouse M-cones are more susceptible to age-dependent degeneration than S-cones (Cunea et al., 2014), suggesting that cone opsin stability might play a role in age-dependent cone degeneration. Regardless of the mechanism affecting loss of cone function in $Rlbp1^{-/-}$ mice, the rescued cone function in animals raised in darkness suggests that minimizing light exposure might be a simple and effective approach for protecting cones from degeneration and preventing photopic vision loss in patients with CRALBP-based visual disorders.

The contribution of two visual cycles to cone function

By selectively rescuing either the RPE or Müller cell visual cycle using AAV-Rlbp1 in $Rlbp1^{-/-}$ mice, we were able to identify the contribution of each visual cycle to supporting normal cone sensitivity and dark adaptation. Our finding that only the rescue of the retina visual cycle, but not the RPE visual cycle, restores normal sensitivity of dark-adapted $Rlbp1^{-/-}$ cones (Figure 2.7) reveals a previously unappreciated function of the retina visual cycle and demonstrates that this pathway plays a crucial role in maintaining long-term cone function. One interesting unexplored possibility emerging from these results is that age-dependent decline in the efficiency of the Müller cell visual cycle contributes to the gradual loss of cone function and is linked to age-related cone visual disorders in patients. Thus, genetic or pharmacological treatments aiming at boosting the retina visual cycle might have therapeutic benefit for age-dependent cone visual loss.

It has been suggested that cone dark adaptation is biphasic, with an initial fast recovery dominated by the retina visual cycle, and a slow subsequent recovery contributed by the RPE visual cycle (Kolesnikov et al., 2011). However, we found that the rescue of either of the two visual cycles in *Rlbp1*$^{-/-}$ mice results in cone dark adaptation in vivo with indistinguishable kinetics (Figure 2.7C). It is not clear at the moment whether this reflects a more complex interplay between the contributions of the two visual cycles than previously appreciated, or a developmental compensatory modulation of one pathway in the absence of the other. Interestingly, neither of the rescues of the two visual cycles restored the maximal cone response, suggesting reduced cone number or phototransduction capacity. One possibility is that both visual cycles are required for normal cone function. Alternatively, it is possible that the loss of cone function in *Rlbp1*$^{-/-}$ mice is caused by chromophore deficiency at an early stage of development and therefore could not be rescued by AAV injections in adult animals. While the two hypotheses are not mutually exclusive, our aging experiments on *Rlbp1*$^{-/-}$ mice (Figure 2.1) support the latter one. Future studies with animals of different ages should resolve these questions and provide invaluable information for the therapeutic potential of such treatments. Notably, we were able to achieve selective and highly efficient CRALBP expression selectively in Müller cells and even in the RPE (Figure 2.6F) with an intravitreal AAV injection.

2.6 Acknowledgements

Chapter 3: Circadian and light-driven regulation of rod dark adaptation

3.1 Abstract

Continuous visual perception and the dark adaptation of vertebrate photoreceptors after bright light exposure require recycling of their visual chromophore through a series of reactions in the retinal pigmented epithelium (RPE visual cycle). Light-driven chromophore consumption by photoreceptors is greater in daytime vs. nighttime, suggesting that correspondingly higher activity of the visual cycle may be required. On the other hand, as rod photoreceptors are saturated in bright light, the continuous turnover of their chromophore by the visual cycle throughout the day would not contribute to vision while still producing toxic chromophore byproducts. Whether the recycling of chromophore that drives rod dark adaptation is regulated by the circadian clock and light exposure is unknown. Here, we demonstrate that mouse rod dark adaptation is slower during the day or after light pre-exposure. This surprising daytime downregulation of the RPE visual cycle was further demonstrated by gene analysis, which revealed light-driven reduction in the expression of *Rpe65*, which encodes a key enzyme of the RPE visual cycle. Notably, only rods in melatonin-proficient C3H/f$^{+/+}$ mice, but not in melatonin-deficient C57BL6/J and 129S2/Sv strains were affected by this daily visual cycle modulation. Our results demonstrate that the circadian clock and light exposure regulate the recycling of chromophore in the RPE visual cycle. This daily modulation of rod dark adaptation is mediated by melatonin and could potentially protect the retina from light-induced damage during the day.

3.2 Introduction

The retina provides vertebrate animals with information about the world around them and the overall light intensity. Detailed visual information is generated by rod and cone photoreceptors, which are responsible for dim- and bright-light vision, respectively. The retina also anticipates the daily changes of ambient light conditions, with a 24-hour intrinsic circadian clock (Storch et al., 2007). This retinal circadian clock regulates many retinal functions, including melatonin synthesis (Tosini and Menaker, 1996), the electrical coupling between photoreceptors (Ribelayga et al., 2008; Jin et al., 2015), and synaptic strength (Emran et al., 2010), to fine-tune visual processing in the retina (Baba et al., 2009). The susceptibility to light-induced retinal damage is also higher in subjective (circadian) night than in subjective day (Organisciak et al., 2000). Although the mechanisms by which the circadian clock regulates this process is not understood, it is likely to be related to the light-sensing visual pigments in photoreceptors.

Light detection in the retina is initiated when light is absorbed by the visual pigment in photoreceptors. This triggers conversion of the visual chromophore 11-*cis* retinal to its all-*trans* form, activating the visual pigment and the phototransduction cascade that ultimately results in the electric response of the cell (Lamb and Pugh, 2004). Resetting of the photoactivated (bleached) visual pigment to its ground state requires removal of the spent all-*trans* chromophore from photoreceptors and its recycling back to its 11-*cis* form in the RPE cells (RPE visual cycle; for both rods and cones) or in the retinal Müller cells (retina visual cycle; for cones only) (Wang and Kefalov, 2011; Saari, 2012). Notably, even though rods are saturated during the day, their visual pigment still continuously cycles through bleaching and regeneration. As a result, rods

consume the bulk of the chromophore recycled by the RPE visual cycle (Wang et al., 2014), while chromophore recycled by the retina visual cycle allows cones to regenerate rapidly their visual pigment (Wang and Kefalov, 2009; Kolesnikov et al., 2011). The accumulation of retinoid byproducts with age or as a result of mutations in the visual cycle can cause retinal degeneration and blindness (Travis et al., 2007).

Chromophore consumption varies greatly during the day-night cycle. During the day, the visual pigments in rods and cones are photobleached at a high rate, whereas a minimal amount of chromophore is used and recycled at night. This day/night difference in chromophore consumption prompted us to ask: Is pigment regeneration under the regulation of the circadian clock, in accordance with chromophore demand? Does light modulate the efficiency of chromophore recycling? Here, we address these questions by electrophysiological recordings and molecular analysis of retinas of melatonin-proficient (C3H/f$^{+/+}$ and CBA/CaJ) and melatonin-deficient (C57/BL6/6J and 129S2/Sv) mouse strains.

3.3　Experimental procedures

Animals. The maintenance and treatment of the mice was in compliance with the protocols approved by the Washington University Animal Studies Committee. Melatonin-deficient C57BL/6J, as well as melatonin-proficient CBA/CaJ and C3H/f$^{+/+}$ mice, were purchased from Jackson Laboratory (Bar Harbor, ME). Melatonin deficient 129S2/Sv mice were purchased from Charles River Laboratories (Wilmington, MA). The C3H/f$^{+/+}$ mice are also known as C3A.BLiA-Pde6b^{+}/J, originally developed by Willem J. de Grip (Erasmus Universiteit, Netherlands) (Schalken et al., 1990; Doyle et al., 2002). Unlike the original C3H strain, the C3H/f$^{+/+}$ mice used in our study were free of the PDE6b mutation that causes retinal degeneration, and had normal retinal morphology and light-driven responses (Baba et al., 2009). All animals used in this study were free of the *rd8* mutation (Mattapallil et al., 2012). The animals were raised in a 12 hr:12 hr light-dark cycle, and entrained in a 420 cd m^{-2} light environment for a week before the experiments. Age-matched animals were grouped into three categories: subjective night, subjective day, and objective day. Subjective night groups were dark-adapted in a light-proof cabinet for 30 hours and tested at 18 circadian time (CT; midnight). Subjective day groups were dark-adapted for 18 hours and tested at CT 6 (noon). Objective day groups were dark-adapted for 1 hour and tested at 6 zeitgeber time (ZT, noon).

In vivo electroretinography (ERG). The method for studying mouse rod dark adaptation *in vivo* using LKC® ERG system had been described in detail previously (Kolesnikov et al., 2011). Briefly, dark-adapted animals were anesthetized with ketamine/xylazine cocktail (100/20 mg/kg) by intraperitoneal injection. The pupils of the anesthetized animals were dilated with a drop of 1% atropine sulfate solution and the animals were transferred to a 37 ℃ heating pad with

a feedback anal thermal probe. The reference electrode was inserted subcutaneously beneath the scalp and 2.5% Gonak hypromellose ophthalmic demulcent solution was applied to the cornea. A contact lens electrode was positioned on the cornea of each eye to detect electrical signals from retina. Excessive Gonak solution was removed from the eyes with tissue paper and the animals were allowed to stabilize in darkness for 15 minutes before beginning the recordings. Test flashes from a 530 nm LED, ranging from 2.5 x 10^{-5} cds m^{-2} to the 25 cds m^{-2} limit, were used to elicit photoresponses from each eye, and white Xenon flashes were used to produce saturated photoresponses. Sufficient time was allowed between individual test flashes to allow full recovery of the retina and avoid gradual response run-down due to light adaptation. For dark adaptation testing, a bright green (505 nm) LED light was applied to both eyes for 30 seconds to photobleach an estimated 90% of the visual pigment. The recovery of the ERG responses was monitored at fixed post-bleach time points within 2 hours after the bleach. The maximal response amplitude, r_{max}, was recorded at the brightest light intensity, and S_f was estimated as the ratio of dim flash response amplitude and the corresponding flash intensity in the linear range of the intensity-response curve, about 20% to 30% of the maximum. The post-bleach maximal amplitude (r_{max}) and sensitivity (S_f) were normalized to their dark adapted pre-bleach level, r^{DA}_{max} and S_f^{DA}, respectively.

RNA-seq. RNA-seq was performed in two biological replicates per condition (objective day vs. subjective day), each consisting of four eyes. Eyes were harvested and rapidly dissected in the dark. The anterior portion of the eye including the lens was removed, and the remaining tissue (posterior sclera, choroid, RPE, and retina) was rinsed in cold sterile HBSS with calcium and magnesium (Gibco) and stored in TRIzol (Invitrogen) at -80 °C. For extraction, the tissue was homogenized with a pestle and then passaged through a needle. Total RNA was extracted

and purified using the RNeasy Mini Kit (Qiagen) with on-column DNaseI digestion (Qiagen).

Integrity of total RNA was verified on a Agilent 2100 Bioanalyzer. Poly-A selection and

synthesis of the cDNA library for sequencing was conducted as described (Shen et al., 2014).

The four samples were indexed and sequenced on a single lane of a HiSeq 2500 sequencer (1 x

50bp). To analyze the sequencing data, raw reads were demultiplexed and aligned to *Mus*

musculus Ensembl release 72 (Flicek et al., 2014) with Tophat v2.0.9 (Trapnell et al., 2009) and

Bowtie2 v2.1.0 (Langmead and Salzberg, 2012) HTseq (Anders et al., 2014) was used to

estimate gene abundance, and differential expression analysis was conducted with EdgeR

(Robinson et al., 2010). Raw and processed RNA-seq data are available at Gene Expression

Omnibus (GEO) accession number GSE68470.

 Quantitative RT-PCR (qRT-PCR). Quantitative RT-PCR was performed in five biological

replicates per condition (objective day vs. subjective day), each consisting of two eyes at 5

weeks old. Eyes were harvested and dissected and total RNA was prepared as described above

for RNA-seq. Complementary DNA (cDNA) was prepared as previously described (Montana et

al., 2011), and qRT-PCR was conducted with SYBR-Green (Applied Biosystems). *Rpe65*

transcript levels were normalized to *Gapdh* transcript levels. *Gapdh* primers (Tsujita et al., 2006)

and *Rpe65* primers (Wright et al., 2014) were previously published. Three technical replicate

PCR reactions were performed for each biological replicate. The ΔCt values from biological

replicates were averaged and the standard deviation across biological replicates was calculated.

The ΔCt values were used to calculate statistical significance with a two-tailed Student's t-test.

 Statistics. Unless noted otherwise, all data is presented as mean ± SEM. Two tailed

unpaired Student's t-test was used to examine the significance of difference between two sample

groups. Statistical significance was reported when $p<0.05$.

3.4 Results

Rod dark adaptation in melatonin-proficient mice is regulated by the circadian clock

The goal of our study was to determine if pigment regeneration is regulated by the circadian clock or by light. These two retinal signals strongly regulate the expression of melatonin, which in turn affects many processes in the retina (Doyle et al., 2002; Tosini et al., 2012). Thus, we investigated rod dark adaptation in melatonin-proficient (C3H/f$^{+/+}$ and CBA/CaJ) and melatonin-deficient (C57/BL6/6J and 129S2/Sv) mouse strains. We began with the C3H/f$^{+/+}$ strain of mice, first testing their *in vivo* ERG responses (Kolesnikov et al., 2011). We observed robust dark-adapted responses with a normal waveform (Figure 3.1A). Measurements of their dark-adapted maximal a-wave amplitudes (r_{max}) at subjective night, 6 hours after the onset of nocturnal activity (18 o'clock circadian time, CT 18), and at subjective day (CT 6) were comparable (Table 3.1). Similarly, scotopic a-wave dim flash sensitivity (S_f) in C3H/f$^{+/+}$ mice was not affected by the time of day of the recordings (Table 3.1). Thus, our results from dark-adapted C3H/f$^{+/+}$ mice revealed no circadian regulation of their dark-adapted scotopic a-wave responses.

In order to determine whether pigment regeneration is regulated by the circadian clock, we next examined the kinetics of rod dark adaptation in C3H/f$^{+/+}$ mice in subjective night and subjective day. The dark adaptation experiments were performed with mice that were dark adapted for 30 hours (for the CT 18 time point) or 18 hours (for the CT 6 time point). As mouse rod pigment regeneration and dark adaptation are typically complete within one hour (Imai et al., 2007; Wang et al., 2014), such conditions allowed for full dark-adaptation prior to the experiment for both time points. This notion was also supported by the comparable scotopic a-wave sensitivities at CT 18 and CT 6 (Table 3.1).

68

Table 3.1 Dark-adapted scotopic in vivo ERG parameters of C3H/f+/+, C57BL/6J and 129S2/Sv mice at subjective night, subjective day and objective day.

	Subjective night	Subjective day	Objective day
C3H/f+/+	(n=15)	(n=16)	(n=7)
a-wave r^{DA}_{max} (μV)	312 $\pm$ 21	291 $\pm$ 31 (NS)	338 $\pm$ 29 (NS)
a-wave S_f^{DA} ($\mu V\ m^2\ cds^{-1}$)	223 $\pm$ 30	267 $\pm$ 39 (NS)	296 $\pm$ 37 (NS)
C57BL/6J	(n=9)	(n=10)	(n=10)
a-wave r^{DA}_{max} (μV)	598 $\pm$ 24	532 $\pm$ 18 (*)	700 $\pm$ 22 (**)
a-wave S_f^{DA} ($\mu V\ m^2\ cds^{-1}$)	751 $\pm$ 39	589 $\pm$ 15 (**)	856 $\pm$ 55 (**)
129S2/Sv	(n=6)	(n=8)	(n=7)
a-wave r^{DA}_{max} (μV)	277 $\pm$ 29	269 $\pm$ 36 (NS)	301 $\pm$ 28 (NS)
a-wave S_f^{DA} ($\mu V\ m^2\ cds^{-1}$)	249 $\pm$ 46	208 $\pm$ 37 (NS)	255 $\pm$ 27 (NS)

r^{DA}_{max} is the maximal amplitude of a-wave. S_f^{DA} is the a-wave sensitivity. NS: $p>0.05$, *$p<0.05$, **$p<0.01$, subjective day: tested with the subjective night group, objective day: tested with the subjective day group.

A bright 30 second light, estimated to bleach >90% of the visual pigment, instantly reduced the a-wave amplitude to near threshold levels (Figure 3.1C), while the a-wave sensitivity declined by ~1000-fold (Figure 3.1D). Consecutive measurements of these parameters in darkness over the next two hours revealed the gradual dark adaptation of the rods as their pigment regenerated. Notably, the recovery of both the amplitude and sensitivity of the a-wave over the first ~30 min of dark adaptation was significantly ($p<0.05$) slower for the subjective day group than for the animals in subjective night (Figure 3.1C & D). Eventually, the recovery levels became comparable, so that the tail of the dark adaptation (final 25% of r_{max} and final 5-fold of S_f recovery) was similar in the two groups. These results demonstrate that the time course of rod dark adaptation in C3H/f$^{+/+}$ mice is delayed during the subjective day compared to subjective night. Thus, mouse rod dark adaptation is modulated by the circadian clock.

We sought to establish the regulation of rod dark adaptation in another melatonin-proficient strain, CBA/CaJ. However, the ERG recordings from these mice revealed a prominent b-wave amplitude loss and extended a- and b-wave implicit times (Figure 3.1B), reminiscent of the phenotype caused by mutation in *Gpr179*, a G-protein coupled receptor in ON-bipolar cells (Peachey et al., 2012; Nishiguchi et al., 2015). Thus, although useful for molecular analysis of the retina circadian clock machinery and regulation (Storch et al., 2007; Ribelayga et al., 2008), this strain of CBA/CaJ mice proved not suitable for our physiological analysis.

Figure 3.1. Effect of the circadian clock on rod dark adaptation in melatonin-proficient mice. (**A**) Representative dark-adapted scotopic *in vivo* ERG responses to various light intensities from melatonin-proficient C3H/f$^{+/+}$ mice. (**B**) Representative dark-adapted scotopic *in vivo* ERG responses from melatonin-proficient CBA/CaJ mice revealing b-wave deficit. (**C**) Normalized *in vivo* ERG scotopic a-wave maximal response (a-wave r_{max} / r^{DA}_{max}) recovery in C3H/f$^{+/+}$ mice following 90% pigment bleach at t=0 at subjective night (solid squares, n=15) and subjective day (open squares, n=16) (*$p<0.05$). (**D**) Normalized *in vivo* ERG scotopic a-wave sensitivity (a-wave S_f / a-wave S_f^{DA}) recovery in C3H/f$^{+/+}$ mice following 90% pigment bleach at t=0 at subjective night (solid squares, n=15) and subjective day (open squares, n=16) (*$p<0.05$).
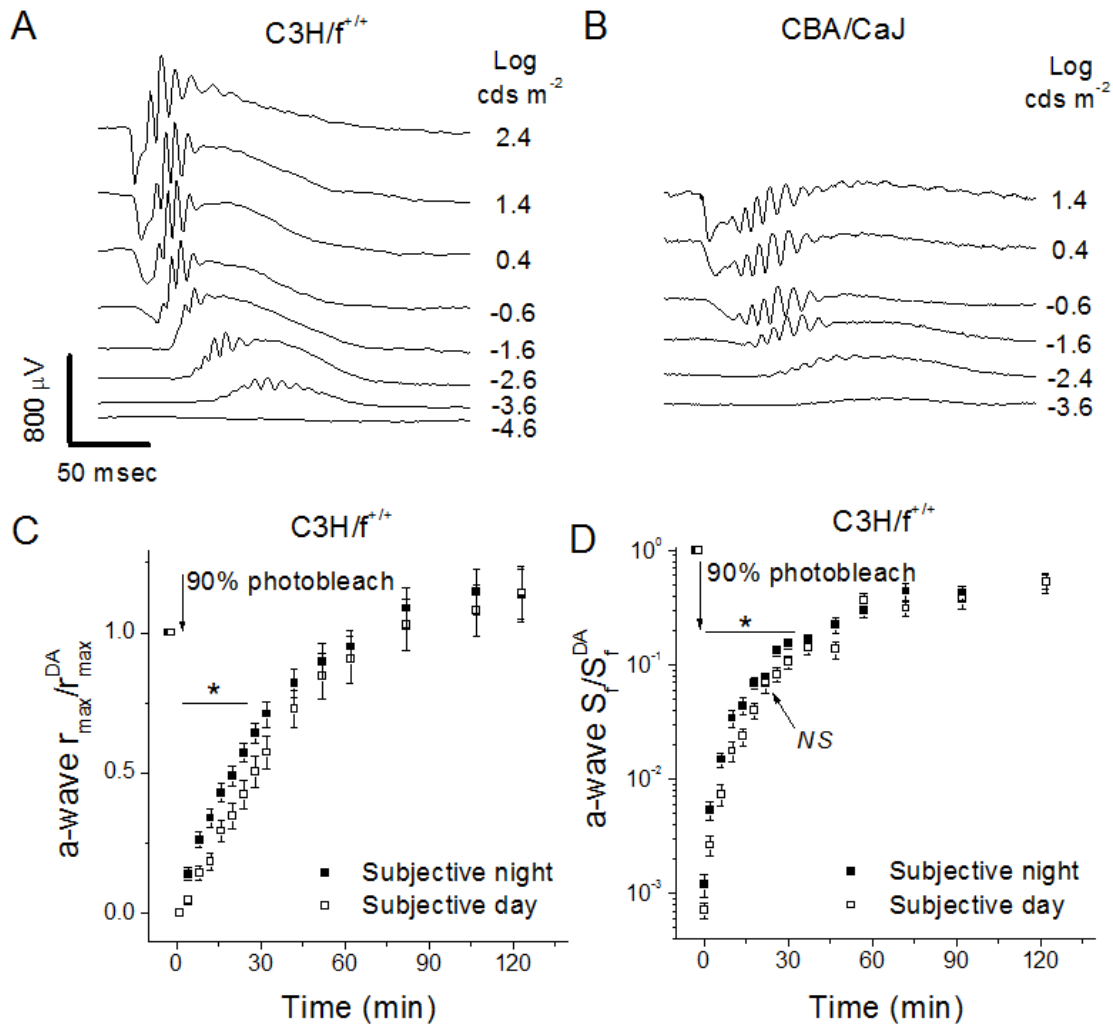
Rod dark adaptation in melatonin-proficient mice is regulated by light history

In addition to the circadian clock, exposure to light may also directly affect animal physiology, particularly in the light-sensitive retina (Emran et al., 2010). Thus, we next sought to determine if rod dark adaptation is also regulated by light history. To accomplish this, we compared the dark adaptation of C3H/f$^{+/+}$ mouse rods *in vivo* at 12 o'clock (noon) but dark adapted for 30 hours (subjective day, CT 6) or pre-exposed to light in the morning and then dark adapted for 1 hour before the experiment (objective day, zeitgeber time ZT 6). The 1 hour of darkness was sufficient to fully dark-adapt the rods in unanesthetized mice and restore their *in vivo* ERG a-wave sensitivity and maximal response amplitude (Table 1, compare values for subjective day, dark-adapted for 18 hours, and objective day, dark-adapted for 1 hour). Comparison of rod dark adaptation in subjective and objective day revealed that both a-wave maximal response (Figure 3.2A) and a-wave sensitivity (Figure 3.2B) recovered significantly slower during the objective day. Thus, our results revealed that rod dark adaptation in melatonin-proficient mice is suppressed by pre-exposure to daylight.

Given the electrophysiological findings that light exposure suppresses rod dark adaptation, we hypothesized that there was an underlying molecular downregulation of the visual cycle in objective day. Accordingly, we conducted RNA-seq and differential expression analysis (Shen et al., 2014) of the eyes of subjective day and objective day groups. A total of 1,460 genes were found to be significantly differentially expressed (FDR = 0.05) (Supplemental Table S1), with most of them (1,298 or 89%) expressed at lower levels in objective day than subjective day. Among the dysregulated genes, we identified two known visual cycle genes, *Rpe65* and *Rdh12* (Figure 3.2C). RPE65 converts all-*trans* retinal esters (atRE) into 11-*cis* retinol (11cROL) in the RPE (Jin et al., 2005), while RDH12 converts all-*trans* retinal (atRAL) to all-*trans* retinol

72

(atROL) in photoreceptors (Wang et al., 2012). Interestingly, *Rpe65* levels were 30% lower in objective day than subjective day, whereas *Rdh12* levels were 29% higher in objective day than subjective day. The downregulation of *Rpe65* would delay the recycling of chromophore in the RPE and the overall visual cycle (Gollapalli and Rando, 2004), whereas *Rdh12* upregulation would accelerate the reduction of toxic all-trans retinal and its clearance from the rods (Saari et al., 1998). To verify the RNA-seq results, we examined *Rpe65* transcript levels by quantitative RT-PCR (qRT-PCR) in an independent set of biological replicates (Montana et al., 2011). In good agreement with RNA-seq, we found that *Rpe65* levels were 27% lower in objective day than subjective day by qRT-PCR (Figure 3.2D). Overall, these molecular studies suggest that *Rpe65* mediates the light-mediated suppression of the visual cycle and rod dark adaptation.

Figure 3.2. Effect of the light history on rod dark adaptation in melatonin-proficient C3H/f$^{+/+}$ mice. (**A**) Normalized *in vivo* ERG scotopic a-wave maximal response (a-wave r_{max} / a-wave r^{DA}_{max}) recovery in C3H/f$^{+/+}$ mice following 90% pigment bleach at t=0 at subjective day (replotted from Figure 3.1C, open squares) and objective day (open triangles, n=7) (*$p<0.05$). (**B**) Normalized *in vivo* ERG scotopic a-wave sensitivity (a-wave S_f / a-wave S^{DA}_f) recovery in C3H/f$^{+/+}$ mice following 90% pigment bleach at t=0 at subjective day (replotted from Figure 3.1D, open squares) and objective day (open triangles, n=7) (*$p<0.05$). (**C**) Components of the RPE visual cycle and their expression by RNA-seq in objective day (OD) vs. subjective day (SD). In the photoreceptor outer segment (OS), the absorption of light by rhodopsin (*Rho*) causes conversion of 11-*cis* retinal (11cRAL) to all-*trans* retinal (atRAL). Next, atRAL is reduced to all-*trans* retinol (atROL) by RDH8 or RDH12 and exported to the RPE. There, atROL is converted to all-*trans* retinyl-ester (atRE) by LRAT. Subsequently, atRE is converted to 11-*cis* retinol (11cROL) by RPE65 in a rate-limiting step. Finally, 11cROL is oxidized to 11cRAL by RDH5 or RDH11 and imported back into the OS. IRBP is a binding protein in the interphotoreceptor matrix. Comparison of gene expression levels in OD vs. SD. Gray shading indicates a significant difference at FDR = 0.05. (Wang et al., 2012) (**D**) *Rpe65* mRNA abundance in objective day (OD) vs. subjective day (SD) as quantified by qRT-PCR. Transcript levels of *Rpe65* were quantified by qRT-PCR with normalization to *Gapdh*. **Error bars represent standard deviation** across five biological replicates per condition. P-value, two-tailed Student's t-test.
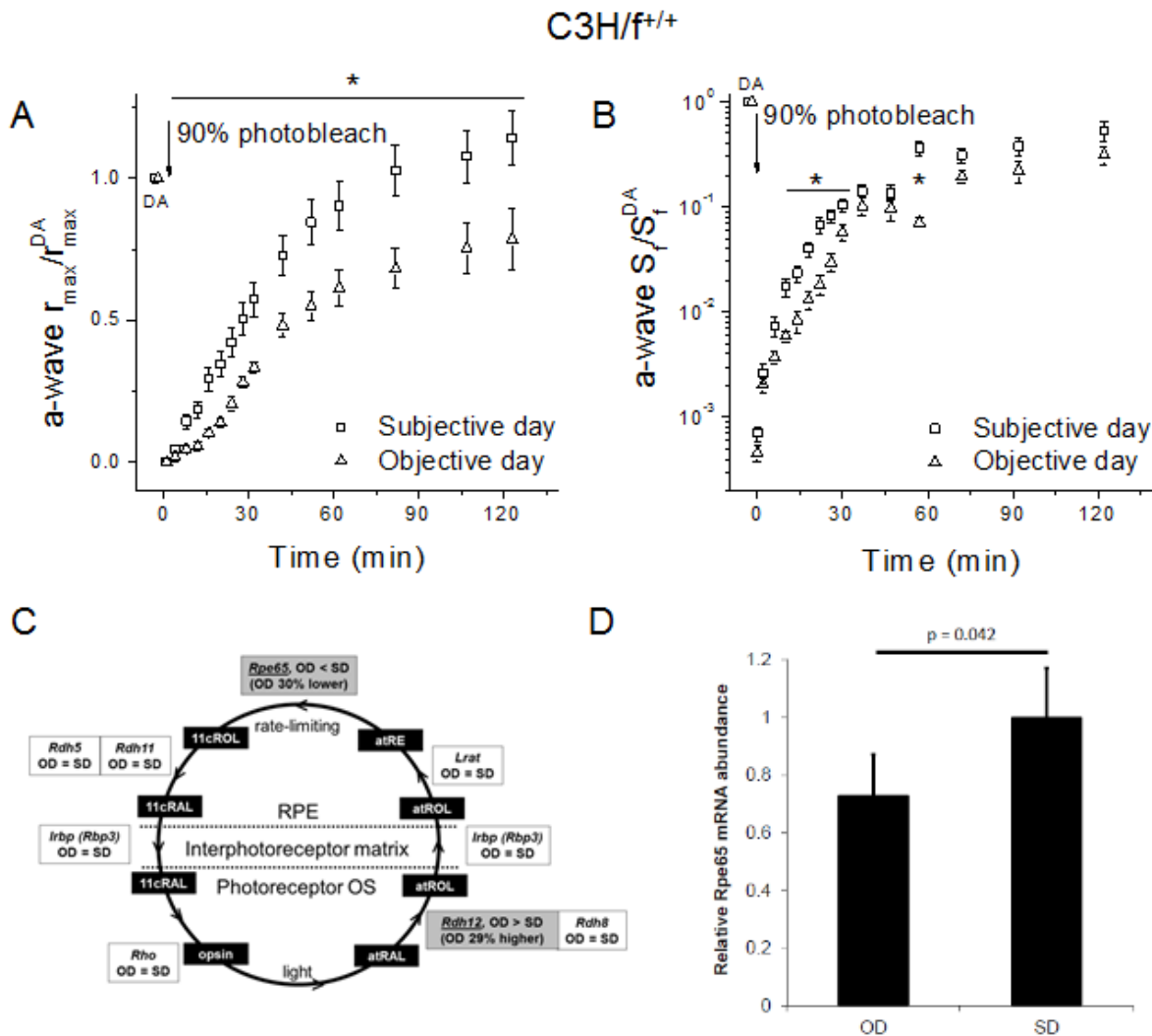
Rod dark adaptation in melatonin-deficient C57BL6/J rods is not affected by the circadian clock or light history

One of the key processes modulated by both the circadian clock and light exposure is melatonin synthesis, which is suppressed during the circadian daytime and by light. Thus, we next investigated whether the changes in dark adaptation we observed in C3H/f$^{+/+}$ mouse rods were mediated by melatonin. To address this question, we examined the function of melatonin-deficient C57BL6/J mouse rods using *in vivo* ERG recordings at subjective day (CT 6), subjective night (CT 18) and objective day (ZT 6). First, we measured the dark-adapted scotopic intensity-response curves at subjective day, subjective night and objective day (Figure 3.3A to C). The results revealed that the ERG a-wave amplitudes were significantly increased in subjective night compared to subjective day and objective day compared to subjective day, but only by a modest amount (Table 1). Then we performed the dark adaptation test as above to probe the operation of the C57BL6/J RPE visual cycle at subjective day, subjective night, and objective day. In contrast to the melatonin-proficient C3H strain, we found that rod dark adaptation at CT 6, CT 18 and ZT 6 was identical as measured by both a-wave amplitude (Figure 3.3D) and sensitivity (Figure 3.3E).

Figure 3.3. Lack of effect by the circadian clock and light history on rod dark adaptation in melatonin-deficient C57BL/6J mice. Representative scotopic *in vivo* ERG responses to various light intensities from C57BL/6J mice at (**A**) subjective night, (**B**) subjective day, and (**C**) objective day. (**D**) Normalized *in vivo* ERG scotopic a-wave maximal response (a-wave r_{max} / a-wave r^{DA}_{max}) recovery in C57BL/6J mice following 90% pigment bleach at t=0 at subjective night (solid squares, n=7), subjective day (open squares, n=6), and objective day (open triangles, n=10). (**E**) Normalized *in vivo* ERG scotopic a-wave sensitivity (a-wave S_f / a-wave S_f^{DA}) recovery in C57BL/6J mice following 90% pigment bleach at t=0 at subjective night (solid squares, n=7), subjective day (open squares, n=6), and objective day (open triangles, n=10).
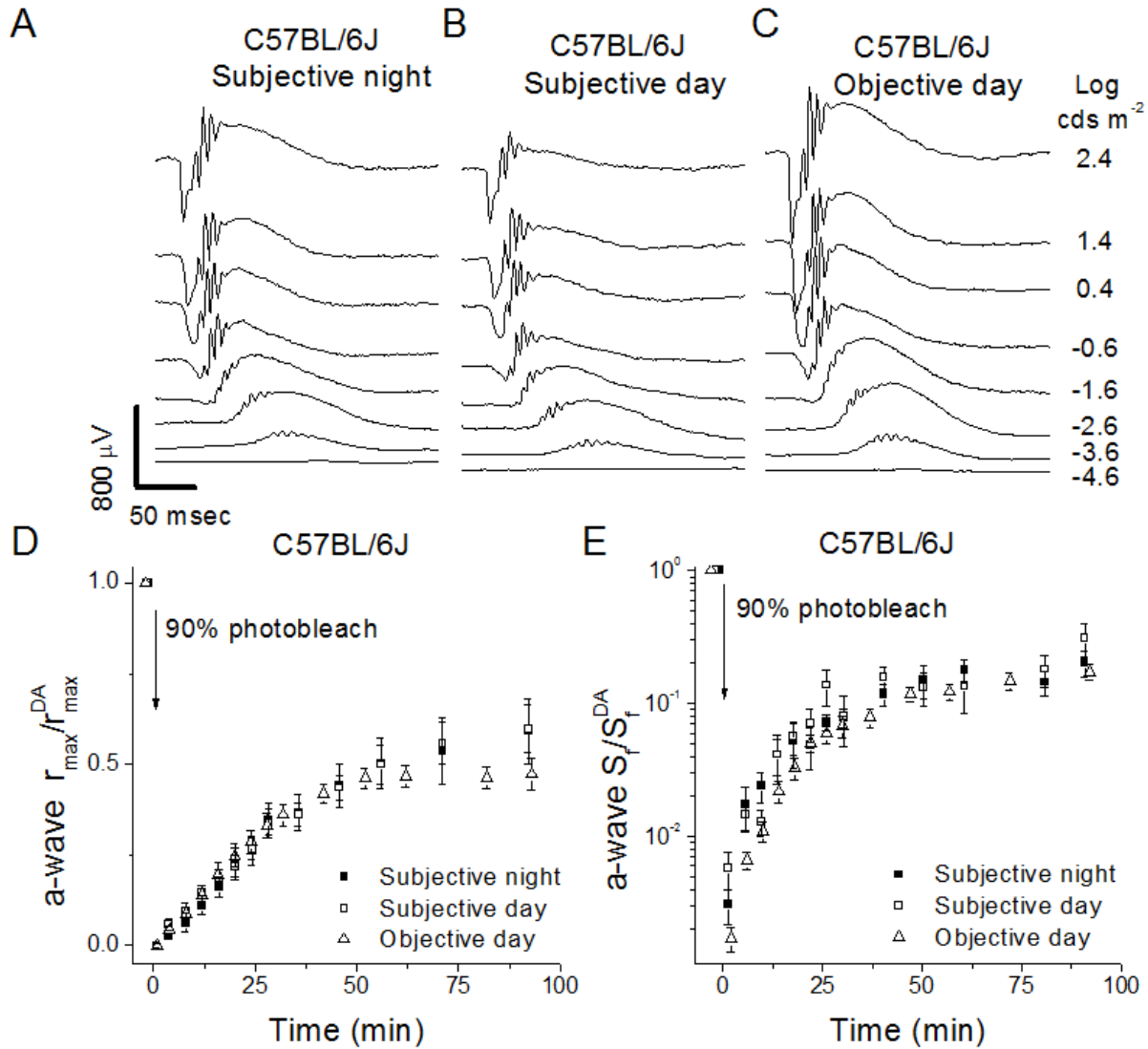
We obtained similar results from another melatonin-deficient mouse strain, 129S2/Sv. Like in C3H mice, the scotopic a-wave maximal amplitude and sensitivity of 129S2/Sv mice were comparable among subjective night, subjective day and objective day (Table 1). However, unlike the case of C3H mice and similar to the C57BL6/J mice, the circadian time or light exposure of 129S2/Sv mice prior to the experiment failed to modulate the dark adaptation of their rods (Figure 3.4A & B). Consistent with this observation, we found no significant difference in the transcript levels of *Rpe65* in objective day vs subjective day of 129S2/Sv mice as examined by qRT-PCR (Figure 3.4C). Thus, rod dark adaptation in melatonin-deficient C57BL6/J and 129S2/Sv mice was not affected by the circadian clock or light exposure history.

Figure 3.4. Lack of effects of the circadian clock and light history on rod dark adaptation in melatonin-deficient 129S2/Sv mice. (**A**) Normalized *in vivo* ERG scotopic a-wave maximal response recovery in 129S2/Sv mice following 90% pigment bleach at t=0 at subjective night (solid squares, n=6), subjective day (open squares, n=8), and objective day (open triangles, n=7). (**B**) Normalized *in vivo* ERG scotopic a-wave sensitivity recovery in 129S2/Sv mice following 90% pigment bleach at t=0 at subjective night (solid squares, n=6), subjective day (open squares, n=8) and objective day (open triangles, n=7). (**C**) *Rpe65* mRNA abundance in objective day (OD) vs. subjective day (SD) in 129/Sv mice as quantified by qRT-PCR. Transcript levels of *Rpe65* were quantified by qRT-PCR with normalization to *Gapdh.* Error bars represent standard error of the mean (SEM) across five biological replicates per condition. P-value, two-tailed Student's t-test.
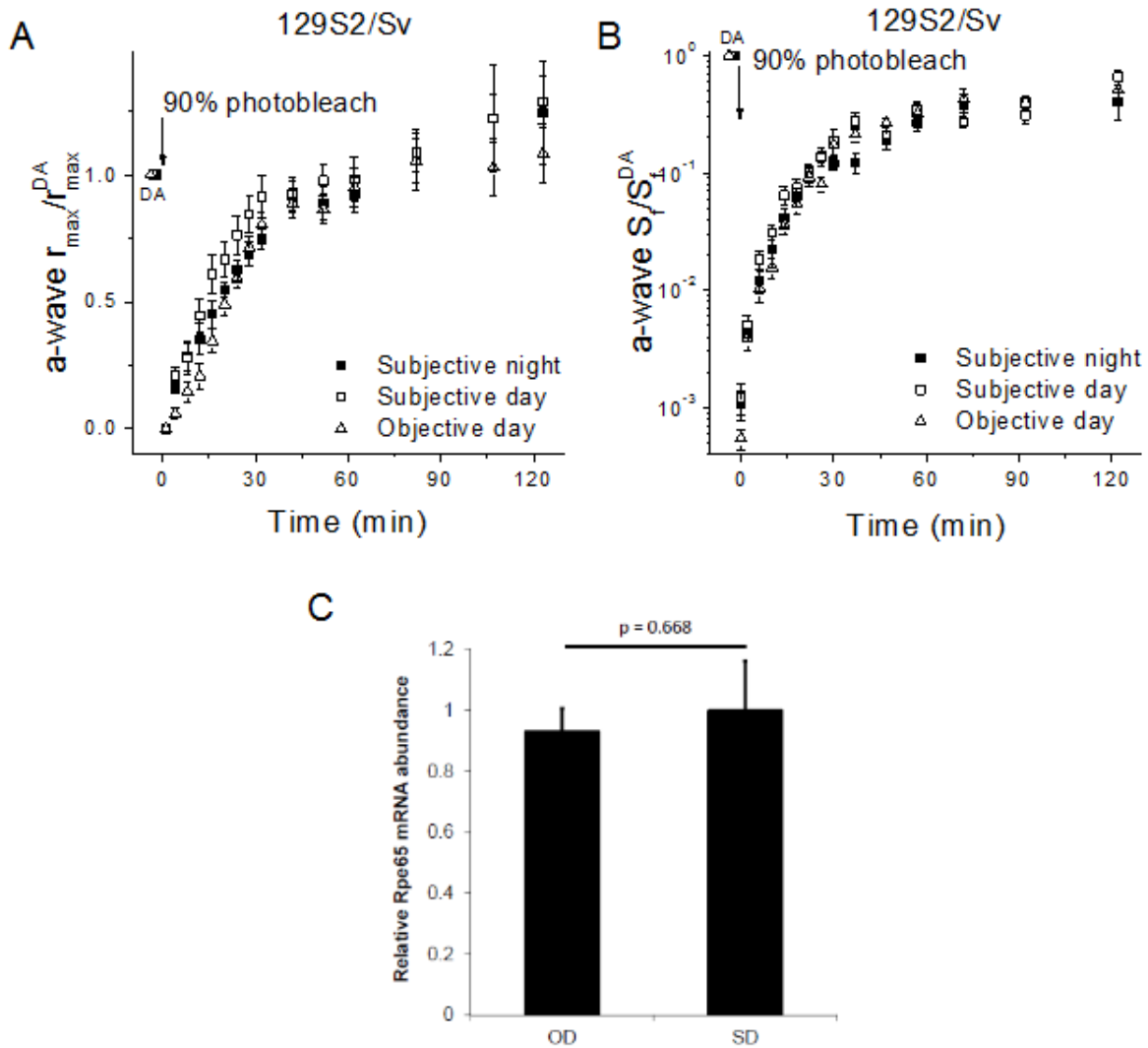
3.5 Discussion

Melatonin-mediated regulation of mouse rod dark adaptation

The circadian clock and light regulate many of the processes in the retina (Tosini et al., 2008). However, despite the large difference in visual pigment photoactivation at night and during the day, it was not previously known whether the recycling of chromophore and the regeneration of visual pigment are also subject to such regulation. Our results clearly demonstrate that both the circadian clock and light exposure slow down the dark adaptation of rods in melatonin-proficient mice during the day. Thus, rod pigment regeneration in these mice is modulated by the circadian clock and by light so that their cumulative effects substantially slow down rod dark adaptation in the daytime when rods are largely saturated.

Although the exact mechanism of this regulation is still unclear, our finding that *Rpe65* expression is suppressed by light, together with its previously described diurnal regulation in CBA/CaJ strain (Storch et al., 2007), suggest that it likely involves modulation of the efficiency of chromophore recycling by the RPE visual cycle. As this is the only mechanism for regeneration of the rod visual pigment and the rate-limiting step for rod dark adaptation (Lamb and Pugh, 2004; Wang et al., 2014), slowing the RPE visual cycle would cause a corresponding delay in the regeneration of rod pigment and in the dark adaptation of rods.

Melatonin is produced by photoreceptor cells in the retina at night (Cahill and Besharse, 1993), and regulates many aspects of mammalian retinal physiology (see Tosini et al., 2012 for review). The rhythmicity of melatonin biosynthesis also drives diurnal retinal dopamine synthesis, which peaks during the day (Doyle et al., 2002), further amplifying the robustness of the retina-intrinsic circadian clock. Melatonin receptors have been identified in various ocular

cell types, including photoreceptors, RPE, and Müller cells (Nash and Osborne, 1995; Baba et al., 2009; Jiang et al., 2012). However, many commonly used strains of laboratory mice, including C57BL6, 129S2/Sv and BALB/c strains, have lost their ability to produce melatonin due to mutations in key melatonin biosynthesis enzymes (Kasahara et al., 2010; Shimomura et al., 2010). In contrast, CBA and C3H mice still retain their ability to synthesize melatonin. Thus, our observation that rod dark adaptation is subject to regulation by the circadian clock and light in C3H, but by neither the circadian clock nor light in C57BL6 and 129S2/Sv mice, suggests a role for melatonin in this process. Thus, the simplest explanation for our results is that the efficiency of the RPE visual cycle is modulated by the daily oscillation of melatonin.

The daily modulation of the RPE visual cycle and rod-mediated vision

The high sensitivity of rods enables them to detect low light levels and mediate dim light vision. However, the high amplification that produces this exquisite rod sensitivity also results in the saturation of the rods at moderately bright light conditions (Green, 1971). Despite this fact, the rod visual pigment continues to undergo bleaching and regeneration throughout the day. As this process involves multiple enzymatic reactions both in the rods and in the RPE cells, it imposes a significant metabolic load on the visual system. Therefore, the downregulation of the RPE visual cycle during the day by both the circadian clock and light history would conserve energy in the eye without significantly compromising rod-mediated vision. The corresponding acceleration of all-*trans* retinal reduction in the rods suggested by the observed upregulation of *Rdh12* would minimize the toxic effects of this compound (Maeda et al., 2009) and prevent the formation and accumulation of related toxic byproducts (Maeda et al., 2008). At the same time, as the cones rely predominantly on the alternative retina visual cycle for the bulk of their dark adaptation (Wang et al., 2009; Kolesnikov et al., 2011) and for chromophore supply during cone

80

opsin synthesis (Xue et al., 2015), the suppression of the RPE visual cycle would not be expected to compromise cone-mediated daytime vision.

Another possible benefit of downregulating the RPE visual cycle during the day is the protection of the retina from light damage. It is known that mice with lower *Rpe65* expression have a slower rod dark adaptation and higher resistance to light-induced rod degeneration (Wenzel et al., 2001), presumably because the slower turnover of visual pigment reduces the accumulation of toxic retinoid byproducts. Similarly, the down-regulation of the RPE visual cycle during the day could be a mechanism to protect photoreceptors from light damage. Consistent with this hypothesis, in rats, retinas are more susceptible to light-induced damage at night (Vaughan et al., 2002; Organisciak and Vaughan, 2010). Our finding that the RPE visual cycle is faster at night provides a mechanistic explanation for this observation. Therefore, a rhythmic melatonin-driven diurnal suppression of the RPE visual cycle may protect the retina from degeneration by lowering the susceptibility of photoreceptors to light damage during the day. Indeed, lack of melatonin-dependent RPE visual cycle regulation could be involved in the enhanced age-dependent retinal degeneration in mice lacking the melatonin receptors MT1 and MT2 (Baba et al., 2009, 2012). Conversely, enhancing the diurnal suppression of the RPE visual cycle by oral intake of melatonin could potentially reduce the risk of human age-related macular degeneration (AMD) (Yi et al., 2005).

3.6 Acknowledgements

Chapter 4: RDH10 is not necessary for the function of retina visual cycle

The work in this chapter is in preparation. The research is conducted and designed by Yunlu Xue, David Razafsky, Didier Hodizc and Vladimir Kefalov (corresponding author).

4.1 Abstract

In retina visual cycle, Müller cells isomerize all-*trans* retinol to 11-*cis* retinol, while vertebrate photoreceptors only use 11-*cis* retinal as the chromophore. Cone photoreceptors, but not rods, can oxidize the 11-*cis* retinol to 11-*cis* retinal and use it for pigment regeneration. However, it is not clear what enzyme is responsible for this 11-*cis* oxidation process in cones. Based on RNA-sequencing results from rd7 mice (Corbo Lab, unpublished data), we hypothesize that retinol dehydrogenase 10 (RDH10) is this unidentified 11-*cis* RDH in cones. Using in vivo electroretinography (ERG) and transretinal recordings, we examined whether knocking out RDH10 in cones modifies cone function and dark adaptation. We also examined if knocking out RDH10 in the retina causes any change to cone function and dark adaptation. The results showed that deletion of RDH10 in cones and retina does not hinder the cones' ability to access the retina visual cycle, and cone function remained normal in the absence of RDH10. Finally, we expressed RDH10 in mouse rods to check whether RDH10 is sufficient for rods to access the retina visual cycle. The results showed no change in rod ERG dark adaptation in these transgenic RDH10 mice. Thus, RDH10 is not sufficient to speed up rod dark adaption, however, future studies, will be required to determine whether the transgenic RDH10 rods can oxidize exogenous 11-*cis* retinol. Taken together, these results suggest that the 11-*cis* RDH in cones remains unidentified.

4.2 Introduction

Upon activation by light, the visual pigment of the vertebrate photoreceptor spends its chromophore, and has to recapture a new one to regenerate itself and become able to capture the next photon. The regeneration of visual pigment together with the chromophore recycling is termed the visual cycle. Chromophore supply is the rate-limiting step of the visual pigment regeneration and photoreceptors dark adaption (Lamb and Pugh, 2004; Wang et al., 2014). Cone photoreceptors, but not rods, can use 11-*cis* retinol from the retina visual cycle as the chromophore (Das et al., 1992; Mata et al., 2002), making them dark adapt faster than rods (Wang et al., 2009). It is unclear what prevents rods from accessing the retina visual cycle. In the past, several hypotheses have been proposed, including rod and cone differences in chromophore trafficking (Jin et al., 1994), and an unidentified cone-specific 11-*cis* retinol dehydrogenase (RDH) which can oxidize the 11-*cis* retinol produced by Müller cells (Mata et al., 2002).

Bringing light to this question, rd7 mice carry *Nr2e3* mutation, which makes the rods express a subset of cone genes (Corbo and Cepko, 2005). In the study of rd7 photoreceptor dark adaptation, these "hybrid" rods were found to dark adapt faster than the wild type rods, and to be capable of accessing the retina visual cycle (Wang et al., 2014), suggesting that rd7 rods express the unidentified 11-*cis* RDH(s). Therefore, we applied RNA-sequencing to the rd7 retina and wild type retina to compare their mRNA content. The results revealed upregulation of *Rdh10* mRNA. RDH10 is a 38 kDA short-chain dehydrogenases/reductases (SDR) family member protein, previously reported to be expressed in the RPE and Müller cells (Wu et al., 2002, 2004; Farjo et al., 2009). Our preliminary results from in situ hybridization suggested that RDH10 is also expressed in the photoreceptor later of $Nrl^{-/-}$ retinas, which only have cone-like

photoreceptors but not rods (Nikonov et al., 2005) as well as sparsely in the photoreceptor layer of wild type mice, consistent with a cone-specific expression. Therefore, we hypothesize that RDH10 enables cones to access the retina visual cycle, and its absence in the rods keeps them from accessing the retina visual cycle, making their dark adaption slower than that of cones.

In this study, we applied loss- and gain- of function experiments to examine the role of RDH10 in the retina visual cycle and cone function. We used electroretinography (ERG) recordings to test cone function and dark adaptation in *Rdh10* cone (HRGP-Cre) and retina (Six3-Cre) conditional knockout mice, as well as rod function and dark adaption in transgenic (GRK1 promoter) *Rdh10* mice.

4.3 Experimental procedures

Animals. All animals except the transgenic *Rdh10* mice were bred to *Gnat1$^{-/-}$* background (obtained from Janis Lem at Tufts University, Boston) as described in Chapter 1.3 Common Experimental Procedures. For this study, both HRGP-Cre and Six3-Cre mice were obtained from Jackson Laboratory (Bar Harbor, ME). *Rdh10$^{flox/flox}$* mice (Sandell et al., 2012) were crossed with HRGP-Cre mice to knockout RDH10 selectively in cones. The HRGP-Cre mice were used as control for the electrophysiology recordings on cone *rhd10* conditional knockout mice. The *Rdh10$^{flox/flox}$* mice crossed with Six3-Cre mice to knockout the RDH10 in the entire retina. Both of the littermate Six3-Cre mice and *Rdh10$^{flox/flox}$* mice were used as the control were used for the recordings on retina *Rdh10* conditional knockout mice

The transgenic *Rdh10* mice were generated by the Transgenic Core at the Department of Ophthalmology at Washington University. The transgene of the mouse *Rdh10* cDNA was introduced to the photoreceptors driven by the human rhodopsin kinase promoter. The sequence of mouse *Rdh10* was described in previous study (Wu et al., 2002). Transgenic *Rdh10* negative littermates were used as controls for these experiments.

Western blot. The RDH10 antibody was obtained from ProteinTech (#14644). Both retinas from each mouse were collected and supplemented with 200ul 2X Laemli/bmercaptoethanol plus zirconium beads. The beating of the retinas lasted 3 min at speed 6, then boiled and centrifuged for 10 min at max speed. 150ul supernatant was taken and loaded at 30 μL/well. For urea gel, 25 μL same lysates plus 5 μL 8M urea were used.

Electrophysiology. The details of in vivo ERG and transretinal recording were described in Section 1.3.

4.4　Results

RDH10 is eliminated in the conditional knockout and overexpressed in transgenic retina

To study the role of RDH10 in the retina visual cycle, we generated RDH10 conditional knockout mice using Cre-Lox recombination technology. Western blot confirmed that the 38 kDa RDH10 was deleted in the entire retina of Six3-Cre $Rdh10^{flox/flox}$, and that the transgenic RDH10 mice overexpressed RDH10 in the retina (Figure 4.1B). However, there was a 150 kDa band in all samples that could not be removed with urea, suggesting non-specific binding to an unknown protein with this RDH10 antibody (Figure 4.1B). Possibly due to this unknown protein, immunofluorescence imaging failed to confirm the deletion of RDH10 in the retina (data not shown). However, this observation did not affect the fact that the 38 kDa RDH10 was removed from the retina and over expressed in the transgenic $Rdh10$ retina. Therefore, the following electrophysiology study on RDH10 provided valuable information about the possible role of RDH10 in the retina visual cycle. We are currently investigating the identity of this 150 kDA protein using immunoprecipitation and mass spectrometry.

Figure 4.1 RDH10 is deleted in Six3-Cre *Rdh10flox/flox* retina and overexpressed in transgenic *Rdh10* retina. (A) Normal western blot of transgenic *rdh10*, transgenic control, Six-Cre *Rdh10flox/flox*, Six3-Cre control retinas. (B) Western blot with urea to disrupt potential RDH10 complexes on the same groups.
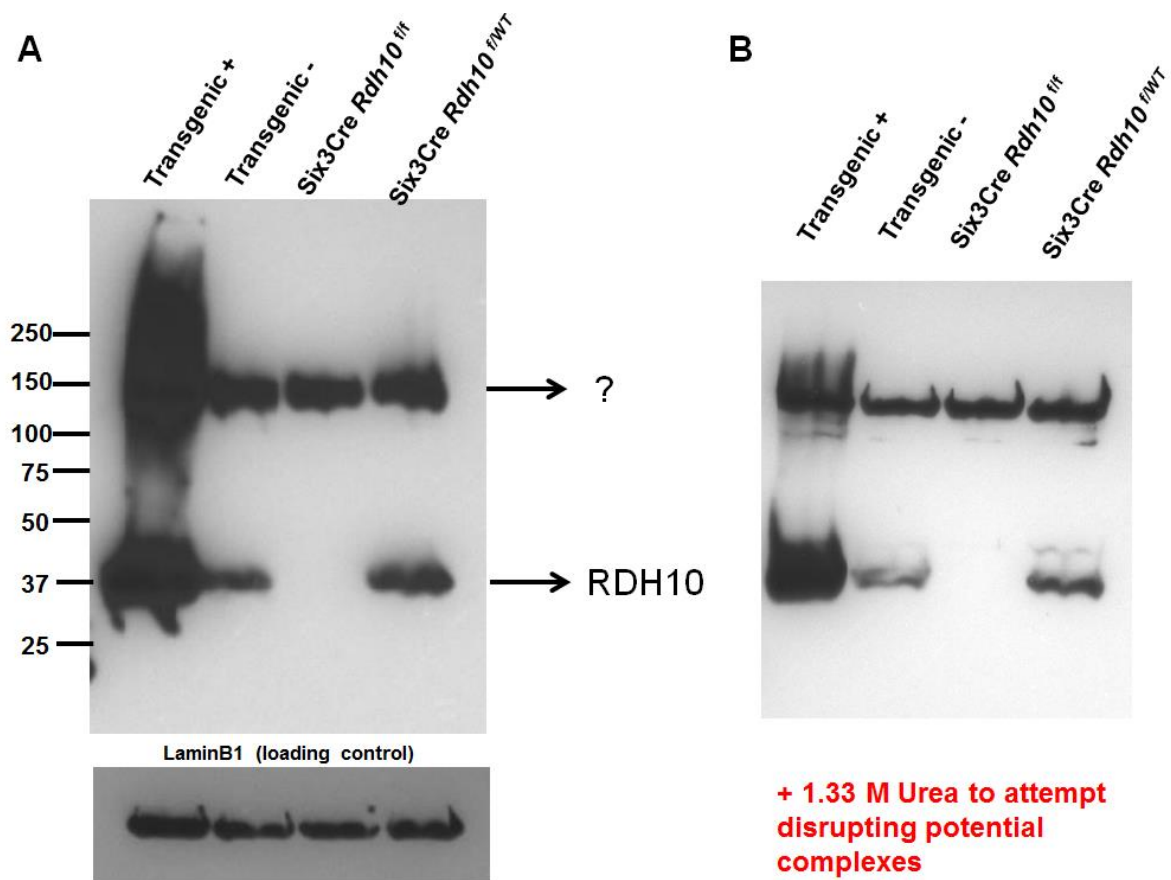
Cone RDH10 is not required for the normal function of cones

To determine if RDH10 is required by the cones for their normal function, the cone responses were recorded and compared between the HRGP-Cre control mice and HRGP-Cre *Rdh10$^{flox/flox}$* mice. We started with in vivo ERG recordings to test the cone b-wave responses (Figure 4.2A). The averaged cone b-wave response amplitude was comparable between the control and the RDH10-deficient cones (Figure 4.2B). The normalized cone b-wave response was also similar between the control and the RDH10 conditional knockout cones (Figure 4.2C). Together, these results suggested that the cone b-wave responses were not affected by the deletion of RDH10 in cones.

To further check if the cone responses were altered by the deletion of RDH10 in cones, we performed transretinal recording with DL-AP4, an mGluR6 antagonist, in the perfusion solution to isolate cone responses. We compared the responses from the control retina and the RDH10 cone conditional knockout retina (Figure 4.3A), and found that the averaged responses were identical in the two groups (Figure 4.3B). The wave shape of averaged dim and bright flash responses were also identical in RDH10 cone conditional knockout group compared to the control. These results suggested that the cone phototransduction cascade and overall cone responses are unaffected by deleting the RDH10 in cones.

Figure 4.2 The deletion of RDH10 in cones does not affect the photopic ERG b-wave responses in mice. (A) Representative in vivo ERG family responses of HRGP-Cre control (left panel, black traces) and cone *Rdh10* knockout (KO) (right panel, red traces) mice. (B) Ensemble-averaged cone b-wave responses of HRGP-Cre control mice (n = 18, black squares) and cone *Rdh10* KO mice (n=18, red circles) as function of flash intensity. (C) Normalized b-wave intensity-response curve of HRGP-Cre control (n = 18, black squares) and cone *Rdh10* KO (n=18, red circles) Mice.
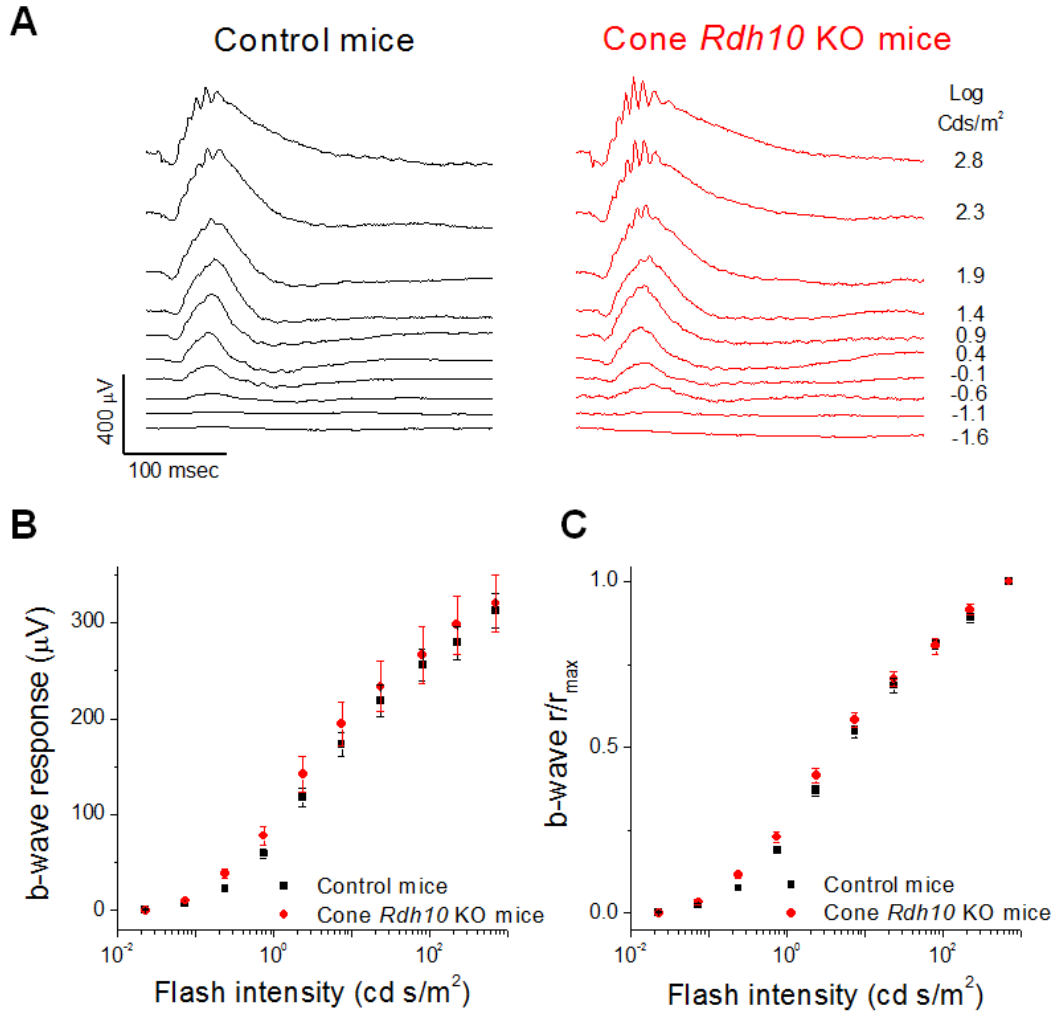
Figure 4.3 The deletion of RDH10 in cones does not affect cone responses. (A) Representative responses of HRGP-Cre control cones (left panel) and *Rdh10* conditional knock-out (CKO) cones (right panel). Red trace flash intensity: 1.4×10^4 photons/μm^2. (B) Ensemble-averaged response of HRGP-Cre control cones (n = 12, black squares) and *Rdh10* CKO cones (n=12, red circles) as function of flash intensity. (C) Ensemble-averaged dim flash responses (intensity: 1.4×10^3 photons/ μm^2) and bright flash responses (intensity: 4.5×10^6 photons/ μm^2) of HRGP-Cre control cones (n = 12) and *Rdh10* CKO cones (n=12).
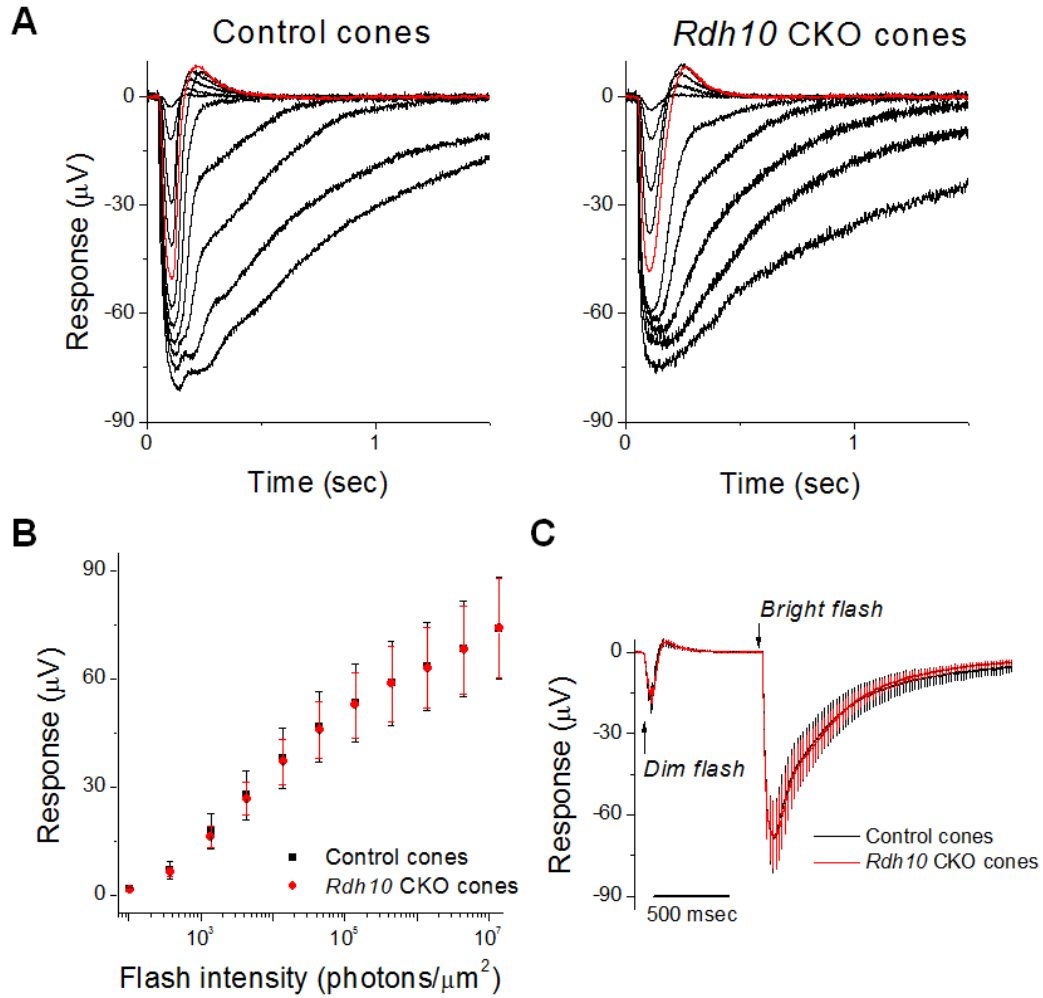
Cone RDH10 is not necessary for cone dark adaptation and retina visual cycle

To examine if cone RDH10 is required by the cones to access the retina visual cycle, we tested the sensitivity recovery of RDH10-deficient cones following a light bleach of over 90% photopigment using transretinal recording (Figure 4.4A). Because the retinas were isolated from the RPE, the dark adaptation recovery was driven by the chromophore recycling only through the retina visual cycle. The measured cone sensitivity was normalized to the prebleach level as described in the experimental procedures. The comparable sensitivity recovery kinetics in the RDH10 conditional knockout and control cones (Figure 4.4A) suggested that the retina visual cycle was unaffected by the deletion of RDH10 in cones.

We also monitored if the overall cone dark adaptation in vivo was affected by the deletion of RDH10 in cones (Figure 4.4B). Measuring cone b-wave recovery, we found comparable recovery kinetics in the two groups, suggesting that neither the retina visual cycle nor the RPE visual cycle was affected by deleting RDH10 in cones (Figure 4.4B). Together, these results suggested that RDH10 is not required for the cone overall dark adaptation or the retina visual cycle.

Figure 4.4 The deletion of RDH10 in cones does not affect cone dark adaptation. (A) Normalized cone sensitivity (S_f / S_f^{DA}) recovery following 90% pigment photobleach in control (n=13, black squares) and *Rdh10* CKO (n=13, red circles) isolated retinas using transretinal recordings. (B) Normalized cone b-wave sensitivity (b-wave S_f / b-wave S_f^{DA}) recovery following 90% pigment photobleach from control (n=18) and cone *Rdh10* KO (n=18) mice using in vivo ERG recordings.
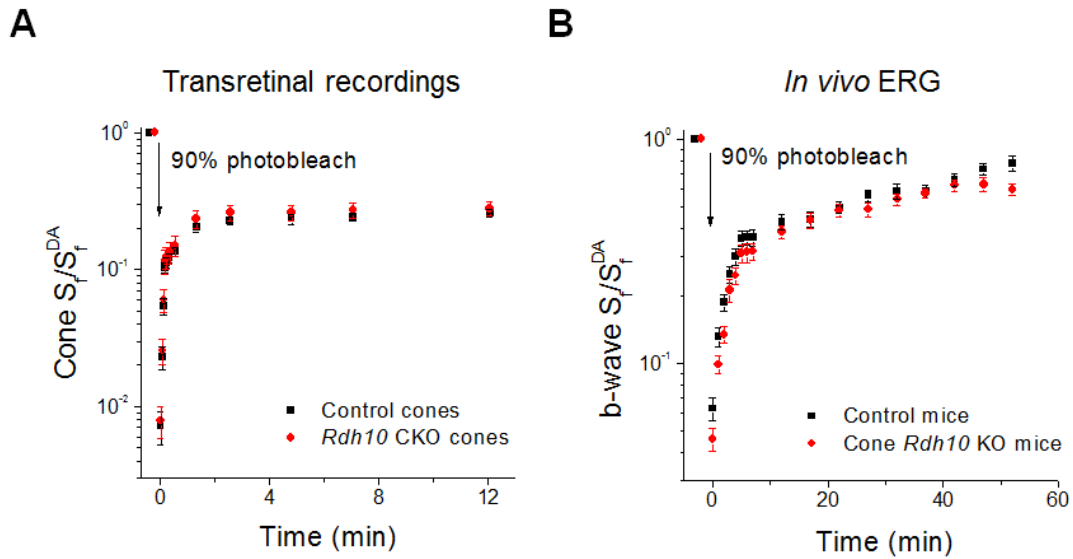
Retina RDH10 is not required for normal cone function

The above results demonstrated that cone RDH10 is not required for normal cone function and cone dark adaptation. In the retina, RDH10 is expressed abundantly in the Müller cells (Wu et al., 2004). In addition, RDH10 in the RPE can facilitate the 11-*cis* retinol to 11-*cis* retinal conversion similar to RDH5 (Farjo et al., 2009). Therefore, we next asked whether RDH10 can convert 11-*cis* retinol to 11-*cis* retinal in Müller cells to contribute to the retina visual cycle in a previously unknown mechanism. How will cone function be affected if RDH10 is removed from the retina?

To study these questions, we first tested the cone b-wave response using in vivo ERG with the retina RDH10 conditional knockout Six3-Cre *Rdh10*$^{flox/flox}$ mice (Figure 4.5A). The averaged cone b-wave response amplitude was similar in the retina RDH10 knockout mice and in the Six3-Cre control (Figure 4.5B). The averaged normalized cone b-wave intensity-response curves of the retina RDH10 knockout and control groups (Figure 4.5C) were also comparable, suggesting that the retina RDH10 is not necessary for maintaining normal cone b-wave responses.

Figure 4.5 The deletion of RDH10 in the retina does not affect the photopic ERG b-wave responses in mice. (A) Representative in vivo ERG family responses of Six3-Cre control (left panel, black traces) and retina *Rdh10* knock-out (KO) (right panel, red traces) mice. (B) Ensemble-averaged cone b-wave responses of Six3-Cre control mice (n = 12, black squares) and retina *Rdh10* KO mice (n=10, red circles) as function of flash intensity. (C) Normalized b-wave intensity-response curve of Six3-Cre control (n = 12, black squares) and retina *Rdh10* KO (n=10, red circles) mice.
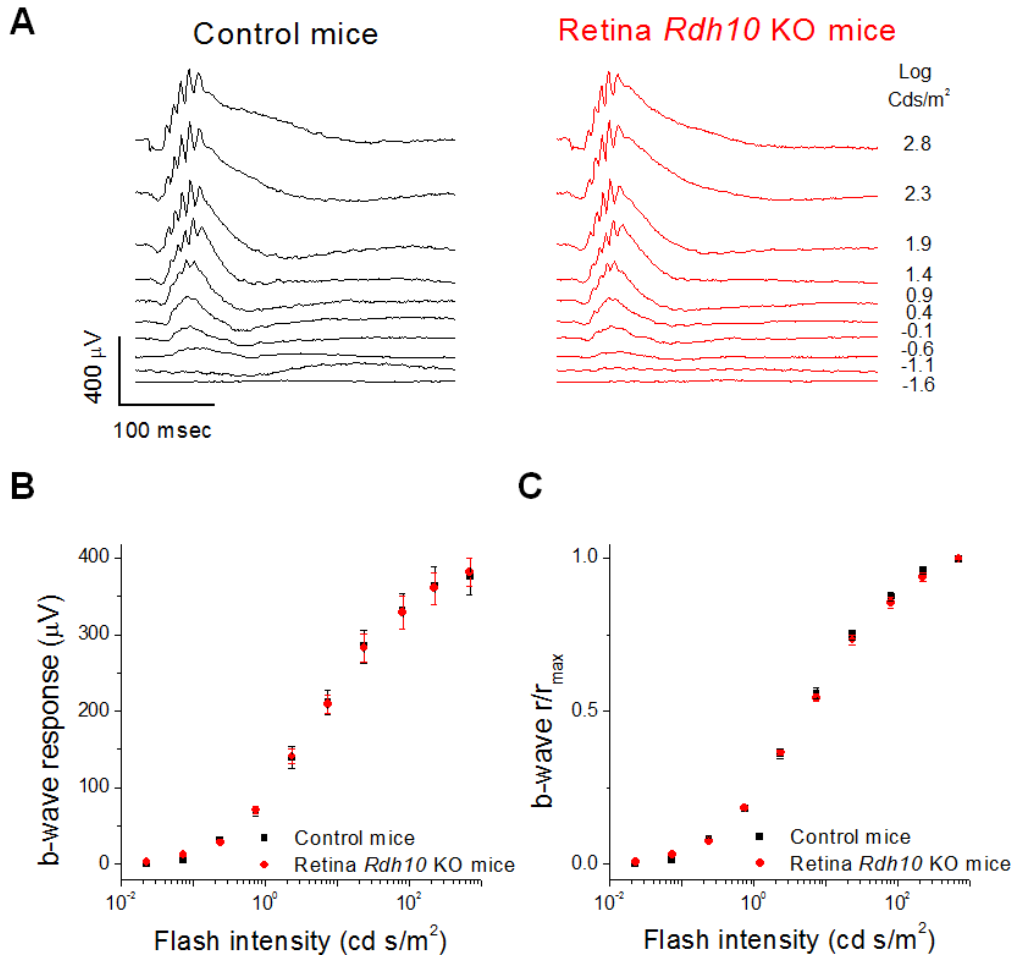
Figure 4.6 The deletion of RDH10 in the retina does not affect cone responses. (A) Representative responses of Six3-Cre control (left panel) and retina *Rdh10* knock-out (KO) (right panel) cones. Red trace flash intensity: 1.4 $\times 10^4$ photons/μm^2. (B) Normalized dim flash responses (r_{dim}/r_{dim}^{peak}) of Six3-Cre control (n = 9, black trace) and retina *Rdh10* KO (n=8, red trace) cones. (C) Ensemble-averaged intensity-response curve of Six3-Cre control (n = 9, black squares) and retina *Rdh10* KO (n=8, red circles) cones. (D) Normalized intensity-response curve of Six3-Cre control (n = 9, black squares) and retina *Rdh10* KO (n=8, red circles) cones.
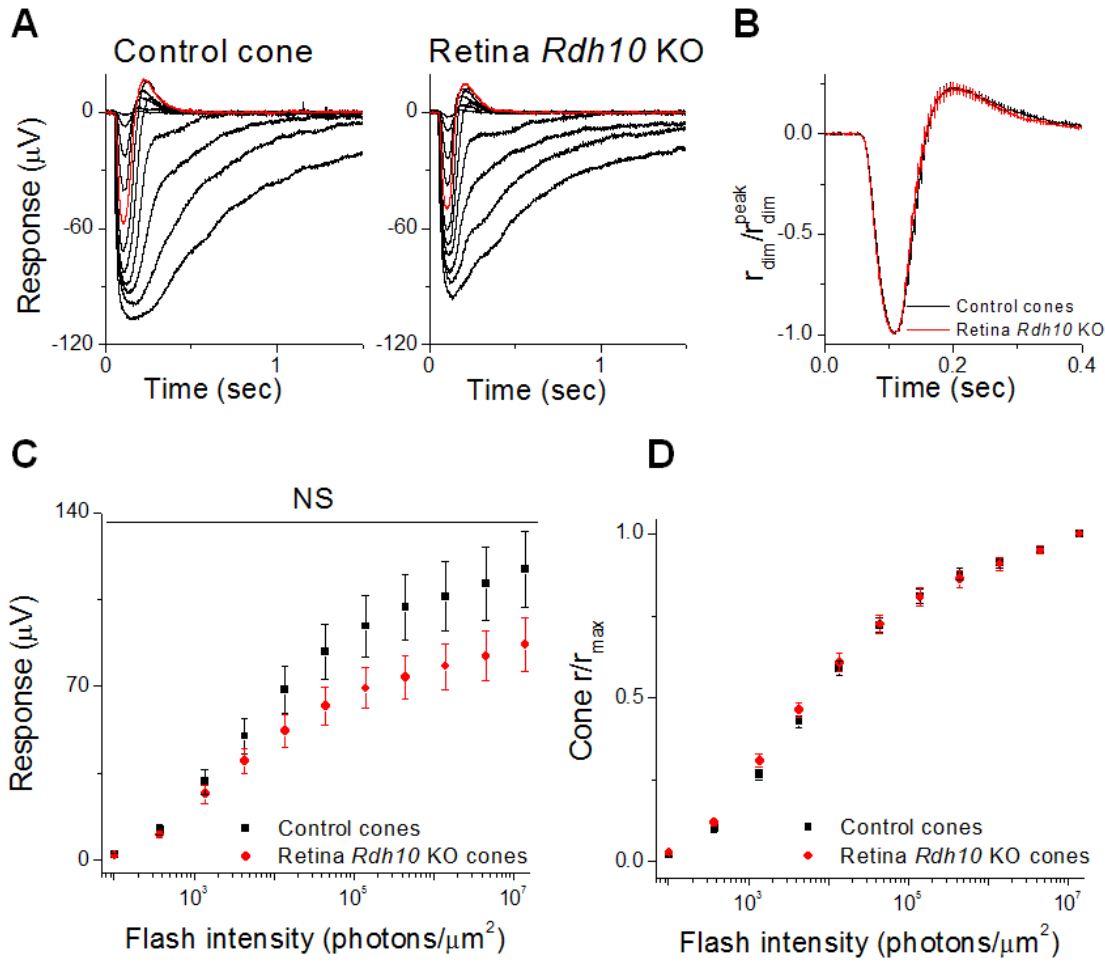
Then we monitored the cone responses with transretinal recordings (Figure 4.6A). The averaged dim flash responses (Figure 4.6B) and normalized intensity response curves (Figure 4.6D) were comparable between the control and retina RDH10 knockout cones, suggesting that the deletion of retina RDH10 does not affect the cone response. The maximal response amplitude of the retina RDH10 knockout cones was also not significantly ($p > 0.05$) different from that of control cones (Figure 4.6C). Together with the cone b-wave responses measured by in vivo ERG (Figure 4.5), these results suggested that cone function is not affected by deleting RDH10 in the retina.

Retina RDH10 is not required for cone dark adaptation and retina visual cycle

It still is not clear what the role of Müller cell RDH10 is in cone dark adaptation. Because RDH10 in the RPE can function as the 11-*cis* retinol dehydrogenase (RDH), converting the retinol to retinal (Wu et al., 2002; Farjo et al., 2009), we speculated that RDH10 may function similarly in the retina by a previously unappreciated reaction, making Müller cells produce 11-*cis* retinal for cone dark adaptation. To examine if this hypothesis is correct, we used transretinal recordings to monitor the cone dark adaptation through the retina visual cycle. However, the recovery kinetics were similar between the retina RDH10 knockout cones and the controls (Figure 4.7A), suggesting that RDH10 in Müller is not required for the retina visual cycle. The in vivo ERG dark adaptation test also confirmed that the deletion of RDH10 in the retina did not affect the overall cone b-wave sensitivity dark adaptation (Figure 4.7B). Together, these results suggest that Müller cell RDH10 is not necessary for the normal cone dark adaptation and the retina visual cycle.

Figure 4.7 The deletion of RDH10 in the retina does not affect cone dark adaptation. (A) Normalized cone sensitivity (S_f / S_f^{DA}) recovery following 90% pigment photobleach in control (n=9, black squares) and retina *Rdh10* KO (n=8, red circles) isolated retinas using transretinal recordings. (B) Normalized cone b-wave sensitivity (b-wave S_f / b-wave S_f^{DA}) recovery following 90% pigment photobleach of control (n=12) and retina *Rdh10* KO (n=10) mice using in vivo ERG recordings.
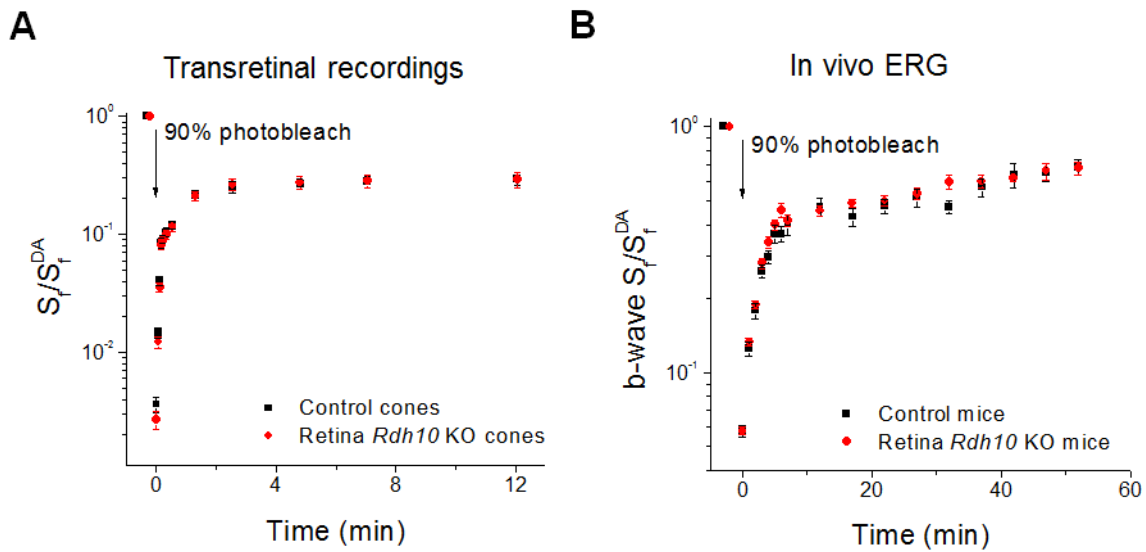
RDH10 is not sufficient to let rods access the retina visual cycle

In the above results, RDH10 in cones and the Müller cells had been demonstrated not necessary for the retina visual cycle. However, if we introduce the RDH10 in the rods, will it enable the rods to access the retina visual cycle, thus accelerating the rod dark adaptation? To answer this question, we generated transgenic *Rdh10* mice with human rhodopsin kinase (GRK1) promoter, which should drive the *Rdh10* expression in all the photoreceptors. We tested the in vivo ERG response of these transgenic *Rdh10* mice (Figure 4.8A), and observed no difference in the scotopic a- and b-wave amplitude between the transgenic *Rdh10* mice and their littermate control (Figure 4.8B & C). The a-wave dark adaptation following strong photobleach was also comparable between the transgenic and control mice (Figure 4.8D & E), suggesting that RDH10 is not sufficient to let rods access the retina visual cycle or to speed up the rod dark adaptation.

Figure 4.8 The expression of RDH10 in the photoreceptors does not affect rod responses or dark adaptation. (A) Representative scotopic in vivo ERG family response traces of control (left panel) and transgenic *Rdh10* (right panel) mice. (B) Ensemble-averaged scotopic a-wave response of control (black squares, n=9) and transgenic *Rdh10* (red circles, n=9) mice by in vivo ERG recordings. (C) Ensemble-averaged scotopic b-wave response of control (black squares, n=9) and transgenic *Rdh10* (red circles, n=9) mice by in vivo ERG recordings. (D) Normalized rod scotopic a-wave maximal response (r_{max} / r^{DA}_{max}) recovery following 90% pigment photobleach in control (n=9, black squares) and transgenic *Rdh10* (n=9, red circles) mice using in vivo ERG. (E) Normalized rod scotopic a-wave sensitivity (S_f / S_f^{DA}) recovery following 90% pigment photobleach of control (black squares, n=9) and transgenic *Rdh10* (red circles, n=9) mice using in vivo ERG recordings.

100
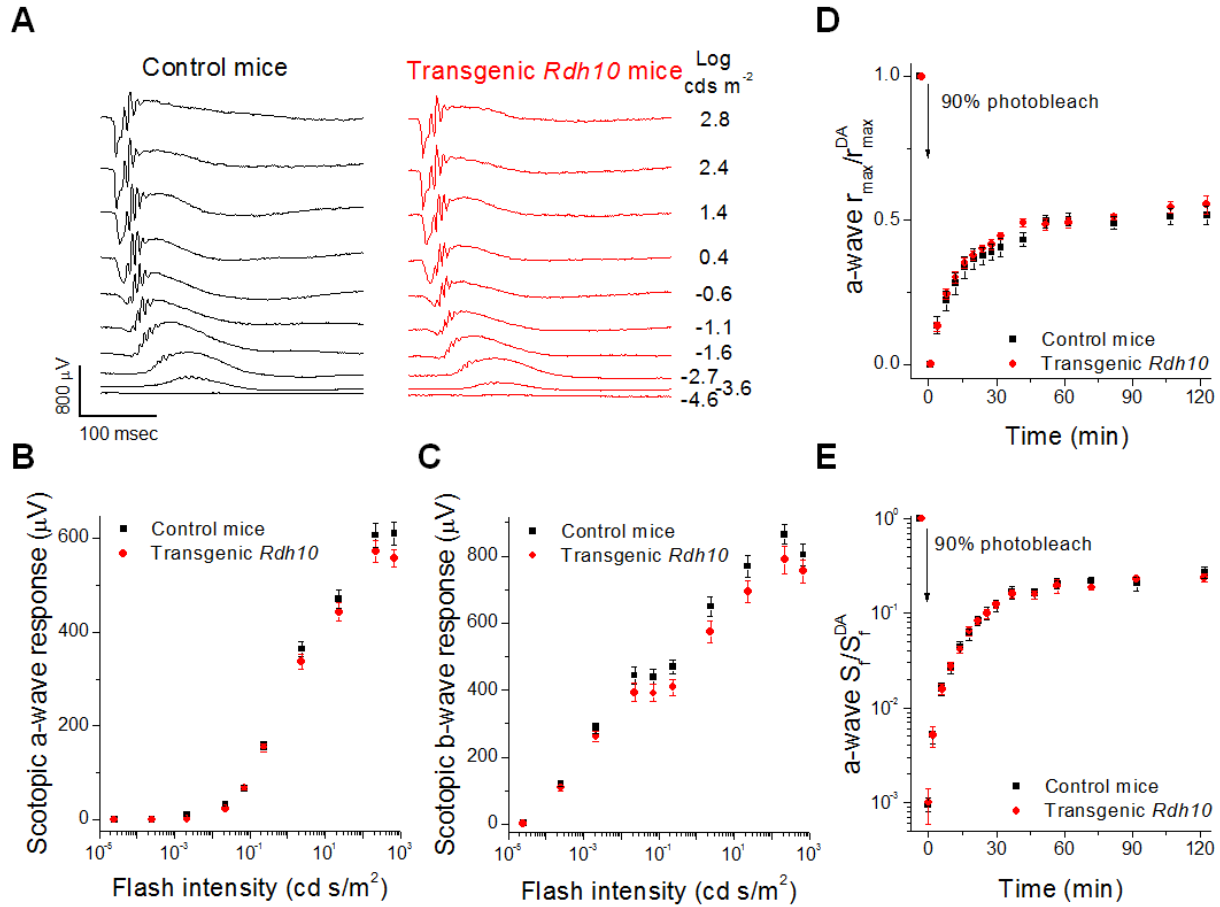
4.5 Discussion

Cones dark adapt faster than rods (Hecht et al., 1937). This rapid dark adaptation is driven by the cones' ability to oxidize 11-*cis* retinol produced by Müller cells (Mata et al., 2002; Wang et al., 2009). Recently, we reported cellular retinaldehyde binding protein (CRALBP) as the first functionally identified player in the retina visual cycle (Xue et al., 2015). However, the rest of the molecular pathway still remains largely unknown. In this study, we examined the possible role of RDH10 as the cone-specific 11-*cis* retinol dehydrogenase. Although the deletion of RDH10 in cones did not affect the cone function and cone dark adaptation (Figure 4.2 - 4.4), it is possible that RDH10 contributes to the oxidation of 11-*cis* retinol with other 11-*cis* RDHs in the cones (Farjo et al., 2009). The importance of the retina visual cycle to cone-mediated vision potentially requires redundancy in the system.

The universal knockout of RDH10 is lethal at embryonic stage (Farjo et al., 2011; Sandell et al., 2012). Our attempt to produce RDH10 Müller cell conditional knockout was unsuccessful using Foxg1-Cre (Ivanova et al., 2010) as we never obtained Foxg1-Cre *Rdh10^{flox/flox}* mice, likely because Foxg1-Cre is not specific to Müller cells but also in telencephalon and other developing head structures (Hébert and McConnell, 2000). This finding is consistent with the report that RDH10 plays an important role in embryonic development (Sandell et al., 2012). RDH10 in RPE and Müller cells has been proposed to support the visual cycle by previous biochemical studies (Wu et al., 2004; Farjo et al., 2009). Our study is the first attempt to functionally identify the 11-*cis* RDH(s) in cones, and also the first attempt to extend the RDH10's function to the retina visual cycle by physiological studies. Because the deletion of RDH10 in the entire retina, including the Müller cells, did not affect cone function and dark adaptation (Figure 4.5 – 4.7),

RDH10 is unlikely to enable the Müller cells to produce previously unappreciated 11-*cis* retinal for the retina visual cycle. RDH10 may be just to support the retinal development by producing the retinaldehyde substrate for retinoid acid synthesis (Farjo et al., 2011; Sandell et al., 2012).

The transgenic *rdh10* rods did not have any improved dark adaptation and their in vivo ERG response remained normal (Figure 4.8), suggesting that RDH10 is not sufficient to enable photoreceptor access to the retina visual cycle. Whereas the transgenic *rdh10* rods still need to be tested for the ability to oxidize and use 11-*cis* retinol as their chromophore, the inability of rods to access the retina visual cycle may be due to other factors like morphology (Jin et al., 1994), or lacking the "correct" RDHs to oxidize the 11-*cis* retinol.

What are the other candidates of 11-*cis* RDH? As reviewed by Parker and Crouch, retSDR1 and RDH8 are found in the cone outer segment, RDH12 found in the cone inner segment, and RDH13 and RDH14 are found in the retina with unknown cellular localization (Parker and Crouch, 2010). Because RDH8 and RDH12 are also expressed in rods, they are unlikely to be the cone-specific RDH we are seeking to identify, making retSDR1, RDH13 and RDH14 remaining candidates. In addition, based on a recent biochemical study on carp cones, mouse RDH14, a homolog of carp RDH13L, is proposed to be the 11-*cis* RDH (Sato et al., 2015). Therefore, we will focus on the role of RDH14 in the retina visual cycle for our future studies.

Chapter 5: Discussion

5.1 Summary

This dissertation reported the most recent research in the mechanism and regulation of mammalian photoreceptor dark adaptation. Building on the past 80 years of dark adaptation research, we advanced the understanding of the retina visual cycle and its role in supporting cone function, as well as the daily variation of RPE visual cycle efficiency in supporting rod function and photoreceptor health, in the following aspects:

In Chapter 2, cellular retinaldehyde binding protein (CRALBP) is demonstrated to be the first functionally identified player in the retina visual cycle. CRALBP is expressed in both RPE and Müller cells. The deletion of CRALBP resulted in impaired cone dark adaptation due to delayed RPE and retina visual cycles in mice (Figure 2.3). CRALBP-deficient mice also present compromised M-cone sensitivity (Figure 2.1 & 2.2), decreased M-cone number (Figure 2.5C), and mislocalized M-opsin (Figure 2.5A). The compromised cone functional in CRALBP-deficient mice can be rescued by dark-rearing but not by exogenous chromophore supply (Figure 2.4), suggesting that the M-cone sensitivity decline is caused by the chronic, but not acute, deprivation of chromophore. Because the rescue of the retina visual cycle, but not the RPE visual cycle, can partially restore the cone-sensitivity (Figure 2.6 & 2.7), we conclude that the retina visual cycle is more important for maintaining mammalian cone function.

In Chapter 3, light history and the circadian clock are shown to down-regulate the RPE visual cycle efficiency in mice during the day. The circadian clock delays the initial dark adaption by about 8 minutes during the day in C3H/f$^{+/+}$ melatonin-proficient mice strain (Figure 3.1). Light exposure further delays the dark adaptation during the day (Figure 3.2A & B). Using

RNA-sequencing and qPCR techniques, we found *Rpe65* mRNA was 30% lower with light history (Figure 3.2C & D). It was also observed that melatonin-deficient strains (i.e. C57BL/6J and 129S2/Sv) do not present this daily variation in RPE visual cycle (Figure 3.3), suggesting that the rhythmic presence of melatonin may be the driving power for RPE visual cycle variation.

In Chapter 4, RDH10 has been demonstrated to be neither necessary for the cones to access the retina visual cycle, nor sufficient for the rods to access the retina visual cycle. The deletion of RDH10 in cones does not affect their function or dark adaptation (Figure 4.2 – 4.4). The deletion of RDH10 in the entire retina also does not change the function or dark adaptation of cones (Figure 4.5 - 4.7). Expressing RDH10 in rods by transgenic technique does not accelerate the rod dark adaptation (Figure 4.8). These results suggest that RDH10 is not the only 11-*cis* dehydrogenase in cones, Müller cell RDH10 is not necessary in retina visual cycle, and there are probably barriers other than lacking 11-*cis* RDHs keeping rods from accessing the retina visual cycle.

In summary, Chapter 2 and 4 provided mechanistic insights about the retina visual cycle's role in supporting cone function, and Chapter 3 revealed previously unknown regulation mechanisms of the RPE visual cycle during the day.

5.2 Implication

5.2.1 Settlement of the "retinoid pool" controversy

As discussed in Chapter 2, there has been controversy about the existence and importance of a second visual cycle in the retina. The opposing side argues that the fast cone dark adaptation originates from a "shared pool of retinoid" (Lamb and Pugh, 2004), while this dissertation is based on the assumption (indeed the fact) that a complete retinoid recycling process exist in the retina through Müller cells to specifically support the fast cone dark adaption. Thus to resolve this debate, a careful examination of the relevant literature is needed.

The concept of "retinoid pool" was created by Rushton in the 1960s through a rod/cone chromophore competition study (Rushton, 1968). This study originally aimed to address the question of whether cone opsin used 11-*cis* retinal as its chromophore similarly to rhodopsin (Rushton, 1968). Rushton believed that this question is under-addressed in Wald's early publication on iodopsin (Wald et al., 1955). Therefore, Rushton carefully designed psychophysical tests to examine human dark adaptation with different wavelengths of bleaching light. If the cone opsins also use 11-*cis* retinal, a competition for the 11-*cis* retinal between rods and cones should be observed in certain dark adaptation scenario. In his experiment, Rushton used red and blue light to bleach each half of the visual field in one eye. The intensity of both bleaching lights was adjusted so that the same amount of rhodopsin was bleached. Because cone opsins had different absorption spectrum from that of rhodopsin, cone visual pigment would be bleached more in the red half of the visual field than the blue half. Then Rushton chose a retina region close to the fovea, which had a 2:1rod to cone ratio, to apply the psychophysical dark adaptation tests.

In this experiment, Rushton observed that the rod dark adaptation was delayed in the red light bleached region, where the cone opsins were more bleached, suggesting a competition for chromophore between rods and cones. Thus he concluded that the cone opsins also used 11-*cis* retinal as their chromophore. However, at a smaller (but still complete) bleaching intensity, the rod dark adaptation was not delayed in the red light region compared to the blue light region. Rushton believed that this unaffected rod dark adaptation was due to the sufficient chromophore supply from a "small store of 11-*cis*", which is now recognized as "shared pool of retinoid" (Lamb and Pugh, 2004), so that there was no competition for chromophore. This "retinoid pool" was inferred based on one of Rushton's earlier studies on the mathematic modeling of visual pigment regeneration, using the data from human reflection densitometry (Rushton and Henry, 1968).

Apparently, Rushton did not intend to use this "retinoid pool" to explain the fast dark adaptation of cones. Therefore, it cannot be used as the direct evidence to challenge the existence of the retina visual cycle. Also, one of the earliest pieces of evidence for the retina visual cycle is that cones can dark adapt in isolated frog retina, while rods cannot (Goldstein, 1970). This "shared retinoid pool" theory could not explain why the cones, but not rods, can dark adapt in isolated retina. Someone may still argue that cones may have the special ability to "plunder" this pool faster over rods. However, the supporting evidence for this argument is weak, and the argument is not consistent with Rushton's calculation and observation that this pool should be "small" and "shared" (Rushton, 1968).

In addition, this "Rushton's pool" is still questionable in its physical presence and even explaining Rushton's own observation. There is no evidence suggesting that a free 11-*cis* retinal storage exist in the retina or RPE (Wald, 1935). The most likely retinoid pools are the all-*trans*

and 11-*cis* retinyl esters in the RPE and Müller cells (Figure 1.5 & 1.6). From Rushton's perspectives, both of the sources could be what the rods and cones competed for. However, in isolated retina where RPE is absent, the amount of Müller cell retinyl ester is limited. Even if this small amount of retinyl ester could specifically support the fast dark adaptation of cones, enzymes and CRALBP would be required for the isomerization, esterification and hydrolysis of the retinyl ester (Kaylor et al., 2014). Due to the requirement of enzymes and supportive proteins, Rushton's pool would fall into the realm of retina visual cycle in this scenario.

Furthermore, Rushton's experiment was done almost 50 years ago. Research on the visual cycle has advanced significantly with more knowledge in the biochemistry and physiology of the two pathways, as introduced extensively in this dissertation. Actually, the down-regulation of the RPE visual cycle by light (see Chapter 3) can provide a novel explanation for Rushton's observation of delayed rod dark adaptation in brighter red light. Therefore, Rushton's observation cannot be used as the evidence against existence of the modern retina visual cycle.

5.2.2 Speculations on the evolution of retina visual cycle

"*Nothing in biology makes sense except in the light of evolution*" (Dobzhansky, 1973). In "*The Origin of Species*", Charles Darwin envisioned the formation of the complicated eye from simple pigment as an ultimate example of natural selection (Darwin, 1872. pp. 143-146).

How does the retina visual cycle fit in the story of evolution?

Partially addressing this question, Lamb wrote two remarkable review articles on the evolution of vertebrate eyes (Lamb et al., 2007; Lamb, 2013). He proposed three milestones for the evolution of visual cycle in vertebrate retina (Lamb, 2013). First, in early chordate evolution,

once ancestral ciliary opsin (C-opsin) attained the ability to release its chromophore, the ancestral photoreceptor needed to get 11-*cis* retinoid from other cells, presumably the Müller cells. Second, when C-opsin lost the ability for photoreversal, the retina visual cycle emerged in later chordate evolution. Finally, the RPE visual cycle emerged with vertebrates, based on the evidence that key RPE visual cycle proteins (RPE65 and LRAT) are present exclusively in vertebrates.

In short, Lamb's hypothesis landmarks the visual cycle evolution into three steps, 1) Müller cell served as the source of 11-*cis* retinoid, 2) modern retina visual cycle emerged, and 3) RPE visual cycle emerged.

Lamb's milestones have brought valuable insights into the evolution of the retina visual cycle, however, one observation casts shadow on this theory, questioning Lamb's first step. This observation is that Müller cells, the key player in retina visual cycle, are born very late in retina development (see Cepko, 2014 for review).

As envisioned by Darwin, the development of embryos provided valuable information on the history of evolution, creating the field of evolutionary developmental biology (Darwin, 1872. pp.386-396). Müller cells appear late in murine retina embryogenesis, even after the rods and cone bipolar cells, suggesting that modern Müller cells emerged late in evolution (Cepko, 2014).

Nonetheless, this observation does not necessarily mean the retina visual cycle occurred late in the evolution. Genetic studies on visual cycle proteins might support an earlier genesis of retina visual cycle. For example, an in silico study suggested that CRALBP, which is crucial to the retina visual cycle (see Chapter 2), emerged in ascidian genome, while RPE65 and LRAT, two key RPE visual cycle proteins, emerged later in vertebrate genome (Albalat, 2012). This

108

result suggests that before the evolution of RPE visual cycle, a Müller cell ancestor probably existed and was able to recycle chromophore for the photoreceptor ancestor.

To reveal the identity of this unknown Müller cell ancestor, which is inferred in Lamb's step 1, the morphology of "living fossil" chordate models, such as ascidian larvae and hagfish, may provide further insights. Ascidian larvae present a structure called ocellus, which has everted photoreceptors (i.e. outer segment facing the light) protruding from a pigmented cell without glia cells presence (Lamb, 2013. Fig. 6). Because of the pigmentation, the ocellus pigmented cell was assumed to be the ancestor of the modern RPE cell. In hagfish eye patch, which is believed to be a prototype of eye in evolution between the ascidian larvae ocellus and vertebrate eye, we see "RPE" and inverted photoreceptors surrounded by "glia" (likely to be the ancestral Müller cell), but no other vertebrate retinal cells except for ancestral ganglion cells (Lamb, 2013. Fig. 9). Therefore, ascidian larvae ocellus might be the common ancestor of hagfish "RPE" and "glia". In addition, as indirect evidence of this hypothesis or speculation, CRALBP (see Chapter 2), CRBP and Retinal G protein coupled receptor (RGR) present in both vertebrate RPE and Müller cells.

Taken together, although the evolution of visual cycle can be reconstructed with other models, the simplest steps fitting with the above observations would be:

1) A common ancestor of Müller cell and RPE emerged as the external source of 11-*cis* retinoid for ancestral photoreceptor. This ancestor is possibly equipped with 11-*cis* isomerase (probably DES1), CRALBP homologs and pigmentation, forming a structure similar to the ascidian larvae ocellus.

2) Photoreceptors got inverted (with their outer segments facing back from the incoming light direction). A lineage of pigmented cells lost their pigmentation to let light through, and became ancestral glia. Another lineage of pigment cells separated from the photoreceptor and the glia, and formed ancestral RPE. These three steps might happen in a short period of time to evolve a structure similar to the hagfish eye patch.

3) The RPE visual cycle emerged with the functional evolution of RPE65 and LRAT in early vertebrates.

4) With the emergence of other retinal cell types complicating the retina structure, the ancestral glia cells underwent morphological changes to support the function of retina, forming the modern retina visual cycle.

To validate the above speculations, future experiments should be conducted, including the detailed molecular mechanism of retina visual cycle, the evolutionary development of RPE, photoreceptors and Müller cells, the molecular genetics of visual cycle proteins, as well as the biochemical and functional studies of prototypical photoreceptors from evolution model organisms, such as ascidian larvae (or their substitute), hagfish and lampreys.

5.2.3 Another challenge in the retina visual cycle

After publishing Chapter 2, we received a comment that there is no genetic evidence of retina visual cycle related human disease, implying that the retina visual cycle is functionally insignificant at least to humans (Jacobson et al., 2015). We disagree with this comment, because as discussed in Chapter 2, the mutations in human CRALBP lead to cone distortions that can be characterized in several forms of retinal diseases.

Furthermore, we speculate that this comment may actually mean "a unique symptom of impaired retina visual cycle has never been observed in humans, while the RPE visual cycle is kept intact". This missing symptom, as explored on the CRALBP-deficient mouse model (Chapter 2), is likely to be poor vision in dim light condition mediated by cones. However, this presumed cone-specific symptom may get compensated by normal rod function in dim ambient light. This presumed symptom can also be easily missed in clinics, because vision in dim light unfortunately is not a standard examination in ophthalmology. Yet there are many clinical cases of cone dystrophy of unknown cause. It is difficult to link these cases with retina visual cycle due to the lack of knowledge in retina visual cycle molecular mechanisms, but the possibility should be kept in mind.

In addition, because this retina visual cycle is Vitamin A based, systemic mutation of a signature molecule in retina visual cycle will probably lead to early embryonic death, such as the case of RDH10 (Farjo et al., 2011; Sandell et al., 2012). Fetuses carrying the mutations may not even survive to birth, and thus will never reach the stage of reporting vision problems. In addition, as discussed in the previous section, the early evolutionary emergence of the retina visual cycle pathway, may lead to redundancy in the system, further lowering the chance of getting retina visual cycle specific disease.

5.3 Future directions

The biggest unknowns that need to be addressed in the future are the identities of the key molecular players in the retina visual cycle. Recently, DES1 and MFAT have been proposed as the 11-*cis* isomerase and 11-*cis* retinyl ester synthase in Müller cells, respectively (Kaylor et al., 2013, 2014). Therefore, the next step is to conduct loss of function study with DES1 and MFAT on *Gnat1*$^{-/-}$ mouse background to examine if the function of retina visual cycle would be altered. Considering the wide expression of DES1 in liver, kidney and skin (Kaylor et al., 2013), systemic knockout may lead to early death of the animal. Therefore, conditional knockout using Cre-LoxP recombinase will likely need to be used.

In terms of future studies along the directions covered within the scope of this dissertation:

First along Chapter 2, the ability of CRALBP in delivering 11-*cis* retinol out of RPE to cones should be examined (Collery et al., 2008). Conventionally, 11-*cis* retinal is thought to be the only recycling product released by the RPE for pigment regeneration. CRALBP carries 11-*cis* retinol and facilitates the catalysis of retinol oxidization in the RPE as in Müller cells. To examine if RPE CRALBP can deliver 11-*cis* retinol out of the RPE, CRALBP-assisted exiting mechanism of 11-*cis* retinol from Müller cell should be studied first. Then it should be studied whether this mechanism can be generalized to RPE. It would be interesting to know if there is 11-*cis* retinol coming from RPE for cone dark adaptation.

Second along Chapter 3, circadian and light regulation should be examined in human subjects with psychophysical studies. The experimental design can be similar to the ERG examination, while the sensitivity recovery could be checked at both the fovea and peripheral

regions. In addition, the mechanism of light regulated RPE65 transcription should be examined carefully. Is it a secondary effect of the retinal melatonin-dopamine oscillation? Is the RPE intrinsically sensitive to light, thus changing the RPE65 gene transcription? Actually, RPE is equipped with light-sensing molecule, which is RPE-retinal G-protein coupled receptor (RGR). RGR responds to light and is expressed in both RPE and Müller cells. RGR modulates the RPE visual cycle in dark and light conditions (Radu et al., 2008). Could RGR contribute to the down-regulation of RPE65 by light? As an extended question, what is the contribution of Müller cell RGR to the retina visual cycle?

Third along Chapter 4, the identity of 11-*cis* RDHs allowing cones to oxidize 11-*cis* retinol should be examined, as discussed in Chapter 4. Furthermore, in addition to the cone-specific 11-*cis* RDH hypothesis, how do evolved structural differences cause rods to lose their ability to access the retina visual cycle? As a first clue, the salamander rods cannot dark adapt if the chromophore is delivered from the inner segment instead of the outer segment (Jin et al., 1994), while the retina visual cycle is likely to use the inner segment because it is close to the Müller cell. As a second clue, rod nuclei are scattered in the ONL, while cone nuclei are aligned well on the top of ONL (Razafsky et al., 2012). Our recent study revealed that the cone dark adaptation was compromised if their nuclei were mislocalized to the bottom of ONL (Razafsky and Xue et al., unpublished data), implying rods are disadvantaged in getting chromophore.

Finally as an additional bold speculation, does the immuno-activated Müller cell affect retina visual cycle and cone function? We recently studied how the deletion of ALMS1, which is a protein involved in Alström syndrome, affected the cone function and retina visual cycle in collaboration with Nishina's group at Jackson Laboratory. We found that ALMS1-deficient mice presented early cone photoreceptor degeneration and accelerated cone dark adaption through the

retina visual cycle, correlating with the activation of Müller cells. In addition, activated Müller cells may be a sign of some neurological diseases. It is reported that one Alzheimer's disease (AD) mouse model presents activated Müller cells (Edwards et al., 2014). Therefore, we explored the photoreceptors dark adaptation on an AD mouse model (APP/PS1 ApoE4$^{+/+}$) in collaboration with Holtzman's Lab at Washington University. Although the results were not significant, we observed that the cone dark adaptation seemed to operate faster in AD mice. Will this difference be significant on $Gnat1^{-/-}$ background AD mice? More importantly, are there any dark adaptation changes in human AD patients? Could the electrophysiology and psychophysical dark adaptation tests help to diagnose neurological diseases in the future?

In summary, there are many exciting research directions in the visual cycle remaining to be explored, including the identities of key molecules in retina visual cycle, the mechanism for light regulation on RPE visual cycle, rod-cone structural differences, the evolutionary origin, and possible implication for the diagnosis of neurological diseases.

References

Ablonczy Z, Crouch RK, Goletz PW, Redmond TM, Knapp DR, Ma J-X, Rohrer B (2002) 11-cis-retinal reduces constitutive opsin phosphorylation and improves quantum catch in retinoid-deficient mouse rod photoreceptors. J Biol Chem 277:40491–40498.

Albalat R (2012) Evolution of the genetic machinery of the visual cycle: a novelty of the vertebrate eye? Mol Biol Evol 29:1461–1469.

Anders S, Pyl PT, Huber W (2014) HTSeq - A Python framework to work with high-throughput sequencing data. Bioinformatics 31:166–169.

Anon (n.d.) Normal eye anatomy. Fam eyecare Spec Available at: http://www.familyeyes.com/images/eye_anatomy.png.

Applebury M., Antoch M., Baxter L., Chun LL., Falk J., Farhangfar F, Kage K, Krzystolik M., Lyass L., Robbins J. (2000) The Murine Cone Photoreceptor. Neuron 27:513–523.

Arshavsky VY, Lamb TD, Pugh EN (2002) G proteins and phototransduction. Annu Rev Physiol 64:153–187.

Aurnhammer C, Haase M, Muether N, Hausl M, Rauschhuber C, Huber I, Nitschko H, Busch U, Sing A, Ehrhardt A, Baiker A (2012) Universal real-time PCR for the detection and quantification of adeno-associated virus serotype 2-derived inverted terminal repeat sequences. Hum Gene Ther Methods 23:18–28.

Baba K, Mazzoni F, Owino S, Contreras-Alcantara S, Strettoi E, Tosini G (2012) Age-related changes in the daily rhythm of photoreceptor functioning and circuitry in a melatonin-proficient mouse strain. PLoS One 7:e37799.

Baba K, Pozdeyev N, Mazzoni F, Contreras-alcantara S, Liu C, Kasamatsu M, Martinez-merlos T, Strettoi E, Iuvone PM, Tosini G (2009) Melatonin modulates visual function and cell viability in the mouse retina via the MT1 melatonin receptor. Proc Natl Acad Sci 106:15043–15048.

Babino D, Perkins BD, Kindermann A, Oberhauser V, von Lintig J (2014) The role of 11-cis-retinyl esters in vertebrate cone vision. FASEB J.

Bok D (1993) The retinal pigment epithelium: a versatile partner in vision. J Cell Sci Suppl 17:189–195.

Bok D, Heller J (1976) Transport of retinol from the blood to the retina: an autoradiographic study of the pigment epithelial cell surface receptor for plasma retinol-binding protein. Exp Eye Res 22:395–402.

Bonilha VL, Bhattacharya SK, West KA, Crabb JS, Sun J, Rayborn ME, Nawrot M, Saari JC, Crabb JW (2004) Support for a proposed retinoid-processing protein complex in apical retinal pigment epithelium. Exp Eye Res 79:419–422.

Burstedt MS, Forsman-Semb K, Golovleva I, Janunger T, Wachtmeister L, Sandgren O (2001) Ocular phenotype of bothnia dystrophy, an autosomal recessive retinitis pigmentosa associated with an R234W mutation in the RLBP1 gene. Arch Ophthalmol 119:260–267.

Burstedt MS, Sandgren O, Holmgren G, Forsman-Semb K (1999) Bothnia dystrophy caused by mutations in the cellular retinaldehyde-binding protein gene (RLBP1) on chromosome 15q26. Invest Ophthalmol Vis Sci 40:995–1000.

Burstedt MSI, Sandgren O, Golovleva I, Wachtmeister L (2003) Retinal function in Bothnia dystrophy. An electrophysiological study. Vision Res 43:2559–2571.

Cahill GM, Besharse JC (1993) Circadian clock functions localized in xenopus retinal photoreceptors. Neuron 10:573–577.

Calvert PD, Krasnoperova N V, Lyubarsky a L, Isayama T, Nicol ó M, Kosaras B, Wong G, Gannon KS, Margolskee RF, Sidman RL, Pugh EN, Makino CL, Lem J (2000) Phototransduction in transgenic mice after targeted deletion of the rod transducin alpha - subunit. Proc Natl Acad Sci U S A 97:13913–13918.

Cameron MA, Barnard AR, Lucas RJ (2008) The electroretinogram as a method for studying circadian rhythms in the mammalian retina. J Genet 87:459–466.

Cepko C (2014) Intrinsically different retinal progenitor cells produce specific types of progeny. Nat Rev Neurosci 15:615–627.

Collery R, McLoughlin S, Vendrell V, Finnegan J, Crabb JW, Saari JC, Kennedy BN (2008) Duplication and divergence of zebrafish CRALBP genes uncovers novel role for RPE- and Muller-CRALBP in cone vision. Invest Ophthalmol Vis Sci 49:3812–3820.

Corbo JC, Cepko CL (2005) A hybrid photoreceptor expressing both rod and cone genes in a mouse model of enhanced S-cone syndrome. PLoS Genet 1:e11.

Cottet S, Michaut L, Boisset G, Schlecht U, Gehring W, Schorderet DF (2006) Biological characterization of gene response in Rpe65-/- mouse model of Leber's congenital amaurosis during progression of the disease. FASEB J 20:2036–2049.

Cunea A, Powner MB, Jeffery G (2014) Death by color: differential cone loss in the aging mouse retina. Neurobiol Aging 35:2584–2591.

Curcio CA, Allen KA, Sloan KR, Lerea CL, Hurley JB, Klock IB, Milam AH (1991) Distribution and morphology of human cone photoreceptors stained with anti-blue opsin. J

Comp Neurol 312:610–624.

Dalkara D, Byrne LC, Klimczak RR, Visel M, Yin L, Merigan WH, Flannery JG, Schaffer D V (2013) In vivo-directed evolution of a new adeno-associated virus for therapeutic outer retinal gene delivery from the vitreous. Sci Transl Med 5:189ra76.

Darwin C (1872) The origin of species by means of natural selection, or the preservation of favoured races in the struggle for life, 6th ed. London: John Murray.

Das SR, Bhardwaj N, Kjeldbye H, Gouras P (1992) Muller cells of chicken retina synthesize 11-cis-retinol. Biochem J 285(3):907–913.

Dobzhansky T (1973) Nothing in Biology Makes Sense except in the Light of Evolution. Am Biol Teach 35:125–129.

Donner KO, Reuter T (1967) Dark-adaptation processes in the rhodopsin rods of the frog's retina. Vision Res 7:17–41.

Dowling JE (1960) Chemistry of visual adaptation in the rat. Nature 188:114–118.

Doyle SE, Grace MS, Mcivor W, Menaker M (2002) Circadian rhythms of dopamine in mouse retina : The role of melatonin. Vis Neurosci:593–601.

Dunn FA, Della Santina L, Parker ED, Wong ROL (2013) Sensory experience shapes the development of the visual system's first synapse. Neuron 80:1159–1166.

Edwards MM, Rodrǵuez JJ, Gutierrez-Lanza R, Yates J, Verkhratsky A, Lutty GA (2014) Retinal macroglia changes in a triple transgenic mouse model of Alzheimer's disease. Exp Eye Res 127:252–260.

Eichers ER, Green JS, Stockton DW, Jackman CS, Whelan J, McNamara JA, Johnson GJ, Lupski JR, Katsanis N (2002) Newfoundland rod-cone dystrophy, an early-onset retinal dystrophy, is caused by splice-junction mutations in RLBP1. Am J Hum Genet 70:955–964.

Emran F, Rihel J, Adolph AR, Dowling JE (2010) Zebrafish larvae lose vision at night. Proc Natl Acad Sci U S A 107:6034–6039.

Esumi N, Oshima Y, Li Y, Campochiaro PA, Zack DJ (2004) Analysis of the VMD2 promoter and implication of E-box binding factors in its regulation. J Biol Chem 279:19064–19073.

Fain GL, Matthews HR, Cornwall MC, Koutalos Y (2001) Adaptation in vertebrate photoreceptors. Physiol Rev 81:117–151.

Farjo KM, Moiseyev G, Nikolaeva O, Sandell LL, Trainor PA, Ma J (2011) RDH10 is the primary enzyme responsible for the first step of embryonic Vitamin A metabolism and retinoic acid synthesis. Dev Biol 357:347–355.

Farjo KM, Moiseyev G, Takahashi Y, Crouch RK, Ma J (2009) The 11-cis-retinol dehydrogenase activity of RDH10 and its interaction with visual cycle proteins. Invest Ophthalmol Vis Sci 50:5089–5097.

Fleisch VC, Schonthaler HB, von Lintig J, Neuhauss SCF (2008) Subfunctionalization of a retinoid-binding protein provides evidence for two parallel visual cycles in the cone-dominant zebrafish retina. J Neurosci 28:8208–8216.

Flicek P et al. (2014) Ensembl 2014. Nucleic Acids Res 42:D749–D755.

Fu Y, Yau K-W (2007) Phototransduction in mouse rods and cones. Pflugers Arch 454:805–819.

Gibson JJ (1933) Adaptation, after-effect and contrast in the perception of curved lines. J Exp Psychol 16:1–31.

Goldman AI, Teirstein PS, Brien PO (1980) Investigative Ophthalmology & Visual Science disc shedding in the rod outer segment of the rat retina. Invest Ophthalmol Vis Sci 19:1257–1267.

Goldstein EB (1970) Cone pigment regeneration in the isolated frog retina. Vision Res 10:1065–1068.

Gollapalli DR, Rando RR (2004) The specific binding of retinoic acid to RPE65 and approaches to the treatment of macular degeneration. Proc Natl Acad Sci U S A 101:10030–10035.

Green DG (1971) Light adaptation in the rat retina: evidence for two receptor mechanisms. Science 174:598–600.

Hagins WA, Penn RD, Yoshikami S (1970) Dark current and photocurrent in retinal rods. Biophys J 10:380–412.

Hattar S, Lucas RJ, Mrosovsky N, Thompson S, Douglas RH, Hankins MW, Lem J, Biel M, Hofmann F, Foster RG, Yau K-W (2003) Melanopsin and rod-cone photoreceptive systems account for all major accessory visual functions in mice. Nature 424:76–81.

Hébert JM, McConnell SK (2000) Targeting of cre to the Foxg1 (BF-1) locus mediates loxP recombination in the telencephalon and other developing head structures. Dev Biol 222:296–306.

Hecht S, Haig C, Chase AM (1937) The influence of light adaptation on subsequent dark adaptation of the eye. J Gen Physiol 20:831–850.

Imai H, Kefalov V, Sakurai K, Chisaka O, Ueda Y, Onishi A, Morizumi T, Fu Y, Ichikawa K, Nakatani K, Honda Y, Chen J, Yau K-W, Shichida Y (2007) Molecular properties of rhodopsin and rod function. J Biol Chem 282:6677–6684.

Insinna C, Daniele LL, Davis JA, Larsen DD, Kuemmel C, Wang J, Nikonov SS, Knox BE,

Pugh EN (2012) An S-opsin knock-in mouse (F81Y) reveals a role for the native ligand 11-cis-retinal in cone opsin biosynthesis. J Neurosci 32:8094–8104.

Ivanova E, Hwang G-S, Pan Z-H (2010) Characterization of transgenic mouse lines expressing Cre recombinase in the retina. Neuroscience 165:233–243.

Jacobson SG, Aleman TS, Cideciyan A V., Heon E, Golczak M, Beltran WA, Sumaroka A, Schwartz SB, Roman AJ, Windsor EAM, Wilson JM, Aguirre GD, Stone EM, Palczewski K (2007) Human cone photoreceptor dependence on RPE65 isomerase. Proc Natl Acad Sci 104:15123–15128.

Jacobson SG, Cideciyan A V, Aguirre GD, Roman AJ, Sumaroka A, Hauswirth WW, Palczewski K (2015) Improvement in vision: a new goal for treatment of hereditary retinal degenerations. Expert Opin orphan drugs 3:563–575.

Jeon CJ, Strettoi E, Masland RH (1998) The major cell populations of the mouse retina. J Neurosci 18:8936–8946.

Jiang T, Chang Q, Zhao Z, Yan S, Wang L, Cai J, Xu G (2012) Melatonin-mediated cytoprotection against hyperglycemic injury in Müller cells. PLoS One 7:e50661.

Jin J, Jones GJ, Cornwall MC (1994) Movement of retinal along cone and rod photoreceptors. Vis Neurosci 11:389–399.

Jin M, Li S, Moghrabi WN, Sun H, Travis GH (2005) Rpe65 is the retinoid isomerase in bovine retinal pigment epithelium. Cell 122:449–459.

Jin M, Li S, Nusinowitz S, Lloyd M, Hu J, Radu RA, Bok D, Travis GH (2009) The role of interphotoreceptor retinoid-binding protein on the translocation of visual retinoids and function of cone photoreceptors. J Neurosci 29:1486–1495.

Jin NG, Chuang AZ, Masson PJ, Ribelayga CP (2015) Rod electrical coupling is controlled by a circadian clock and dopamine in mouse retina. J Physiol 593:1597–1631.

Jones GJ, Crouch RK, Wiggert B, Cornwall MC, Chader GJ (1989) Retinoid requirements for recovery of sensitivity after visual-pigment bleaching in isolated photoreceptors. Proc Natl Acad Sci U S A 86:9606–9610.

Kasahara T, Abe K, Mekada K, Yoshiki A, Kato T (2010) Genetic variation of melatonin productivity in laboratory mice under domestication. Proc Natl Acad Sci U S A 107:6412–6417.

Katsanis N, Shroyer NF, Lewis RA, Cavender JC, Al-Rajhi AA, Jabak M, Lupski JR (2001) Fundus albipunctatus and retinitis punctata albescens in a pedigree with an R150Q mutation in RLBP1. Clin Genet 59:424–429.

Kawaguchi R, Yu J, Honda J, Hu J, Whitelegge J, Ping P, Wiita P, Bok D, Sun H (2007) A membrane receptor for retinol binding protein mediates cellular uptake of vitamin A. Science 315:820–825.

Kaylor JJ, Cook JD, Makshanoff J, Bischoff N, Yong J, Travis GH (2014) Identification of the 11-cis-specific retinyl-ester synthase in retinal Müller cells as multifunctional O-acyltransferase (MFAT). Proc Natl Acad Sci U S A 111:7302–7307.

Kaylor JJ, Yuan Q, Cook J, Sarfare S, Makshanoff J, Miu A, Kim A, Kim P, Habib S, Roybal CN, Xu T, Nusinowitz S, Travis GH (2013) Identification of DES1 as a vitamin A isomerase in Müller glial cells of the retina. Nat Chem Biol 9:30–36.

Kefalov VJ (2012) Rod and cone visual pigments and phototransduction through pharmacological, genetic, and physiological approaches. J Biol Chem 287:1635–1641.

Keller C, Grimm C, Wenzel A, Hafezi F, Remé C (2001) Protective effect of halothane anesthesia on retinal light damage: inhibition of metabolic rhodopsin regeneration. Invest Ophthalmol Vis Sci 42:476–480.

Kim J-Y, Zhao H, Martinez J, Doggett TA, Kolesnikov A V, Tang PH, Ablonczy Z, Chan C-C, Zhou Z, Green DR, Ferguson TA (2013) Noncanonical autophagy promotes the visual cycle. Cell 154:365–376.

Kiser PD, Golczak M, Palczewski K (2014) Chemistry of the retinoid (visual) cycle. Chem Rev 114:194–232.

Klimczak RR, Koerber JT, Dalkara D, Flannery JG, Schaffer D V (2009) A novel adeno-associated viral variant for efficient and selective intravitreal transduction of rat Müller cells. PLoS One 4:e7467.

Kolb H (1970) Organization of the outer plexiform layer of the primate retina: electron microscopy of Golgi-impregnated cells. Philos Trans R Soc Lond B Biol Sci 258:261–283.

Kolesnikov A V, Golobokova EY, Govardovskii VI (2003) The identity of metarhodopsin III. Vis Neurosci 20:249–265.

Kolesnikov A V, Tang PH, Parker RO, Crouch RK, Kefalov VJ (2011) The Mammalian cone visual cycle promotes rapid m/l-cone pigment regeneration independently of the interphotoreceptor retinoid-binding protein. 2. J Neurosci 31:7900–7909.

Lamb TD (2013) Evolution of phototransduction, vertebrate photoreceptors and retina. Prog Retin Eye Res 36:52–119.

Lamb TD, Collin SP, Pugh EN (2007) Evolution of the vertebrate eye: opsins, photoreceptors, retina and eye cup. Nat Rev Neurosci 8:960–976.

Lamb TD, Pugh EN (2004) Dark adaptation and the retinoid cycle of vision. Prog Retin Eye Res 23:307–380.

Langmead B, Salzberg SL (2012) Fast gapped-read alignment with Bowtie 2. Nat Methods 9:357–359.

Liu T, Jenwitheesuk E, Teller DC, Samudrala R (2005) Structural insights into the cellular retinaldehyde-binding protein (CRALBP). Proteins 61:412–422.

Lucas RJ, Hattar S, Takao M, Berson DM, Foster RG, Yau K-W (2003) Diminished pupillary light reflex at high irradiances in melanopsin-knockout mice. Science 299:245–247.

Maeda A, Maeda T, Golczak M, Chou S, Desai A, Hoppel CL, Matsuyama S, Palczewski K (2009) Involvement of all-trans-retinal in acute light-induced retinopathy of mice. J Biol Chem 284:15173–15183.

Maeda A, Maeda T, Golczak M, Palczewski K (2008) Retinopathy in mice induced by disrupted all-trans-retinal clearance. J Biol Chem 283:26684–26693.

Mahroo OAR, Lamb TD (2012) Slowed recovery of human photopic ERG a-wave amplitude following intense bleaches: a slowing of cone pigment regeneration? Doc Ophthalmol 125:137–147.

Masland RH (2012) The neuronal organization of the retina. Neuron 76:266–280.

Mata NL, Radu RA, Clemmons RS, Travis GH (2002) Isomerization and Oxidation of Vitamin A in Cone-Dominant Retinas. Neuron 36:69–80.

Mattapallil MJ, Wawrousek EF, Chan C-C, Zhao H, Roychoudhury J, Ferguson TA, Caspi RR (2012) The Rd8 mutation of the Crb1 gene is present in vendor lines of C57BL/6N mice and embryonic stem cells, and confounds ocular induced mutant phenotypes. Invest Ophthalmol Vis Sci 53:2921–2927.

Matthews G (1983) Physiological characteristics of single green rod photoreceptors from toad retina. J Physiol 342:347–359.

Maw MA, Kennedy B, Knight A, Bridges R, Roth KE, Mani EJ, Mukkadan JK, Nancarrow D, Crabb JW, Denton MJ (1997) Mutation of the gene encoding cellular retinaldehyde-binding protein in autosomal recessive retinitis pigmentosa. Nat Genet 17:198–200.

Miyazono S, Shimauchi-Matsukawa Y, Tachibanaki S, Kawamura S (2008) Highly efficient retinal metabolism in cones. Proc Natl Acad Sci U S A 105:16051–16056.

Mondal MS, Ruiz A, Bok D, Rando RR (2000) Lecithin retinol acyltransferase contains cysteine residues essential for catalysis. Biochemistry 39:5215–5220.

Montana CL, Lawrence KA, Williams NL, Tran NM, Peng G-H, Chen S, Corbo JC (2011)

Transcriptional regulation of neural retina leucine zipper (Nrl), a photoreceptor cell fate determinant. J Biol Chem 286:36921–36931.

Morimura H, Berson EL, Dryja TP (1999) Recessive mutations in the RLBP1 gene encoding cellular retinaldehyde-binding protein in a form of retinitis punctata albescens. Invest Ophthalmol Vis Sci 40:1000–1004.

Muniz A, Betts BS, Trevino AR, Buddavarapu K, Roman R, Ma J-X, Tsin ATC (2009) Evidence for two retinoid cycles in the cone-dominated chicken eye. Biochemistry 48:6854–6863.

Mustafi D, Engel AH, Palczewski K (2009) Structure of cone photoreceptors. Prog Retin Eye Res 28:289–302.

Napoli JL (2000) A gene knockout corroborates the integral function of cellular retinol-binding protein in retinoid metabolism. Nutr Rev 58:230–236.

Nash MS, Osborne NN (1995) Pertussis toxin-sensitive melatonin receptors negatively coupled to adenylate cyclase associated with cultured human and rat retinal pigment epithelial cells. Invest Ophthalmol Vis Sci 36:95–102.

Nawrot M, West K, Huang J, Possin DE, Bretscher A, Crabb JW, Saari JC (2004) Cellular retinaldehyde-binding protein interacts with ERM-binding phosphoprotein 50 in retinal pigment epithelium. Invest Ophthalmol Vis Sci 45:393–401.

Naz S, Ali S, Riazuddin SA, Farooq T, Butt NH, Zafar AU, Khan SN, Husnain T, Macdonald IM, Sieving PA, Hejtmancik JF, Riazuddin S (2011) Mutations in RLBP1 associated with fundus albipunctatus in consanguineous Pakistani families. Br J Ophthalmol 95:1019–1024.

Nikonov SS, Daniele LL, Zhu X, Craft CM, Swaroop A, Pugh EN (2005) Photoreceptors of Nrl - /- mice coexpress functional S- and M-cone opsins having distinct inactivation mechanisms. J Gen Physiol 125:287–304.

Nikonov SS, Kholodenko R, Lem J, Pugh EN (2006) Physiological features of the S- and M-cone photoreceptors of wild-type mice from single-cell recordings. J Gen Physiol 127:359–374.

Nishiguchi KM, Carvalho LS, Rizzi M, Powell K, Holthaus S-MK, Azam SA, Duran Y, Ribeiro J, Luhmann UFO, Bainbridge JWB, Smith AJ, Ali RR (2015) Gene therapy restores vision in rd1 mice after removal of a confounding mutation in Gpr179. Nat Commun 6:6006.

Okajima TI, Pepperberg DR, Ripps H, Wiggert B, Chader GJ (1989) Interphotoreceptor retinoid-binding protein: role in delivery of retinol to the pigment epithelium. Exp Eye Res 49:629–644.

Organisciak DT, Darrow RM, Barsalou L, Kutty RK, Wiggert B (2000) Circadian-dependent

retinal light damage in rats. Invest Ophthalmol Vis Sci 41:3694–3701.

Organisciak DT, Vaughan DK (2010) Retinal light damage: mechanisms and protection. Prog Retin Eye Res 29:113–134.

Papermaster DS, Reilly P, Schneider BG (1982) Cone lamellae and red and green rod outer segment disks contain a large intrinsic membrane protein on their margins: An ultrastructural immunocytochemical study of frog retinas. Vision Res 22:1417–1428.

Parker RO, Crouch RK (2010) Retinol dehydrogenases (RDHs) in the visual cycle. Exp Eye Res 91:788–792.

Parker RO, Fan J, Nickerson JM, Liou GI, Crouch RK (2009) Normal cone function requires the interphotoreceptor retinoid binding protein. J Neurosci 29:4616–4621.

Peachey NS et al. (2012) GPR179 is required for depolarizing bipolar cell function and is mutated in autosomal-recessive complete congenital stationary night blindness. Am J Hum Genet 90:331–339.

Pugh EN, Lamb TD (1993) Amplification and kinetics of the activation steps in phototransduction. Biochim Biophys Acta 1141:111–149.

Purves D, Augustine GJ, Fitzpatrick D, Katz LC, LaMantia A-S, McNamara JO, Williams SM (2001) Anatomical Distribution of Rods and Cones..

Radu RA, Hu J, Peng J, Bok D, Mata NL, Travis GH (2008) Retinal pigment epithelium-retinal G protein receptor-opsin mediates light-dependent translocation of all-trans-retinyl esters for synthesis of visual chromophore in retinal pigment epithelial cells. J Biol Chem 283:19730–19738.

Ramón y Cajal S (1900) Structure of the Mammalian Retina, Madrid. Available at: https://en.wikipedia.org/wiki/Santiago_Ram%C3%B3n_y_Cajal#/media/File:Cajal_Retina.jpg.

Razafsky D, Blecher N, Markov A, Stewart-Hutchinson PJ, Hodzic D (2012) LINC complexes mediate the positioning of cone photoreceptor nuclei in mouse retina. PLoS One 7:e47180.

Redmond TM, Yu S, Lee E, Bok D, Hamasaki D, Chen N, Goletz P, Ma JX, Crouch RK, Pfeifer K (1998) Rpe65 is necessary for production of 11-cis-vitamin A in the retinal visual cycle. Nat Genet 20:344–351.

Reichenbach A, Bringmann A (2010) Müller Cells in the Healthy and Diseased Retina. New York, NY: Springer New York.

Reuter T (1969) Visual pigments and ganglion cell activity in the retinae of tadpoles and adult frogs (Rana temporaria L.). Acta Zool Fenn 122:1–64.

Reuter T (2011) Fifty years of dark adaptation 1961-2011. Vision Res 51:2243–2262.

Ribelayga C, Cao Y, Mangel SC (2008) The circadian clock in the retina controls rod-cone coupling. Neuron 59:790–801.

Richardson TM (1969) Cytoplasmic and ciliary connections between the inner and outer segments of mammalian visual receptors. Vision Res 9:727–731.

Robinson MD, McCarthy DJ, Smyth GK (2010) edgeR: a Bioconductor package for differential expression analysis of digital gene expression data. Bioinformatics 26:139–140.

Rohrer B, Goletz P, Znoiko S, Ablonczy Z, Ma J, Redmond TM, Crouch RK (2003) Correlation of regenerable opsin with rod ERG signal in Rpe65-/- mice during development and aging. Invest Ophthalmol Vis Sci 44:310–315.

Ruiz A, Winston A, Lim YH, Gilbert BA, Rando RR, Bok D (1999) Molecular and biochemical characterization of lecithin retinol acyltransferase. J Biol Chem 274:3834–3841.

Rushton WA (1961) Rhodopsin measurement and dark-adaptation in a subject deficient in cone vision. J Physiol 156:193–205.

Rushton WA (1968) Rod/cone rivalry in pigment regeneration. J Physiol 198:219–236.

Rushton WA, Henry GH (1968) Bleaching and regeneration of cone pigments in man. Vision Res 8:617–631.

Saari JC (2012) Vitamin A metabolism in rod and cone visual cycles. Annu Rev Nutr 32:125–145.

Saari JC, Crabb JW (2005) Focus on molecules: cellular retinaldehyde-binding protein (CRALBP). Exp Eye Res 81:245–246.

Saari JC, Garwin GG, Van Hooser JP, Palczewski K (1998) Reduction of all-trans-retinal limits regeneration of visual pigment in mice. Vision Res 38:1325–1333.

Saari JC, Nawrot M, Kennedy BN, Garwin GG, Hurley JB, Huang J, Possin DE, Crabb JW (2001) Visual cycle impairment in cellular retinaldehyde binding protein (CRALBP) knockout mice results in delayed dark adaptation. Neuron 29:739–748.

Saari JC, Nawrot M, Stenkamp RE, Teller DC, Garwin GG (2009) Release of 11-cis-retinal from cellular retinaldehyde-binding protein by acidic lipids. Mol Vis 15:844–854.

Sakurai K, Chen J, Kefalov VJ (2011) Role of guanylyl cyclase modulation in mouse cone phototransduction. J Neurosci 31:7991–8000.

Sakurai K, Chen J, Khani SC, Kefalov VJ (2015) Regulation of mammalian cone phototransduction by recoverin and rhodopsin kinase. J Biol Chem 290:9239–9250.

Sandell LL, Lynn ML, Inman KE, McDowell W, Trainor PA (2012) RDH10 oxidation of Vitamin A is a critical control step in synthesis of retinoic acid during mouse embryogenesis. Henrique D, ed. PLoS One 7:e30698.

Sato S, Miyazono S, Tachibanaki S, Kawamura S (2015) RDH13L, an enzyme responsible for the aldehyde-alcohol redox coupling reaction (AL-OL coupling reaction) to supply 11-cis retinal in the carp cone retinoid cycle. J Biol Chem 290:2983–2992.

Schalken JJ, Janssen JJM, Sanyal S, Hawkins RK, de Grip WJ (1990) Development and degeneration of retina in rds mutant mice: immunoassay of the rod visual pigment rhodopsin. Biochim Biophys Acta - Gen Subj 1033:103–109.

Shen SQ, Turro E, Corbo JC (2014) Hybrid Mice Reveal Parent-of-Origin and Cis- and Trans-Regulatory Effects in the Retina. PLoS One 9:e109382.

Shichida Y, Imai H, Imamoto Y, Fukada Y, Yoshizawa T (1994) Is chicken green-sensitive cone visual pigment a rhodopsin-like pigment? A comparative study of the molecular properties between chicken green and rhodopsin. Biochemistry 33:9040–9044.

Shimomura K, Lowrey PL, Vitaterna MH, Buhr ED, Kumar V, Hanna P, Omura C, Izumo M, Low SS, Barrett RK, LaRue SI, Green CB, Takahashi JS (2010) Genetic suppression of the circadian Clock mutation by the melatonin biosynthesis pathway. Proc Natl Acad Sci 107:8399–8403.

Steinberg RH (1985) Interactions between the retinal pigment epithelium and the neural retina. Doc Ophthalmol 60:327–346.

Stone J, Dreher Z (1987) Relationship between astrocytes, ganglion cells and vasculature of the retina. J Comp Neurol 255:35–49.

Storch K-F, Paz C, Signorovitch J, Raviola E, Pawlyk B, Li T, Weitz CJ (2007) Intrinsic circadian clock of the mammalian retina: importance for retinal processing of visual information. Cell 130:730–741.

Stratton GM (1897) Vision without inversion of the retinal image. Psychol Rev 4:463–481.

Sundermeier TR, Vinberg F, Mustafi D, Bai X, Kefalov VJ, Palczewski K (2014a) R9AP overexpression alters phototransduction kinetics in iCre75 mice. Invest Ophthalmol Vis Sci 55:1339–1347.

Sundermeier TR, Zhang N, Vinberg F, Mustafi D, Kohno H, Golczak M, Bai X, Maeda A, Kefalov VJ, Palczewski K (2014b) DICER1 is essential for survival of postmitotic rod photoreceptor cells in mice. FASEB J 28:3780–3791.

Thomas MM, Lamb TD (1999) Light adaptation and dark adaptation of human rod

photoreceptors measured from the a-wave of the electroretinogram. J Physiol 518 (Pt 2:479–496.

Thompson DA, Gal A (2003) Vitamin A metabolism in the retinal pigment epithelium: genes, mutations, and diseases. Prog Retin Eye Res 22:683–703.

Tosini G, Baba K, Hwang CK, Iuvone PM (2012) Melatonin: an underappreciated player in retinal physiology and pathophysiology. Exp Eye Res 103:82–89.

Tosini G, Menaker M (1996) Circadian Rhythms in Cultured Mammalian Retina. Science (80-) 272:419–421.

Tosini G, Pozdeyev N, Sakamoto K, Iuvone PM (2008) The circadian clock system in the mammalian retina. Bioessays 30:624–633.

Trapnell C, Pachter L, Salzberg SL (2009) TopHat: discovering splice junctions with RNA-Seq. Bioinformatics 25:1105–1111.

Travis GH, Golczak M, Moise AR, Palczewski K (2007) Diseases caused by defects in the visual cycle: retinoids as potential therapeutic agents. Annu Rev Pharmacol Toxicol 47:469–512.

Tsujita Y, Muraski J, Shiraishi I, Kato T, Kajstura J, Anversa P, Sussman MA (2006) Nuclear targeting of Akt antagonizes aspects of cardiomyocyte hypertrophy. Proc Natl Acad Sci U S A 103:11946–11951.

Tu DC, Owens LA, Anderson L, Golczak M, Doyle SE, McCall M, Menaker M, Palczewski K, Van Gelder RN (2006) Inner retinal photoreception independent of the visual retinoid cycle. Proc Natl Acad Sci U S A 103:10426–10431.

Vaughan DK, Nemke JL, Fliesler SJ, Darrow RM, Organisciak DT (2002) Evidence for a circadian rhythm of susceptibility to retinal light damage. Photochem Photobiol 75:547–553.

Vinberg F, Kolesnikov A V, Kefalov VJ (2014) Ex vivo ERG analysis of photoreceptors using an in vivo ERG system. Vision Res 101:108–117.

Vinberg F, Koskelainen A (2010) Calcium sets the physiological value of the dominant time constant of saturated mouse rod photoresponse recovery. PLoS One 5:e13025.

Wald G (1935) Carotenoids and the visual cycle. J Gen Physiol 19:351–371.

Wald G, Brown PK, Smith PH (1955) Iodopsin. J Gen Physiol 38:623–681.

Wang H, Cui X, Gu Q, Chen Y, Zhou J, Kuang Y, Wang Z, Xu X (2012) Retinol dehydrogenase 13 protects the mouse retina from acute light damage. Mol Vis 18:1021–1030.

Wang J, Nymark S, Frederiksen R, Estevez ME, Shen SQ, Corbo JC, Cornwall MC, Kefalov VJ

(2014) Chromophore supply rate-limits mammalian photoreceptor dark adaptation. J Neurosci 34:11212–11221.

Wang J-S, Estevez ME, Cornwall MC, Kefalov VJ (2009) Intra-retinal visual cycle required for rapid and complete cone dark adaptation. Nat Neurosci 12:295–302.

Wang J-S, Kefalov VJ (2009) An alternative pathway mediates the mouse and human cone visual cycle. Curr Biol 19:1665–1669.

Wang J-S, Kefalov VJ (2011) The cone-specific visual cycle. Prog Retin Eye Res 30:115–128.

Wang M, Wong WT (2014) Microglia-Müller cell interactions in the retina. Adv Exp Med Biol 801:333–338.

Wenzel A, Reme CE, Williams TP, Hafezi F, Grimm C (2001) The Rpe65 Leu450Met variation increases retinal resistance against light-induced degeneration by slowing rhodopsin regeneration. J Neurosci 21:53–58.

Wong K (2013) Intrinsically Photosensitive Retinal Ganglion Cells (ipRGCs) Depend on the Retinal Pigment Epithelium (RPE) to Regenerate Melanopsin. Invest Ophthalmol Vis Sci 54:400.

Wright CB, Chrenek MA, Feng W, Getz SE, Duncan T, Pardue MT, Feng Y, Redmond TM, Boatright JH, Nickerson JM (2014) The Rpe65 rd12 allele exerts a semidominant negative effect on vision in mice. Invest Ophthalmol Vis Sci 55:2500–2515.

Wu BX, Chen Y, Chen Y, Fan J, Rohrer B, Crouch RK, Ma J-X (2002) Cloning and characterization of a novel all-trans retinol short-chain dehydrogenase/reductase from the RPE. Invest Ophthalmol Vis Sci 43:3365–3372.

Wu BX, Moiseyev G, Chen Y, Rohrer B, Crouch RK, Ma J-X (2004) Identification of RDH10, an All-trans Retinol Dehydrogenase, in Retinal Muller Cells. Invest Ophthalmol Vis Sci 45:3857–3862.

Xue T, Do MTH, Riccio A, Jiang Z, Hsieh J, Wang HC, Merbs SL, Welsbie DS, Yoshioka T, Weissgerber P, Stolz S, Flockerzi V, Freichel M, Simon MI, Clapham DE, Yau K-W (2011) Melanopsin signalling in mammalian iris and retina. Nature 479:67–73.

Xue Y, Shen SQ, Jui J, Rupp AC, Byrne LC, Hattar S, Flannery JG, Corbo JC, Kefalov VJ (2015) CRALBP supports the mammalian retinal visual cycle and cone vision. J Clin Invest 125:727–738.

Yau K-W, Hardie RC (2009) Phototransduction motifs and variations. Cell 139:246–264.

Yi C, Pan X, Yan H, Guo M, Pierpaoli W (2005) Effects of melatonin in age-related macular degeneration. Ann N Y Acad Sci 1057:384–392.

Zhang H, Fan J, Li S, Karan S, Rohrer B, Palczewski K, Frederick JM, Crouch RK, Baehr W (2008) Trafficking of membrane-associated proteins to cone photoreceptor outer segments requires the chromophore 11-cis-retinal. J Neurosci 28:4008–4014.

Zhou XE, Melcher K, Xu HE (2012) Structure and activation of rhodopsin. Acta Pharmacol Sin 33:291–299.

Znoiko SL, Rohrer B, Lu K, Lohr HR, Crouch RK, Ma J-X (2005) Downregulation of cone-specific gene expression and degeneration of cone photoreceptors in the Rpe65-/- mouse at early ages. Invest Ophthalmol Vis Sci 46:1473–1479.